Defense Nuclear Agency
Alexandria, VA 22310-3398

DNA-TR-92-20

Urban Fire Simulation Version 2

James C. Sanderlin, et al.
Mission Research Corporation
P.O. Drawer 719
Santa Barbara, CA 93102-0719

February 1993

Technical Report

CONTRACT No. DNA 001-82-C-0071

Destroy this report when it is no longer needed. Do not return to sender.

PLEASE NOTIFY THE DEFENSE NUCLEAR AGENCY, ATTN: CSTI, 6801 TELEGRAPH ROAD, ALEXANDRIA, VA 22310-3398, IF YOUR ADDRESS IS INCORRECT, IF YOU WISH IT DELETED FROM THE DISTRIBUTION LIST, OR IF THE ADDRESSEE IS NO LONGER EMPLOYED BY YOUR ORGANIZATION.

DISTRIBUTION LIST UPDATE

This mailer is provided to enable DNA to maintain current distribution lists for reports. (We would appreciate your providing the requested information.)

NOTE:
Please return the mailing label from the document so that any additions, changes, corrections or deletions can be made easily.

☐ Add the individual listed to your distribution list.

☐ Delete the cited organization/individual.

☐ Change of address.

NAME: _____

ORGANIZATION: _____

OLD ADDRESS	CURRENT ADDRESS
_____	_____
_____	_____
_____	_____

TELEPHONE NUMBER: (___) _____

DNA PUBLICATION NUMBER/TITLE	CHANGES/DELETIONS/ADDITIONS, etc.) *(Attach Sheet if more Space is Required)*
_____	_____
_____	_____
_____	_____

DNA OR OTHER GOVERNMENT CONTRACT NUMBER: _____

CERTIFICATION OF NEED-TO-KNOW BY GOVERNMENT SPONSOR (if other than DNA):

SPONSORING ORGANIZATION: _____

CONTRACTING OFFICER OR REPRESENTATIVE: _____

SIGNATURE: _____

CUT HERE AND RETURN

DEFENSE NUCLEAR AGENCY
ATTN: TITL
6801 TELEGRAPH ROAD
ALEXANDRIA, VA 22310-3398

DEFENSE NUCLEAR AGENCY
ATTN: TITL
6801 TELEGRAPH ROAD
ALEXANDRIA, VA 22310-3398

REPORT DOCUMENTATION PAGE

Form Approved
OMB No. 0704-0188

1. AGENCY USE ONLY (Leave blank)	2. REPORT DATE	3. REPORT TYPE AND DATES COVERED
	930201	Technical 811210 – 830214

4. TITLE AND SUBTITLE
Urban Fire Simulation Version 2

5. FUNDING NUMBERS
C - DNA 001-82-C-0071
PE - 62715H
PR - 854CAXY
TA - X
WU - DH005885

6. AUTHOR(S)
James C. Sanderlin, Joseph A. Ball, Gary A. Johanson, and Larry E. Ewing

7. PERFORMING ORGANIZATION NAME(S) AND ADDRESS(ES)
Mission Research Corporation
P.O. Drawer 719
Santa Barbara, CA 93102-0719

8. PERFORMING ORGANIZATION REPORT NUMBER
MRC-R-1390

9. SPONSORING/MONITORING AGENCY NAME(S) AND ADDRESS(ES)
Defense Nuclear Agency
6801 Telegraph Road
Alexandria, VA 22310-3398
RARP/Auton

10. SPONSORING/MONITORING AGENCY REPORT NUMBER
DNA-TR-92-20

11. SUPPLEMENTARY NOTES
This work was sponsored by the Defense Nuclear Agency under RDT&E RMSS Code B3450 82466 854CAXY X 00004 H2590D.

12a. DISTRIBUTION/AVAILABILITY STATEMENT
Approved for public release; distribution is unlimited.

12b. DISTRIBUTION CODE

13. ABSTRACT *(Maximum 200 words)*

A model of mass fire onset and propagation is described. This is Version 2 of a model developed earlier for DNA. This computer model takes the simulation from the detonation of one, or a few, nuclear weapons over an urban site. The detonation(s) ignite fires, generally paper and fabrics, within rooms of houses and offices that are in view of a burst point. Blast wave(s) extinguish some of the initial ignitions, cause secondary ignitions, and can turn a region from Ground Zero into rubble. As ignited structures burn they, in turn, ignite other structures, until an eventual lack of fuel allows the fire to burn out. The rate at which fuel is used, i.e., the rate at which energy is released, governs the indraft surface winds, which also affect fire propagation. Indraft conditions can be great enough that a fire storm exists. The user describes an urban area geometrically as triangular tracks with the number of structures in each occupancy class (Residential, High Rise, Industrial, etc.), locates the weapon detonation points, and weapon yields. Output requests produce graphical tract maps of wind, track burning status, and energy release at selected times.

14. SUBJECT TERMS
Mass Fire, Fire Storm, Simulation Models, Fire Behavior, Nuclear Burst, Fire Ignition, Nuclear Blast, Urban Site

15. NUMBER OF PAGES
116

16. PRICE CODE

17. SECURITY CLASSIFICATION OF REPORT	18. SECURITY CLASSIFICATION OF THIS PAGE	19. SECURITY CLASSIFICATION OF ABSTRACT	20. LIMITATION OF ABSTRACT
UNCLASSIFIED	UNCLASSIFIED	UNCLASSIFIED	SAR

CLASSIFIED BY:
N/A since Unclassified.

DECLASSIFY ON:
N/A since Unclassified.

CONVERSION TABLE

Conversion factors for U.S. Customary to metric (SI) units of measurement

MULTIPLY → / TO GET ←	BY → / BY ←	TO GET / DIVIDE
angstrom	1.000000 x E -10	meters (m)
atmosphere (normal)	1.01325 x E +2	kilo pascal (kPa)
bar	1.000000 x E +2	kilo pascal (kPa)
barn	1.000000 x E -28	meter^2 (m^2)
British thermal unit (thermochemical)	1.054350 x E +3	joule (J)
calorie (thermochemical)	4.184000	joule (J)
cal (thermochemical) / cm^2	4.184000 x E -2	mega joule/m^2 (MJ/m^2)
curie	3.700000 x E +1	*giga becquerel (GBq)
degree (angle)	1.745329 x E -2	radian (rad)
degree Farenheit	$t_K = (t_F + 459.67)/1.8$	degree kelvin (K)
electron volt	1.60219 x E -19	joule (J)
erg	1.000000 x E -7	joule (J)
erg/second	1.000000 x E -7	watt (W)
foot	3.048000 x E -1	meter (m)
foot-pound-force	1.355818	joule (J)
gallon (U.S. liquid)	3.785412 x E -3	meter^3 (m^3)
inch	2.540000 x E -2	meter (m)
jerk	1.000000 x E +9	joule (J)
joule/kilogram (J/kg) (radiation dose absorbed)	1.000000	Gray (Gy)
kilotons	4.183	terajoules
kip (1000 lbf)	4.448222 x E +3	newton (N)
kip/inch^2 (ksi)	6.894757 x E +3	kilo pascal (kPa)
ktap	1.000000 x E +2	newton-second/m^2 (N-s/m^2)
micron	1.000000 x E -6	meter (m)
mil	2.540000 x E -5	meter (m)
mile (international)	1.609344 x E +3	meter (m)
ounce	2.834952 x E -2	kilogram (kg)
pound-force (lbs avoirdupois)	4.448222	newton (N)
pound-force inch	1.129848 x E -1	newton-meter (N-m)
pound-force/inch	1.751268 x E +2	newton/meter (N/m)
pound-force/foot^2	4.788026 x E -2	kilo pascal (kPa)
pound-force/inch^2 (psi)	6.894757	kilo pascal (kPa)
pound-mass (lbm avoirdupois)	4.535924 x E -1	kilogram (kg)
pound-mass-foot^2 (moment of inertia)	4.214011 x E -2	kilogram-meter^2 (kg-m^2)
pound-mass/foot^3	1.601846 x E +1	kilogram/meter^3 (kg/m^3)
rad (radiation dose absorbed)	1.000000 x E -2	**Gray (Gy)
roentgen	2.579760 x E -4	coulomb/kilogram (C/kg)
shake	1.000000 x E -8	second (s)
slug	1.459390 x E +1	kilogram (kg)
torr (mm Hg, 0° C)	1.333220 x E -1	kilo pascal (kPa)

*The becquerel (Bq) is the SI unit of radioactivity; 1 Bq = 1 event/s.
**The Gray (Gy) is the SI unit of absorbed radiation.

TABLE OF CONTENTS

LIST OF ILLUSTRATIONS

LIST OF ILLUSTRATIONS (continued)

LIST OF ILLUSTRATIONS (continued)

LIST OF TABLES

SECTION 1

INTRODUCTION

This section presents a brief history of the Urban Fire Simulation (UFS) development, together with a discussion of the conclusions drawn from the work performed, recommendations regarding future related work, and a brief summary of this report.

1.1 BACKGROUND.

During FY 81 Mission Research Corporation (MRC) undertook to develop for the Defense Nuclear Agency (DNA) a concept for a model to predict the onset and development of mass fires in urban areas as a result of a nuclear attack. A review of the literature showed that a considerable amount of well organized work had been done toward the development of a model to predict primary ignitions resulting from nuclear weapons detonations, that a great deal of highly fragmented work had been done in studying phenomena that could be applicable to various aspects of fire behavior and fire propagation in an urban environment, and that on-going work was addressing flame extinguishment due to blast wave passage, the relationship between blast wave structural damage and secondary ignitions, and the relationship between building structural characteristics and building burning characteristics.

It was concluded that a simulation could be developed to describe urban fire effects resulting from a nuclear detonation. It was also concluded that the highest risk components in such a simulation would probably be those that dealt with the burning characteristics of buildings, fire effects on the ambient winds, and the growth and propagation of uncontrolled fires in an urban environment.

In order to show feasibility of the concept that was developed and to provide a working software structure which would show how the concept could be implemented, a demonstration version of the Urban Fire Simulation (UFS-1) structure was developed as part of the FY 81 effort (Reference 1). The demonstration simulation was designed to accept all initial ignitions as input data. The UFS-1 development concentrated on the simulation structure. However development of models for the UFS-1 addressed the overall geometry, descriptions of the characteristics of burning buildings and burning blocks of buildings in a fire suppression-free urban environment, effects of the fire on the ambient winds, and the effects of local winds on the growth and propagation of the fire.

The fire behavior and propagation models developed for UFS-1 represented a first attempt to put together some to the results of the fragmented fire-related research work into an organized set of models describing the behavior of uncontrolled fires in an urban environment. These models were developed primarily for demonstration purposes. As such, they did not represent a final product and were expected to be the subject of careful review, revision and, where possible, validation.

During FY 82 MRC continued the development for DNA of the Urban Fire Simulation. Specifically the FY 82 development addressed:

- A grid system to partition the urban area into manageable pieces and methods of incorporating subgrid resolution.
- Data to describe the urban area for fire ignition and fire spread purposes.
- Control interfaces, data interfaces and rudimentary models for simulating ignitions

related to nuclear weapon detonation.

- Review and revision of models simulating fire effects on the ambient winds and local wind effects on fire behavior and propagation.

- Parametric executions of UFS-1 to show simulation sensitivity to variations in key variables.

The Urban Fire Simulation was expanded as part of the FY 82 effort. The expanded version (UFS-2) incorporates, in addition to the functions included in UFS-1, a more flexible geometry, together with the data and control interfaces required to support a detailed description of the urban area, primary ignitions, blast extinguishment, and secondary ignitions. These features have been incorporated into the structure in such a way that a scenario can be run starting with weapon detonation, proceeding through primary and secondary ignitions, to fire spread, growth and eventual burnout.

1.2 CONCLUSIONS AND RECOMMENDATIONS.

The triangular grid used in UFS-2 is much more flexible than the rectangular grid that was used in UFS-1. The location, orientation and size of each triangular tract can be tailored to fit the urban area being analyzed. Use of the triangular grid is expected to alleviate the potential storage problem encountered in UFM-1 as a result of using uniform block-sized rectangular tracts.

Data and control interfaces allow detailed descriptions of urban area ignition and burning characteristics, given sufficiently abundant data. Alternatively, simplified descriptions can be used if only sparse data are available.

The amount of detail that can be included in the description of ignition characteristics is limited by a combination of storage capacity and acceptable execution time. The storage and execution time requirements for each tract are independent of tract size. However, the total number of tracts is dependent upon average tract size. Thus, execution time is linearly dependent upon average tract size and urban area size. Execution time is strongly dependent and storage requirements are weakly dependent upon the number of occupancy classes in a tract. The sensitivity or execution time to tract complexity can be simply avoided by subdividing complex tracts to provide a larger number of less complex tracts.

The most logical future directions for the urban fire simulation project that are consistent with the past development and the need to provide a product that can be useful for targeting are:

- The development of appropriately accurate and detailed models and data to allow prediction of primary ignitions.

- Testing and validation, where possible, of the models and the overall structure.

This is the most conservative definition of the potential extent of fire damage. However, it is also probably the most reliable.

The development of additional models and data beyond primary ignition to include the effects of blast damage, secondary ignitions and fire spread is also consistent with past work and the need to provide a useful product; however, the potential utility of these models and data is less clear, because of their lower anticipated predictive reliability.

1.3 SUMMARY.

In Section 2 the Urban Fire Simulation (UFS-1) concept is reviewed and the additions and modifications that have been included to define UFS-2 are briefly described. These additions and modifications affect the grid system, data management system, subgrid calculations, the events used, and the modules required to execute events.

In Section 3 the triangular grid system is discussed, additions to the data management system are described, and alterations to the Event Transfer List are identified.

In Section 4 the nuclear detonation (NUCDET) event is described, together with the models and data involved in NUCDET event execution.

In Section 5 the blast effects (BLSEFF) event is described, together with the models and data involved in BLSEFF event execution.

In Section 6 example model results are presented and discussed.

SECTION 2

URBAN FIRE SIMULATION STRUCTURE AND CONCEPT

In this section the UFS-1 concept is briefly reviewed. The structural and conceptual additions and modifications to UFS-1 are discussed.

2.1 BACKGROUND.

A detailed description of the UFS-1 concept and structure is given in Reference 1. We will present here a brief summary to provide a background for discussing the work leading to UFS-2.

The UFS-1 structure accepted an initial set of ignitions as input data and addressed the problem of fire behavior and growth from that point. Since the set of ignitions was a given, ignition characteristics were not required. Only minimal combustion characteristics were included, since all executions considered a uniform fuel distribution to prevent masking the effects of other variables.

Each block-sized cell was ignited and allowed to burn until burnout with a variable burn rate that depended upon the number of ignitions and the local wind velocities. Cells adjacent to burning cells could be ignited by convection or conduction. A fire was defined to consist of a set of contiguous burning cells. Each fire was subdivided into appropriately symmetrical subfires. Brands were considered to be lofted from burning cells on the periphery of each fire.

The resolution used in UFS-1 was considered to be too fine. It resulted in a limit on urban area size of about 10,000 blocks as a result of requirements for storing cell data. The use of several cell states required maintenance of a cell state map. Additionally, the definition and maintenance of lists of fires, subfires and fire perimeters was required. The large number of cells used, together with the considerable number of operations necessary to keep the simulation moving forward cell-by-cell, and to maintain records of the state of each cell, fire, subfire, fire perimeter, etc. involved the use of a great deal of computation resources and storage capacity.

2.2 CURRENT STATUS.

A flexible grid system has been incorporated into the UFS-2 structure. This allows the urban area to be partitioned into triangular tracts. The orientation of the tracts is arbitrary, however restrictions are placed on their size and shape. Average tract size is limited by the urban area and the maximum desired number of tracts, in view of the related run time and storage requirements. Maximum and minimum tract sizes are generally limited by the variability of tract characteristics and the allowed size ranges for fires, since each tract is treated as a fire.

Nuclear detonation and blast effect events have been incorporated into the UFS-2 structure. These events include the modules appropriate to simulate primary and secondary ignitions.

Data files, interfaces and initiating routines have been included in the UFS-2 structure to specify urban area characteristics related to ignition and combustion. Tracts are defined in terms of fractional occupancy classes. Data are specified in terms of "global data", which apply to the entire urban area and "occupancy class" data, which apply to each occupancy class. Data for each tract are calculated from the fractional distribution of occupancy classes in each tract and the distributions of characteristics that describe each occupancy class. This makes possible the description of a large number of different tract types while requiring the user to only describe the global and occupancy class characteristics.

2.3 TRIANGULAR TRACTS.

A triangular grid structure was chosen to partition the urban area into tracts because of its flexibility and because it produces a surface containing no unnecessary step discontinuities. Geometrically, tracts of arbitrary size, orientation and aspect ratio (ratio of maximum to minimum side length) may be used. In this case limitations are placed upon the tract size and aspect ratio.

Symmetrical fires are assumed by the fire modeling equations. Since each ignited tract is treated as a fire, this condition is satisfied by limiting the tract aspect ratio to be no greater than two.

The average tract size is determined by the urban area and the desired number of tracts. A maximum tract area is dictated by the minimum usable resolution. Storage requirements and run time are essentially independent of tract size. The minimum tract size should be chosen to be consistent with the largest of the tract sizes dictated by storage requirements, execution time, and the maximum usable resolution.

The final number of tracts obtained will generally be larger than the planned number. This results from subdividing tracts to simplify, where required, the number of occupancy classes per tract. It is desirable to limit the number of occupancy classes per tract, because (NUCDET, BSLEFF) execution time for a tract increases exponentially with the number of occupancy classes per tract, while it increases linearly with the number of tracts used.

Figure 1 shows an example of a hypothetical urban area that has been partitioned into triangular tracts. In this case the urban area had been previously partitioned into square tracts. Although the resulting grid was used to define the rectangular coordinate system, the presence of the square tracts impeded the definition of triangular tracts by making the occupancy class boundaries more difficult to fit with triangular tracts.

Several attempts, based on different rationales, were made to partition the urban area shown in Figure 1. The rationale that served as the basis for the partitioning shown in Figure 1, and used in the example calculations is described below.

Define the maximum number (Nmx) and the minimum number (Nmn) of tracts to be used. Given the urban area AU, the maximum and minimum average tract areas are given by

$$Amx = AU/Nmn \tag{1}$$

and

$$Amn = AU/Nmx. \tag{2}$$

If equilateral tracts are assumed, the maximum and minimum tract sides are given by

$$Smx = (Amx/2)^{\frac{1}{2}} \tag{3}$$

and

$$Smn = (Amn/2)^{\frac{1}{2}}. \tag{4}$$

Lay out the tracts on the urban area occupancy class map so that tract boundaries follow as closely as possible the boundaries between occupancy classes, without violating (3), (4) or the maximum aspect ratio (ARmx). An additional constraint imposed on the tracts is that each tract is required to have exactly three vertices. Thus, it is not possible for a vertex of a tract to fall on the side of an adjacent tract.

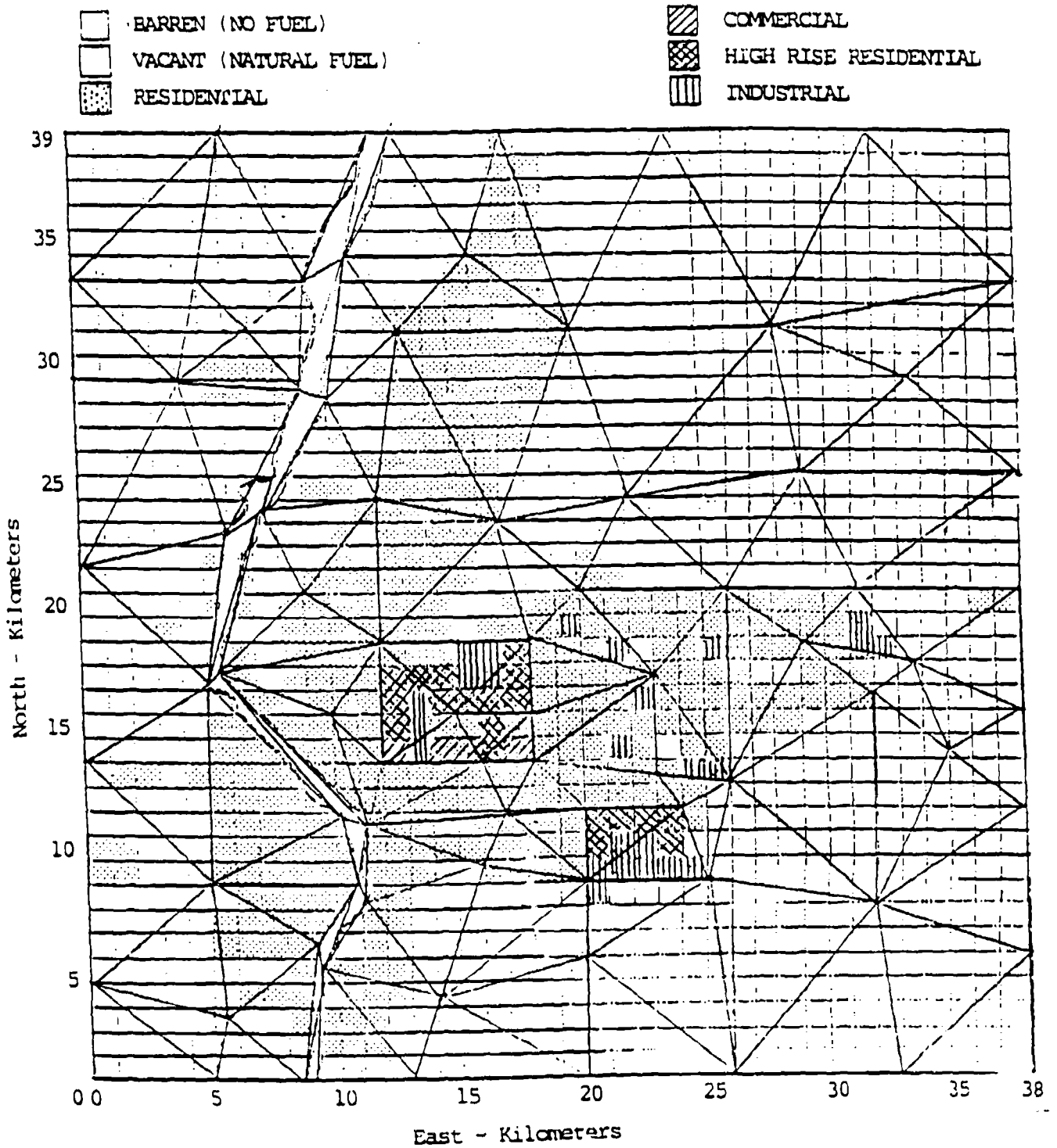

Figure 1. Layout and composition of tracts in hypothetical urban area.

A river flows from north to south down the west side of the urban area shown in Figure 1. In partitioning the river into triangular tracts, the maximum aspect ratio was clearly violated, although (3) and (4) were observed. The aspect ratio could be violated, because these tracts cannot burn and, thus, will never be represented as fires. It was necessary to observe (3) and (4), because the sides or the tracts defining the river are also sides of the adjacent tracts, which may contain fuel and thus be represented as fires.

After the first partitioning the central business/ industrial area was found to be contained in a few tracts, each of which exhibited several occupancy classes. This area was repartitioned to arrive at the configuration shown in Figure 1.

In repartitioning the central business/industrial area to reduce the number of occupancy classes per tract, constraints (3) and (4) were related while ARmx was observed. Figure 1 still shows tracts containing as many as four occupancy classes. These were left in order to be able to test the effect of the number of occupancy classes on tract execution time.

Although triangular tracts are used, the computational coordinate system is still rectangular. Thus, provisions must be made to transform back and forth between these two coordinate systems. To accomplish this, the tracts are numbered as shown in Figure 2 and the tract vertices are numbered as shown in Figure 3. The data associated with tracts is contained in data table TRaCT Data (TRCTD), and the data associated with tract vertices is contained in data table VERTex Data (VERTD). The format for data table TRCTD is:

ITRACT, IV1, IV2, IV3, NNOC, IOCT, FOCT, TRACT CENTER, TRACT AREA

where

ITRACT is the tract identification number
IV1, IV2, IV3 are the identification numbers of subject tract vertices
NNOC is the number of occupancy classes in subject tract
IOCT is the occupancy class identification number
FOCT is the fraction of subject tract occupied by this occupancy class
TRACT CENTER is the (X,Y,Z) coordinates of tract center
TRACT AREA is the area of tract in meters^2.

The tract data table is entered with the tract ID number to obtain the above tract characteristics. The format for data table VERTD is:

IVERT, VX, VY, VZ, NAT, IAT

where

IVERT is the vertex identification number
VX, VY, VZ are the (X,Y,Z) coordinates of subject vertex
NAT is the number of tracts to which the subject vertex belongs
IAT is the set of identification numbers of the tracts to which the subject vertex belongs.

The tract vertex table is entered with a vertex ID number (obtained from TRCTD) to obtain the above vertex characteristics.

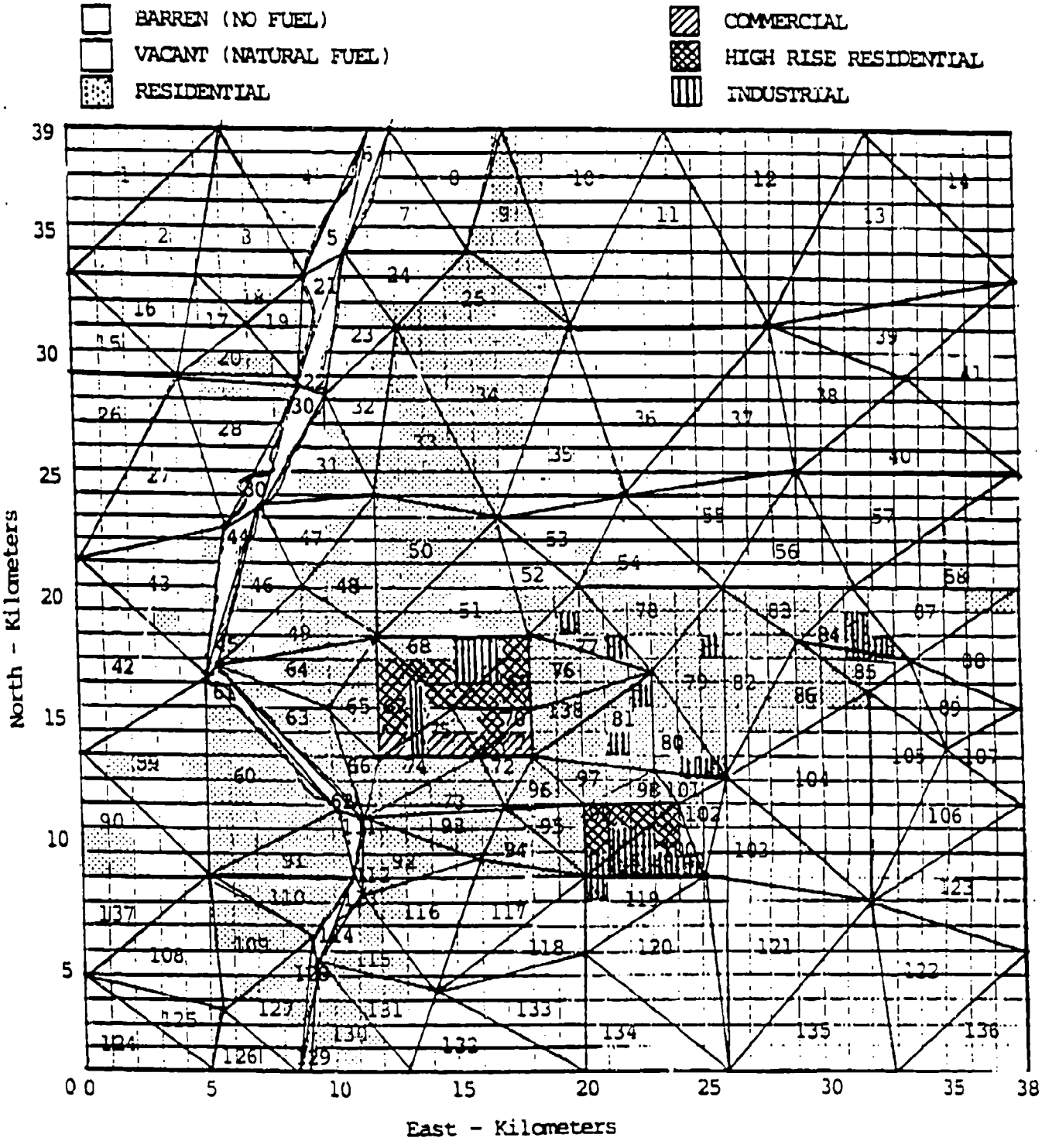

Figure 2. Tract identification numbers.

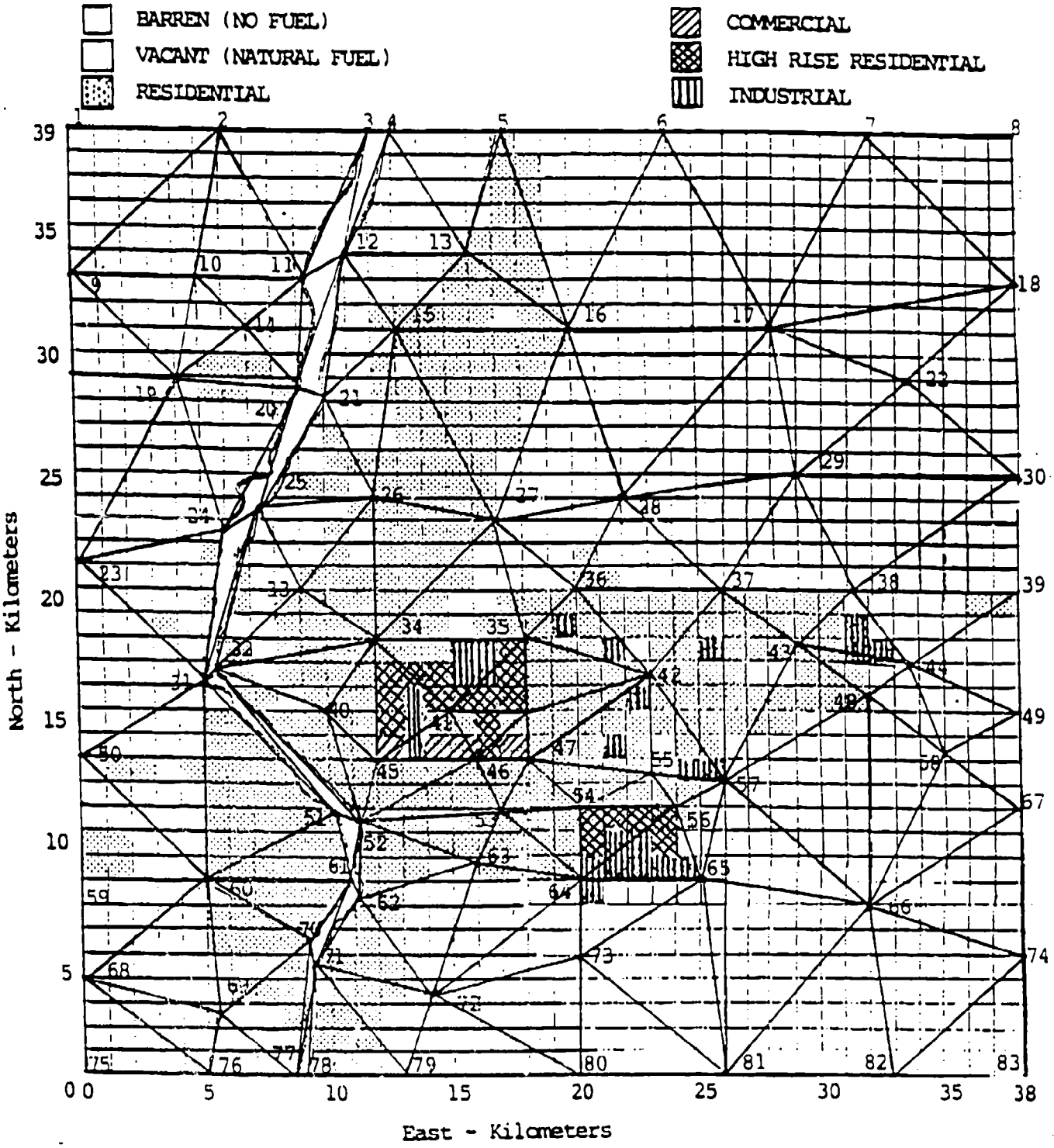

Figure 3. Tract identification numbers.

2.4 CONTROL INTERFACES.

The major modification that has been made to the control interfaces of UFS-1 is the addition of two new Events, the NUClear DETonation (NUCDET) Event and the BLaSt EFFects (BLSEFF) Event. A number of minor alterations made to the control interfaces will be included in the detailed descriptions of these events.

Table 1 shows the UFS-2 Event Transfer Table, which defines the intermodule control interfaces. The NUCDET and BLSEFF Events have been added to the table, together with the modules, models, data interfaces, and intramodule control interfaces required to execute the events.

2.5 DATA INTERFACES.

Three classes of data are used by UFS-2. These are; (1) data which are user defined and entered prior to any execution, (2) data which are calculated (i.e. preprocessed) from user defined data and entered prior to execution, and (3) data which are calculated during execution. The data sets belonging to Class 1 and the approach used in generating the data sets belonging to Class 2 will be described here. Descriptions of the data sets belonging to Class 3 will be included in the descriptions of the modules and models in which they are used.

2.5.1 Class 1 Data Sets.

Tract and vertex data, shown in Figure 4, are user specified from an occupancy class map of the urban area to be analyzed. Currently these data are manually specified and entered; however, provisions can be made to allow digitizer entry of much of this data directly from the occupancy class map. The above data for each tract are used by a preprocessor to calculate the area of each tract and the coordinates of the center of each tract.

The data which describe the details of the urban area for purposes of ignition, combustion and propagation of nuclear weapon induced fires are contained in a collection of "global" data sets. The global data sets, which are shown in Figure 5, identify characteristics which apply over the entire urban area. The contents of the global data sets are currently user specified and manually entered. However, the global data are of limited extent and they need only be defined initially, and updated when the urban area characteristics are changed.

The data which describe the details of each occupancy class in the urban area for purposes of ignition, combustion and propagation of nuclear weapon induced fires are contained in a collection of "occupancy class" data sets. The occupancy class data sets, which are shown in Figure 6, define the distributions of characteristics which apply to each occupancy class. These data sets are also global in the sense that the defined distributions apply to each occupancy class no matter where it is found in the urban area. The contents of the occupancy class data sets are currently user specified and manually entered. However, the occupancy class data are of limited extent and need be defined only for the number of occupancy classes to be used in the urban area to be analyzed.

Additional user defined data include runtime data, grid data, and environmental data, which are shown in Figure 7, together with weapon data, and initialization data for fireball and irradiance calculations, which are shown in Figure 8.

An effort has been made to limit the amount and detail of data that the user is required to define, while including enough descriptive detail to allow adequate description of the ignition and burning characteristics of the urban area.

Table 1. Event transfer table for urban fire simulation.

READIN	INPUTS			
WRITOT	OUTPUT			
SETUP(M)	MODULE(M)			
UPDATE(M)	MODULE (M)			
FINISH(M)	MODULE(M)			
NUCDET	TPULSE	INBLST	WNDMOD	IGNITE
BSDEFF	BSLPRP	QUENCH	FULMOD	SECIGN
BURN(K)	BCUPDT(K)	BRNDG(K)		
ADJCNT(N)	ACUPDT(N)			
FUPDT(L)	UPDTF(L)			
STOWV	WVMAP			
STOCS	CSMAP			
STOQ	QMAP			

Define the Events and Modules which appear in the Event-Module Transfer Table.

TERM	DEFINITION
READIN	Event to read input data
INPUTS	Module to specify data to be read in and its formats
WRITOT	Event to write output data
OUTPUT	Module to specify data to be output and its formats
SETUP(M)	Event to setup module (M)
MODULE(M)	ID of module (M)
UPDATE(M)	Event to bring the pertinent data elements of module(M) up to date
FINISH(M)	Event to terminate module(M)
NUCDET	Event to perform calculations associated with nuclear weapon detonation
TPULSE	Module to calculate free-field thermal irradiance (j/m^2) as a function of yield, burst height, and visibility at a specified number of ranges from ground zero
INBLST	Module to calculate free-field blast effects of peak overpressure, positive phase duration, flow velocity and time of arrival at a specified number of ranges from ground zero as a function of yield and burst height
WNDMOD	Module to modify wind field to account for column formation at the burst location as a function of yield, burst height and time after detonation.
IGNITE	Module to calculate ignitions from this NUCDET in all affected tracts
BLSEFF	Event to calculate blast effects from this NUCDET in all affected tracts
BLSPRP	Module to calculate free field blast parameters in a specific tract and to modify them to account for shadowing, orientation, and reflection
QUENCH	Module to calculate ignitions extinguished by blast effects in a specific tract
FULMOD	Module to calculate blast induced fuel modifications in a specific tract
SECIGN	Module to calculate blast related secondary ignitions in a specific tract
BURN(K)	Event to bring up to date the burning characteristics of burning track (K)
BCUPDT(K)	Module to update the data elements of burning tract (K)
BRNDG(K)	Module to calculate brand generation and propagation for burning tract (K)

Table 1. Event transfer table for urban fire simulation (continued).

ADJCNT(N)	Event to update the characteristics of tract (N), which is adjacent to a burning tract
ACUPDT(N)	Module to update the data elements of tract (N)
FUPDT(L)	Event to update the characteristics of fire (L)
UPDTF(L)	Module to update the data elements of fire (L)
STOWV	Event to store data for a wind velocity map
WVMAP	Module to specify the data formats for wind velocity maps
STOWCS	Event to store data for a tract state map
CSMAP	Module to specify the data formats for tract state maps
STOQ	Event to store data for a heat release rate map
QMAP	Module to specify the data formats for heat release rate maps

For each tract

- Tract ID number
- Three vertex ID numbers
- Number of occupancy classes in tract
- ID number of each occupancy class in tract
- Fraction of tract occupied by each occupancy class

For each vertex

- Vertex ID number
- X,Y,Z coordinates of vertex
- Number of tracts to which each vertex belongs
- ID number of each tract belonging to each vertex

Figure 4. User defined tract and vertex data.

Building Heights

Height of a story (m)
Number of building heights used
Heights of buildings used (m)

Building Classes

Number of building classes used
ID numbers of building classes used

Building Separation Distances

Number of building separation distances used
Building separation distances used (m)

Foliage-Building Separation Distances

Number of foliage-building separation distances used
Foliage-building separation distances used (m)

Foliage Heights

Number of foliage heights used
Foliage heights used (m)
Transmissivity of each foliage height used

Occupancy Classes

Number of occupancy classes used
Building density of occupancy class (No. Bldgs./m^2)
Building fuel loading of occupancy class per floor (kg/m^2/Floor)
Building fuel loading of occupancy class (kg/m^2)

Room Furnishings

Number of room furnishing types (critical ignition energies) used
Critical ignition energy of each type of room furnishing (j/m^2)

Room Sizes

Number of room sizes allowed
Room cell linear dimension (m)
Depth of each room size (m)
Width of each room size (m)

Figure 5. Global data - user defined characteristics of the overall urban area.

Street Azimuth Angles

Number of street azimuth angles used
Azimuth angles of streets (rad)

Street Widths

Number of street widths used
Widths of streets (m)

Window Sizes

Window transmissivity
Number of window sizes used
Height of each window size (m)
Width of each window size (m)

Window Coverings

Number of window covering types (critical ignition energies) used
Critical ignition energy of each window covering type (j/m^2)

Figure 5. Global data - user defined characteristics of the overall urban area (continued).

Building Heights

Number of building heights in each occupancy class
ID number of each building height in each occupancy class
Fraction of buildings in each height class per occupancy class

Building Classes

Number of building classes in each occupancy class
ID number of each building class in each occupancy class
Fraction of buildings in each building class per occupancy class

Building Separations

Number of building separation distances in each occupancy class
ID number of each building separation distance in each occupancy class
Fraction of buildings in each separation distance class per occupancy class

Foliage-Building Separation Distances

Number of foliage-building separation distances in each occupancy class
ID number of each foliage-building separation distance in each occupancy class
Fraction of foliage in each separation distance class per occupancy class

Foliage Heights

Number of foliage heights in each occupancy class
ID number of each foliage height in each occupancy class
Fraction of foliage in each height class per occupancy class

Room Furnishings

Number of room furnishing types (critical ignition energies) in each occupancy class
ID number of each room furnishing type in each occupancy class
Fraction of room furnishings of each type per occupancy class

Room Sizes

Number of room sizes in each occupancy class
ID number of each room size in each occupancy class
Fraction of rooms in each size class per occupancy class

Street Widths

Number of street widths in each occupancy class
ID number of each street width in each occupancy class
Fraction of streets in each width class per occupancy class

Figure 6. Occupancy class data - user defined characteristics of occupancy classes over the urban area.

Window sizes

Number of window sizes in each occupancy class
ID number of each window size in each occupancy class
Fraction of windows in each size class per occupancy class

Window Coverings

Number of window covering, types (critical ignition energies) in each occupancy class
ID number of each window covering type in each occupancy class
Fraction of window coverings in each type class per occupancy class

Figure 6. Occupancy class data - user defined characteristics of occupancy classes over the urban area (continued).

Runtime Data

- Maximum simulation run time (s)
- Simulation time to start diagnostic writing
- Number of cells to be diagnosed
- ID numbers of cells to be diagnosed

Grid Data

- Square cell side length (m)
- X,Y coordinates of Southwest corner of cell system
- Number of East-West cells (columns)
- Number of North-South cells (rows)

Environmental Data

- Time of data (s)
- Ambient wind speed (m/s)
- Ambient wind direction (rad)
- Relative humidity
- Temperature (deg. C)
- Low cloud layer height (m) above sea level
- Low cloud layer type
- High cloud layer height (m) above sea level
- Surface albedo
- Visibility index

Figure 7. User defined runtime, grid and environmental data.

Nuclear Weapon Characteristics

Weapon (detonation) ID number
X,Y coordinates of detonation point (m)
Height of detonation above sea level (m)
Total weapon yield (m)
Detonation time (s)
Maximum effects range (m)
Minimum effects range (m)

Radiation Circle Rows

Maximum number of rows on a side with no step
Maximum number of rows
Array of X,Y locations for the centers of radiation circle elements

Irradiance Calculation Ranges and Values

ID number of weapon
Number of ranges at which irradiance is to be calculated
Value of irradiance at each calculation range

Figure 8. User defined weapon data and initialization data for fireball radiation and irradiance calculations.

2.5.2 Class 2 Data Sets.

Class 2 data are calculated from user defined data and entered in the simulation data prior to execution. These precalculated data are not recalculated for each execution, and, in general, need be recalculated only if the user defined data are altered.

The user defined tract and vertex data are shown in Figure 4. These data are used to calculate the area of each tract and the location of the center of each tract. These data are loaded together with the user defined tract and vertex data into a single data file.

The tract fractional occupancy class specifications (Figure 4), the global data characteristics (Figure 5), and the occupancy class data characteristics (Figure 6) are used in a preprocessor to define the distributions of the characteristics for each identified tract in the urban area.

For each tract the fractional occupancy class data are of the form:

Ioc(l, Noc) = the ID number of each occupancy class in the tract,

Foc(Ioc) = the fraction of each occupancy class in the tract.

The data for each global variable (see Table 2) are of the form:

Igv(l, Ngv) = the ID number of each value of the global variable that is used throughout the urban area,

Vgv(Igv) = the magnitude of each value of the global variable.

The data for each occupancy class variable (see Table 3) are of the form:

Iov(l, Nov) = the ID number of each value of the global variable that is used in the occupancy class,

Fov(Iov) = the Fraction of each value of the global variable that is used in the occupancy class.

Each occupancy class ID number (Ioc) must belong to the corresponding set of global ID numbers (Igv). Thus, the characteristics that make up any occupancy class data set constitute a subset of, and can be obtained from, the corresponding global data set. The occupancy class ID number (Iov) is used to obtain the value of the variable in the form Vgv(Iov).

The number of values of a global variable in each tract (Ntv) is calculated from the number of values exhibited by the global variable in all of the occupancy classes of the tract. The ID numbers of the global variable values in each tract are the ID numbers of the global variable values in all of the occupancy classes of the tract. The fraction of each global variable value in each tract is calculated from

$$Ftv(Iov) = \sum_{Ioc} Foc(Ioc)\, Fov(Iov) \qquad (5)$$

where

Ftv is the fraction of the global variable value in the tract,
Foc is the fraction of the occupancy class in the tract,
Fov is the fraction of the global variable value in the occupancy class.

The preprocessor uses the above calculations to define tract data sets corresponding to the global and occupancy class data sets which are of the form:

It = the tract ID number,

Itv(1,Ntv) = the ID number of each global variable value in the tract,

Ftv(Itv) = the fraction of each global variable value in the tract.

The data sets which are defined by the preprocessor for each tract are shown in Figure 9.

2.5.3 Class 3 Data Sets.

Class 3 data sets are calculated by the various modules and models during execution. The format and contents of the Class 3 data sets will be described as part of the detailed discussions of the Events, modules and models with which they are associated.

In the following paragraphs the control and data interfaces defined for the modules and models associated with the nuclear detonation and blast effects events will be discussed. These discussions will be followed by a presentation and discussion of example results from UFS-2.

Building Height

Number of building heights in tract
ID numbers of building heights in tract
Fraction of buildings of each height in tract

Building Classes

Number of building (structural) classes in tract
ID numbers of building classes in tract
Fraction of buildings of each class in tract

Building Separation Distances

Number of building separation distances in tract
ID numbers of building separation distances in tract
Fraction of buildings separated by each separation class

Foliage-Building Separation Distances

Number of foliage-building separation distances in tract
ID numbers of foliage-building separation distances in tract
Fraction of foliage separated by each separation class

Foliage Heights

Number of foliage heights in tract
ID numbers of foliage heights in tract
Fraction of foliage of each height in tract

Room Furnishings

Number of room furnishing types (critical ignition energies) in tract
ID numbers of room furnishing types in tract
Fraction of room furnishings of each type in tract

Room Sizes

Number of room sizes in tract
ID numbers of room sizes in tract
Fraction of rooms of each size in tract

Figure 9. Tract characteristics - calculated characteristics of each in the urban area.

Street Azimuth Angles

Number of street azimuths in tract
ID numbers of street azimuths in tract
Fraction of streets at each azimuth in tract

Street Widths

Number of street widths in tract
ID numbers of street widths in tract
Fraction of streets of each width in tract

Window Sizes

Number of window sizes in tract
ID numbers of window sizes in tract
Fraction of windows of each size in tract

Window Coverings

Number of window covering types (critical ignition energies) in tract
ID numbers of window covering types in tract
Fraction of window coverings of each type in tract

Figure 9. Tract characteristics - calculated characteristics of each in the urban area (continued).

SECTION 3

THE NUCLEAR DETONATION (NUCDET) EVENT

The NUCDET Event provides the initialization for all nuclear weapon caused ignitions, and these, in turn, provide the initialization for the BURN (fire behavior and spread) event. The NUCDET event includes modules for calculating, throughout the urban area of interest, the thermal irradiance (TPULSE), blast characteristics (INBLST), wind velocity (WNDMOD), and primary ignitions (IGNITE) resulting from detonation of a nuclear weapon.

The structure of the NUCDET event, and of UFS-2 in general, is designed to accommodate single or multiple-sequential nuclear weapon detonations. In order for two detonations to be considered sequential, their time spacing must be greater than the arrival time of the blast wave from the first detonation at the maximum range of interest. This calculational criterion decouples sequential detonations by not allowing the calculation of primary or secondary ignitions for the first detonation to be affected by the second detonation. Of course, both primary and secondary ignitions due to the first detonation will be affected by the second detonation, and these effects will be calculated.

3.1 THERMAL IRRADIANCE.

Fire effects are usually of interest over the extent of an annulus centered on ground zero. The inner radius of the annulus is defined by blast effects of such severity that fire effects are generally of little interest. The outer radius of the annulus is defined by fire effects of less severity than specified, and essentially insignificant blast effects. Within the annulus both blast and fire effects are considered. This is necessary, because blast induced fuel modifications affect secondary ignitions.

A potentially large number of tracts may be included in the annulus, and it is generally not necessary to calculate the thermal irradiance in each tract. This is particularly true if (as in the present case) it is assumed that thermal irradiance is a function only of distance from the burst point (i.e. no terrain shadowing). To avoid calculating thermal irradiance for every tract in the annulus, thermal irradiance can be calculated at a user specified number of equally spaced distances from ground zero. Irradiance data at other distances from ground zero are obtained by interpolating on these data. Alternatively, a set of monotonic decreasing values of irradiance can be specified by the user. The corresponding ranges from ground zero will be calculated.

Thermal irradiance data are calculated by module TPULSE, which is shown in Figure 10. Upon entry to TPULSE, environmental data (ENVD, Figure 7) are accessed to obtain the visible range. Reference to Figure 7 shows that a number of additional variables are also included. Data interfaces have been included to permit use of an irradiance model such as described in Reference 2, although a much simpler demonstration model is used. Given the visible range (Rv), the scattering coefficient (Cs) is calculated from the definition of visible range (Reference 3) by

$$Cs = 0.105/Rv. \qquad (6)$$

The weapon data (WEPD, Figure 8) and the initialization irradiance calculation data are accessed to obtain the weapon, detonation, and calculation parameters needed to calculate thermal irradiance at specified locations in the urban area.

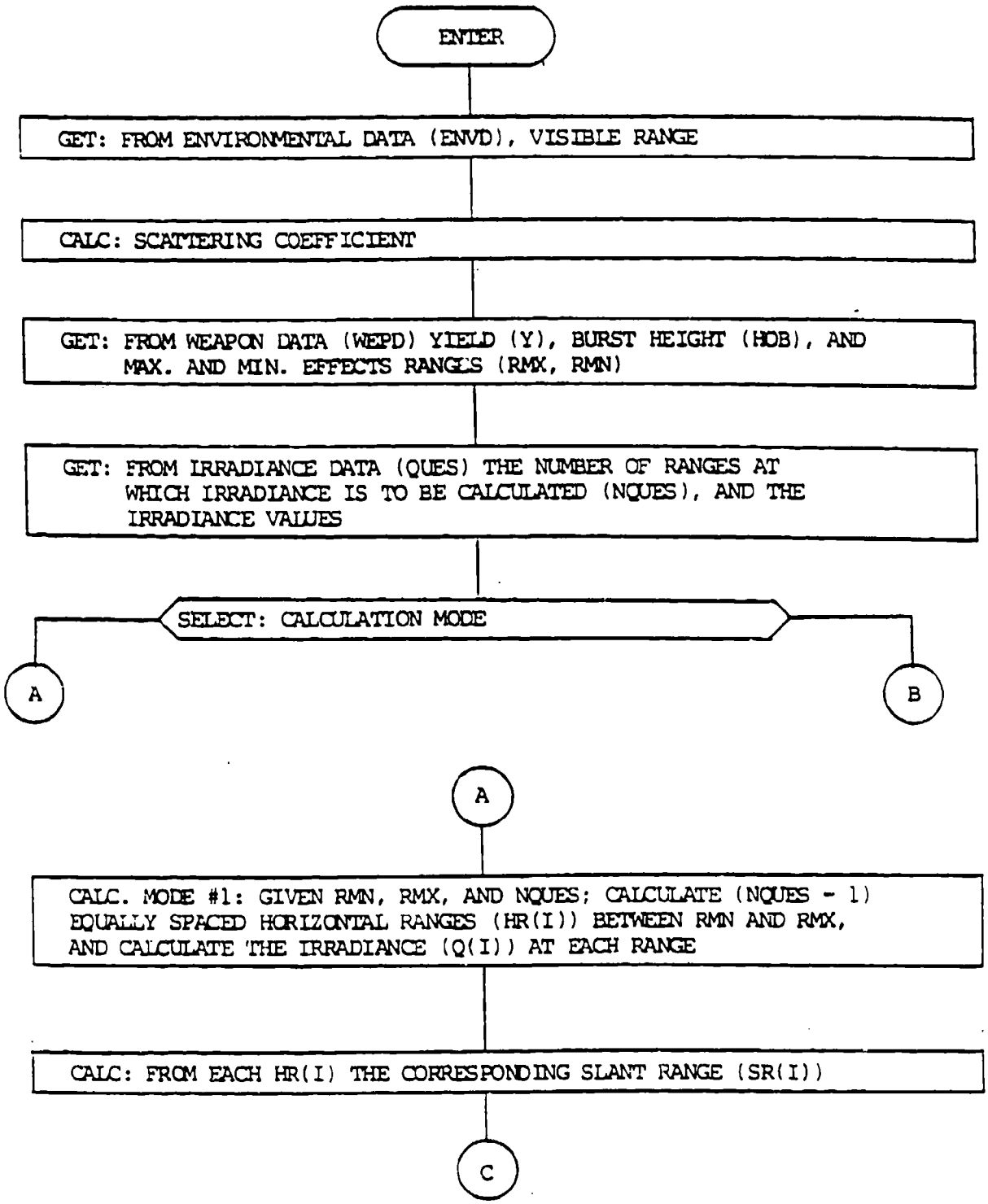

Figure 10. Logic flow diagram for module TPULSE.

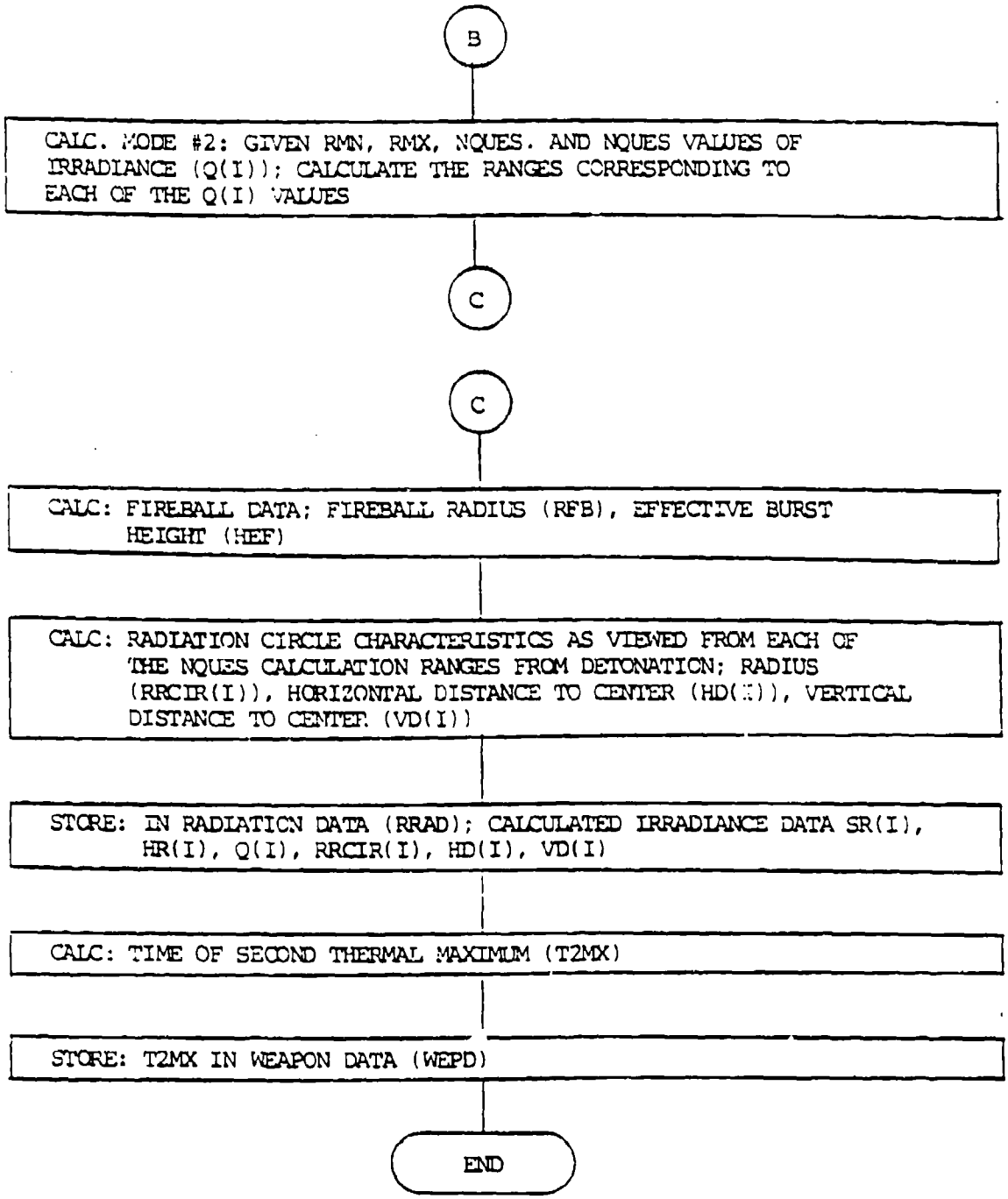

Figure 10. Logic flow diagram for module TPULSE (continued).

Two calculation modes are allowed. In Mode 1, at label (A) of Figure 10, the inner and outer annulus radii and the number of calculation ranges are user specified. The specified number or equally spaced horizontal (Rh) and slant (Rs) ranges from the detonation point, and the corresponding free field irradiances at these ranges are calculated. In Mode 2, at label (B) of Figure 10, the inner and outer annulus radii, the number of calculation ranges, and the desired irradiances at each of the calculation ranges are user specified. The horizontal and slant ranges are calculated at which the specified irradiances will occur.

Free field thermal irradiance at each range is calculated from the radiant exposure-distance relationship (Reference 4, pp. 316-317)

$$Q = 85.6\ (f\ W\ t)/(R^2) \qquad (7)$$

where Q is the thermal irradiance at distance R (cal/cm^2),
f is the thermal fraction of yield (taken to be 0.3),
W is the weapon yield (KT),
t is the transmittance,
R is the distance from detonation point (Kft).

At label (C) of Figure 10 the fireball radius and radiation circle characteristics are calculated following (Reference 5, pp 88-91). The fireball radius is given by

$$Rf = K\ \ (Y^{0.35})\ Exp(0.465Hb) \qquad (8)$$

where Rf is the fireball radius (mi),
K is the 0.53 for surface burst,
K is the 0.47 for Hb below 40 miles,
K is the 0.41 for Hb above 40 miles,
Y is the weapon yield (MT).

The radius of the radiation circle is given by

$$Rrc = Rf\ (1.0 - (Rf/Rs)^2)^{\frac{1}{2}} \qquad (9)$$

where Rrc is the radius of radiation circle (m),
Rf is the fireball radius (m),
Rs is the distance to detonation point (m).

The horizontal and vertical distances to the center of the radiation circle are given by

$$Dh = Rh\ (1.0 - (Rf/Rs)^2)^{\frac{1}{2}} \qquad (10)$$

and

$$Dv = Rv\ (1.0 - (Rf/Rs)^2)^{\frac{1}{2}} \qquad (11)$$

where Dh is the horizontal distance to center of radiation circle (m),
Rh is the horizontal range to center of fireball (m),
Dv is the vertical distance to center of radiation circle (m),
Rv is the vertical range to center of fireball (m),
Rf is the fireball radius (m)
Rs is the range to fireball center (m).

These data are stored in the radiation data array RRAD, which is shown in Figure 11.

Thermal Irradiance Data (RRAD)

Weapon (detonation) ID Number (for each detonation in this scenario)

Number of ranges at which irradiance is to be calculated
Slant range to detonation (m)
Horizontal range to detonation (m)
Irradiance at this range (j/m^2)
Radius of radiation circle at this range (m)
Horizontal distance to radiation circle center at this range (m)
Vertical distance to radiation circle center at this range (m)

Augmented Weapon Data (WEPD)

Weapon (detonation) ID number (for each detonation in this scenario)

X,Y coordinates of detonation point (m)
Height of burst above sea level (m)
Total weapon yield (MT)
Detonation time (s)
Maximum effects range (m)
Minimum effects range (m)
Time of second thermal maximum (s)
ID number of tract under burst point

Figure 11. Thermal irradiance and augmented weapon data.

The time of second thermal maximum is calculated from the relationships (Reference 4, pp 309-312)

$$T2mx = 0.0417\ W^{0.44}, \text{ if Hb less than 15 Kft} \quad (12)$$

$$T2mx = 0.038\ W^{0.44}\ (p(h)/p)^{0.36}, \text{ if Hb higher than 15 Kft} \quad (13)$$

where T2mx is the time of second thermal maximum (s),
W is the weapon yield (KT),
p(h)/p is the atmospheric density ratio as a function of height.

The time of second thermal maximum is stored in the weapon data set WEPD and module TPULSE is exited. Figure 8 shows WEPD as it was initiated and contained only user specified data. Figure 11 shows WEPD after execution of TPULSE, when it has been augmented by inclusion of the calculated variables T2mx and the ID number of the tract containing ground zero.

3.2 INITIAL BLAST PARAMETERS.

Blast wave parameters are of interest for estimating the quenching effect of blast wave passage on primary ignitions, the interaction of the blast wave with structures, structure contents, and primary ignitions in producing secondary ignitions, and the loss of structural integrity due to blast damage.

Research into quenching of primary ignitions by blast wave passage (Reference 6) is just beginning to produce results that can be used to develop a predictive model. A predictive model has been developed (Reference 7) for secondary ignitions resulting from blast wave interaction with structures and their contents. On-going work is expected to refine both the secondary ignition model, and the data it uses. Additional information is required on the effects of low level blast parameters on structural integrity, and the effect of loss of structural integrity on building burning characteristics.

Calculation of blast wave parameters are performed by module INitial BLaST, which is shown in Figure 12. Blast wave parameter calculations are based on the data presented in Reference 4 on pages 109 to 121, together with the scaling rules presented in Reference 4 on pages 100 to 105.

Upon entry to module INBLST, pressure, distance, and time scaling data are obtained from the blast atmospheric data (BLASTD). BLASTD provides altitude scaling factors at several altitudes between sea level and 150,000 feet. These data were obtained from Reference 4, p. 104, is invariant, and has been hard coded into the module. Data are obtained from BLASTD for altitudes above and below the altitude of interest. Pressure, distance and time scaling factors are then calculated at the altitude of interest by interpolating on these data.

Data file RRAD (Figure 11) is accessed to obtain the irradiance calculation ranges that were used in module TPULSE. Blast wave parameters are calculated at the same set of ranges that were used for calculating irradiance. As in the case of irradiance, blast parameters are modeled for demonstration as functions only of distance from ground zero.

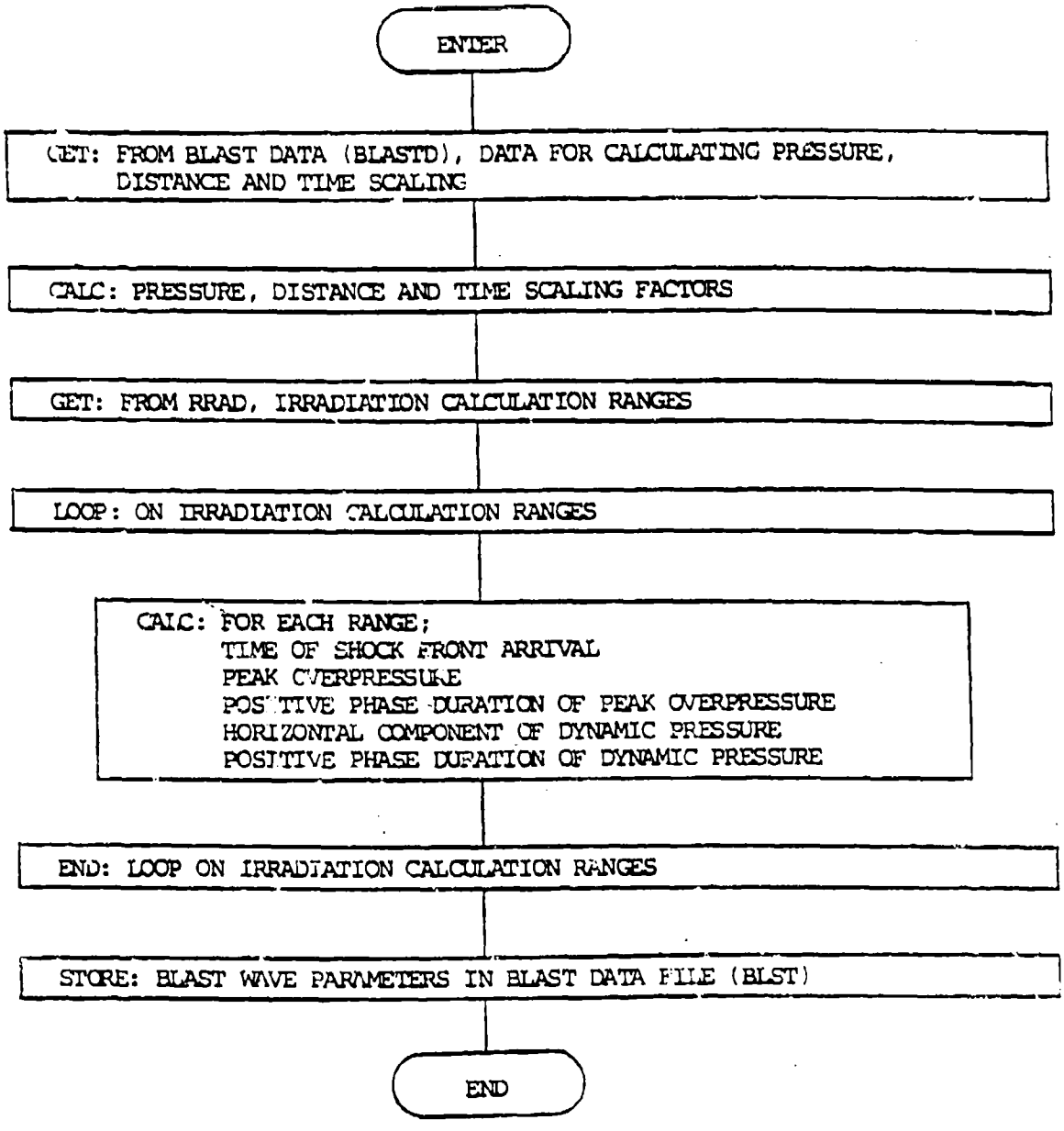

Figure 12. Logic flow diagram for module INBLST.

The blast wave parameters are calculated at each irradiance calculation range and stored in the blast data file BLST, which is shown in Figure 13.

3.3 WIND MODULE (WNDMOD).

The description of this module is included in the description of the combustion and propagation models.

3.4 PRIMARY IGNITIONS MODULE (IGNITE).

The primary ignitions module IGNITE uses the irradiance calculated by module TPULSE and the calculated tract characteristics shown in Figure 9 to calculate probabilities of room and structure ignition, and subsequent flashover. Module IGNITE is divided into two parts; a part that calculates global ignition (GLBIGN) variables, and a part that calculates tract ignition (TRTIGN) variables.

Ignition related calculations that apply to all tracts and occupancy classes are performed by submodule GLBIGN in order to set up global probability distribution of the irradiance of window coverings and of room furnishings as a function of selected variables. Ignition related calculations that apply to each tract and to the occupancy classes it contains are performed by submodule TRTIGN in order to establish probability distributions of room ignitions, structure ignitions, and structure flashovers.

3.4.1 Global Ignition Calculations (GLBIGN).

The thermal irradiance of window coverings and room furnishings is calculated at each of the irradiance (and blast) calculation ranges relative to ground zero. These results will be used in TRTIGN to determine the irradiance of window coverings and room furnishings in each tract, taking into account tract geometry, shadowing, etc. By using the global calculations, the window covering and room furnishing irradiance calculations are only performed for five to ten ranges from ground zero, instead of for each of potentially several hundred tracts.

A simplified calculation of window covering and room furnishing irradiance is used for demonstration. The radiation source is assumed to lie on, and be perpendicular to, the line connecting the window center and the radiation circle center, as shown in Figure 15. Later, in TRTIGN, a correction is made to these results to account for orientation of the building with respect to the radiation source. A more detailed calculation in GLBIGN would include a loop over several azimuth angles. These data could then be interpolated in TRTIGN to obtain irradiance as a function of building orientation.Module GLBIGN is shown in Figure 14. Upon entry to GLBIGN the following data are accessed:

The radiation data calculated by module TPULSE and stored in data file RRAD (Figure 11),

The blast data calculated by module INBLST and stored in data file BLST (Figure 13),

The user defined weapon data stored in data file WEPD (Figure 11).

Weapon (detonation) ID number

Weapon detonation time (s)

Number of ranges for blast calculations

Time of shock front arrival (s)
Peak overpressure (kg/m^2)
Positive phase duration of overpressure (s)
Horizontal component of dynamic pressure (kg/m^2)
Positive phase duration of dynamic pressure (s)

Figure 13. Blast wave parameter data (BLST).

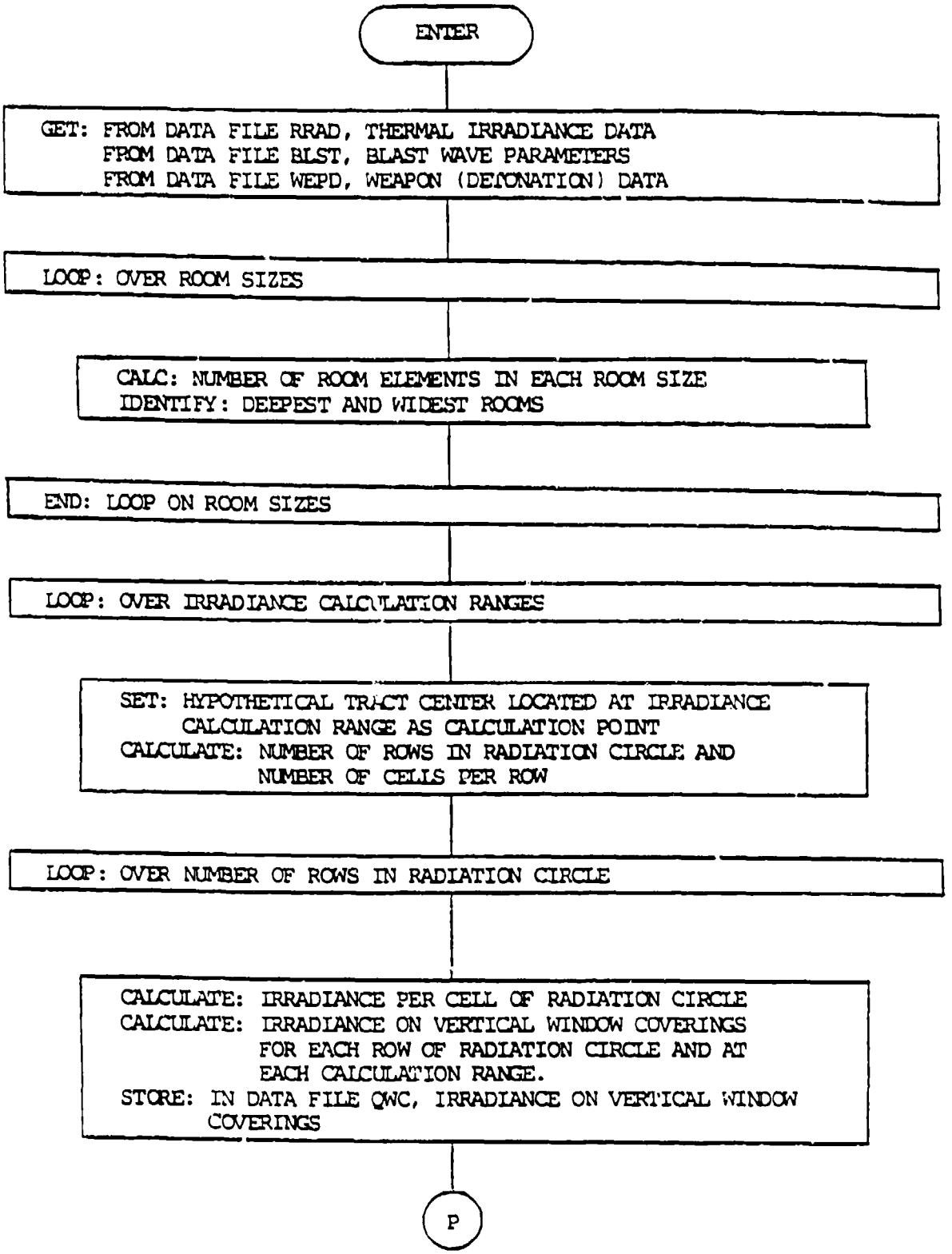

Figure 14. Logic flow diagram for submodule GLBIGN.

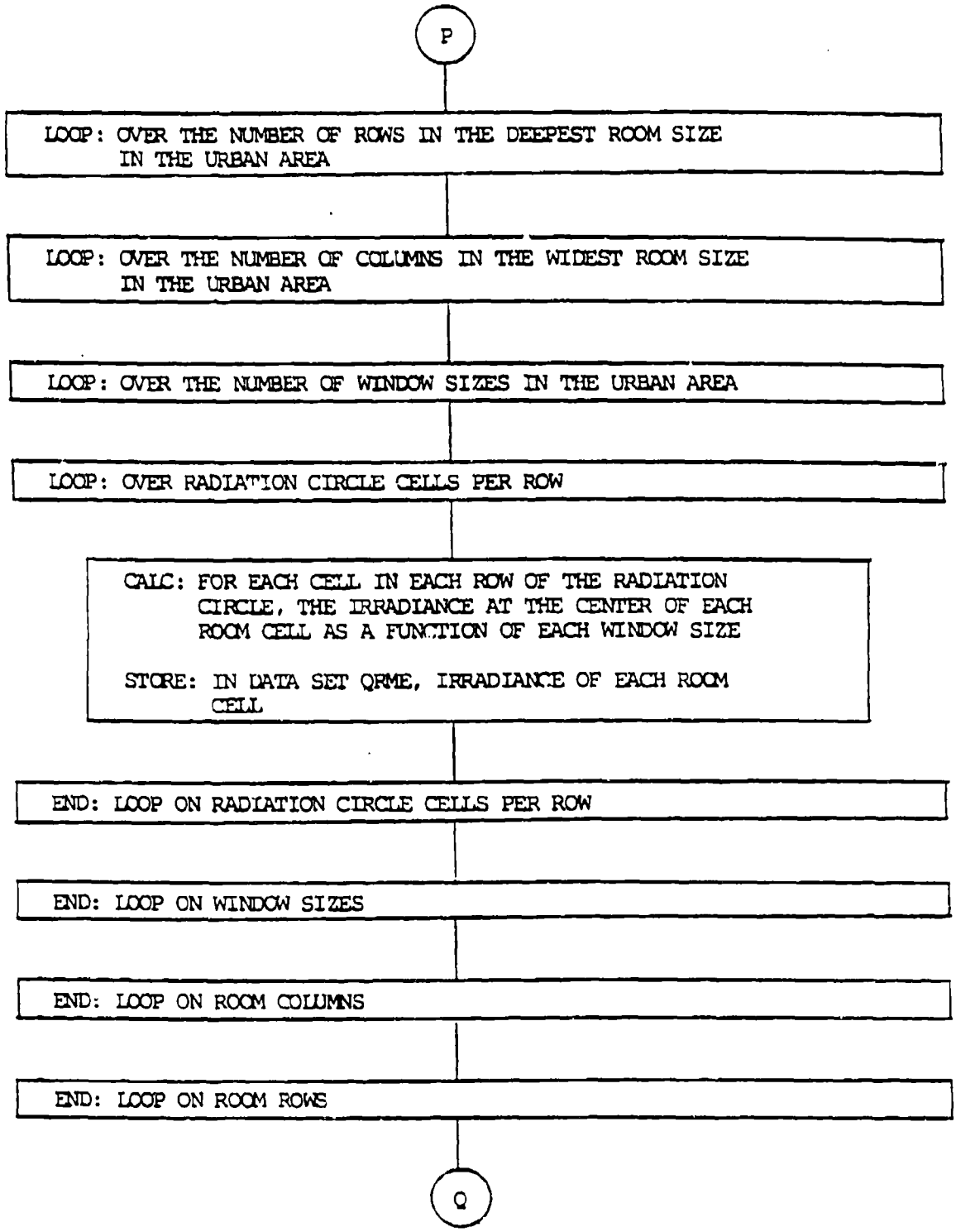

Figure 14. Logic flow diagram for submodule GLBIGN (continued).

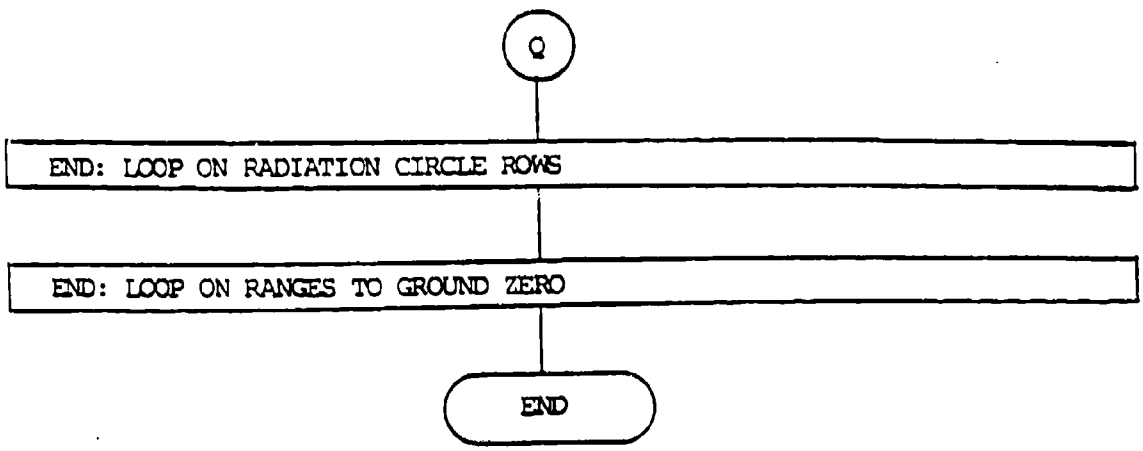

Figure 14. Logic flow diagram for submodulc GLBIGN (continued).

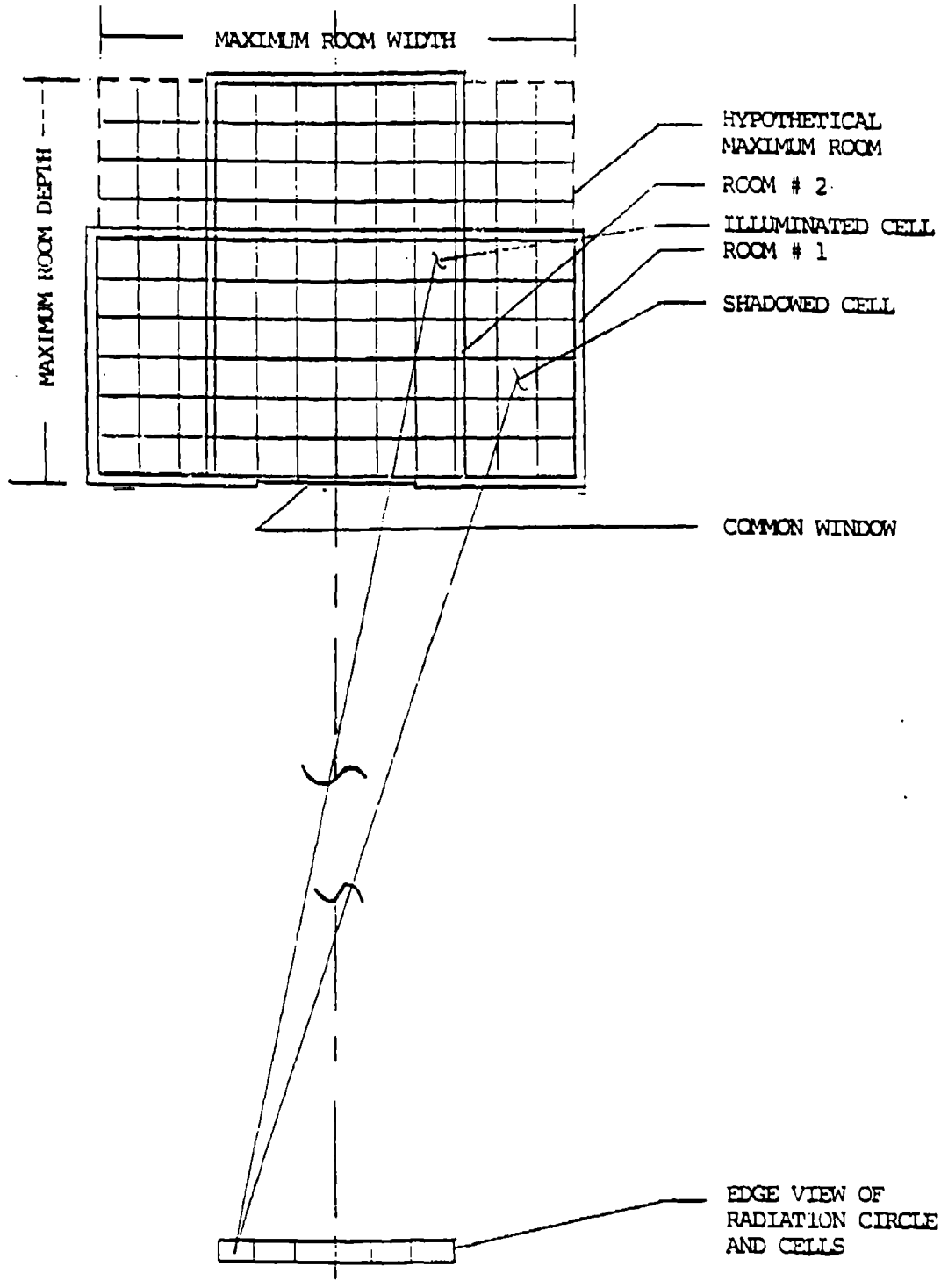

Figure 15. Irradiance geometry for room cells of two nested rooms.

Each room size used in the urban area description is partitioned into elements, and the number of rows and columns of elements are identified in the deepest and widest rooms, respectively. For calculation of room cell irradiance, all rooms are assumed to be nested about the center of a window which faces the center of the radiation circle. The window is oriented perpendicular to the line connecting the center of the window with the center of the radiation circle, as shown in Figure 15. The irradiance of each room cell is calculated for one hypothetical room whose width and depth are equal to those of the widest and deepest rooms used in the urban area.

A loop is formed over the irradiance calculation ranges that were used in TPULSE to calculate the free field irradiance data stored in RRAD (Figure 11).

The radiation circle is partitioned into rows and columns by specifying the number of elements to appear in the first row. The number of rows and number of elements per row are then calculated from the number of elements in the first row and the radiation circle radius, as shown in Figure 16. Partitioning the radiation circle allows inclusion of the effects of partial radiation circle visibility on the probability of room ignition. The necessity for this can be shown by considering the fireballs from 1 MT and 10 MT bombs detonated at heights that maximize their 2 psi overpressure radii. At the 2 psi overpressure radius, the radiation circle will subtend about 18 degrees for the 1 MT weapon, and about 54 degrees for the 10 MT weapon. These are not extreme conditions, but represent a range of cases that might require from slight to significant levels of radiation circle partitioning.

A loop is formed over the number of rows in the radiation circle. Assuming uniform radiation circle irradiance, the irradiance of each row is calculated from the total number of elements per row. The irradiance of vertical window coverings is calculated at each irradiance calculation range, and accumulated for each number of radiation circle rows (from top to bottom of the radiation circle). These calculations assume no shadowing, normal incidence in the horizontal plane, and vertical incidence as defined by range from ground zero and detonation height.

The resulting window covering irradiance data are stored in the two dimensional array,

QWC(RGZ, NROWS)

where

RGZ is the range from ground zero, and
NROWS is the number of radiation circle rows used.

Loops are formed over the number of rows in the deepest, and the number of columns in the widest rooms used in the urban area.

Loops are formed over the number of window sizes used in the urban area and the number of radiation circle cells in the row under evaluation.

For each irradiance calculation range and each row of the radiation circle, the irradiance of vertical room furnishings is calculated in each room cell as a function of each window size. In the case of room furnishings, the irradiance from each radiation circle cell must be examined because of different degrees of horizontal shadowing by the different window sizes. Vertical window shadowing is accounted for by radiation circle rows. The possibility of shadowing is determined by testing whether or not the center of each radiation circle cell is visible from the center of each room cell.

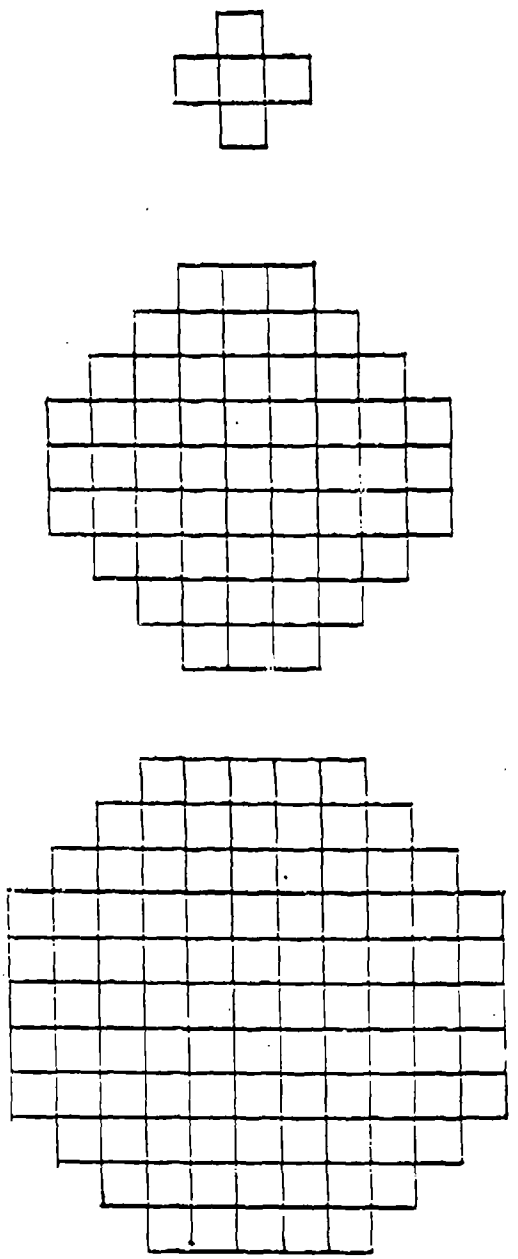

NUMBER OF CELLS IN:		
FIRST ROW	MAX. ROW	TOTAL
1	3	5
3	7	37
5	11	97

Figure 16. Radiation circle partitioning.

The room cell irradiance is stored in the five dimensional array,

QRME(RGZ, NROWS, ROWRM, COLRM, WNDSIZ)

where

ROWRM, COLRM are the coordinates of the room cell, and
WNDSIZ is the window size.

The successive loops over radiation circle cells per row, window sizes, room columns, room rows, radiation circle rows, and ranges to ground zero are closed. Upon completion of all the loops, module GLBIGN is exited.

3.4.2 Tract Ignition Calculations (TRTIGN).

The tract ignition calculation module makes use of global, occupancy class, and tract characteristics, together with calculated irradiance data to estimate the number of buildings that will be ignited in each tract.

Upon entry to submodule TRTIGN, shown in Figure 17, the following data are initialized in the form of data statements:

A data set which specifies the probability of a room fire occurring given ignition of window coverings (RFWCI),

A data set which specifies the probability of room furnishings being in each room cell (FRFRC),

A data set which specifies the probability of a room fire occurring given ignition of window coverings (RFRFI),

A data set specifying the probability of building flash over given flash over of at least one room in the building (FBFO).

These data sets will be described in the following discussions of the parts of the module where they are used. Weapon and detonation data are obtained from data file WEPD (Figure 11), and thermal irradiance data at specified ranges from ground zero are obtained from data file RRAD (Figure 11).

A loop is established over all of the tracts in the urban area, and a file is generated containing all of the tracts whose centers lie within the effects calculation annulus. The effects calculation annulus is defined by the user specified minimum and maximum effects ranges (see WEPD, Figure 11).

A loop is formed over all of the tracts in the effects calculation annulus. At label (P) the tract center coordinates and tract occupancy classes are obtained from the tract and vertex data (Figure 4). The tract characteristics (Figure 9) are accessed to obtain distributions of the tract ignition descriptors.

The vertical, horizontal and slant ranges are calculated from the tract center to the detonation point. The horizontal range from tract center to ground zero is used to interpolate the irradiance data of RRAD (Figure 11) and the blast parameters of BLST (Figure 13) to the center of the subject tract.

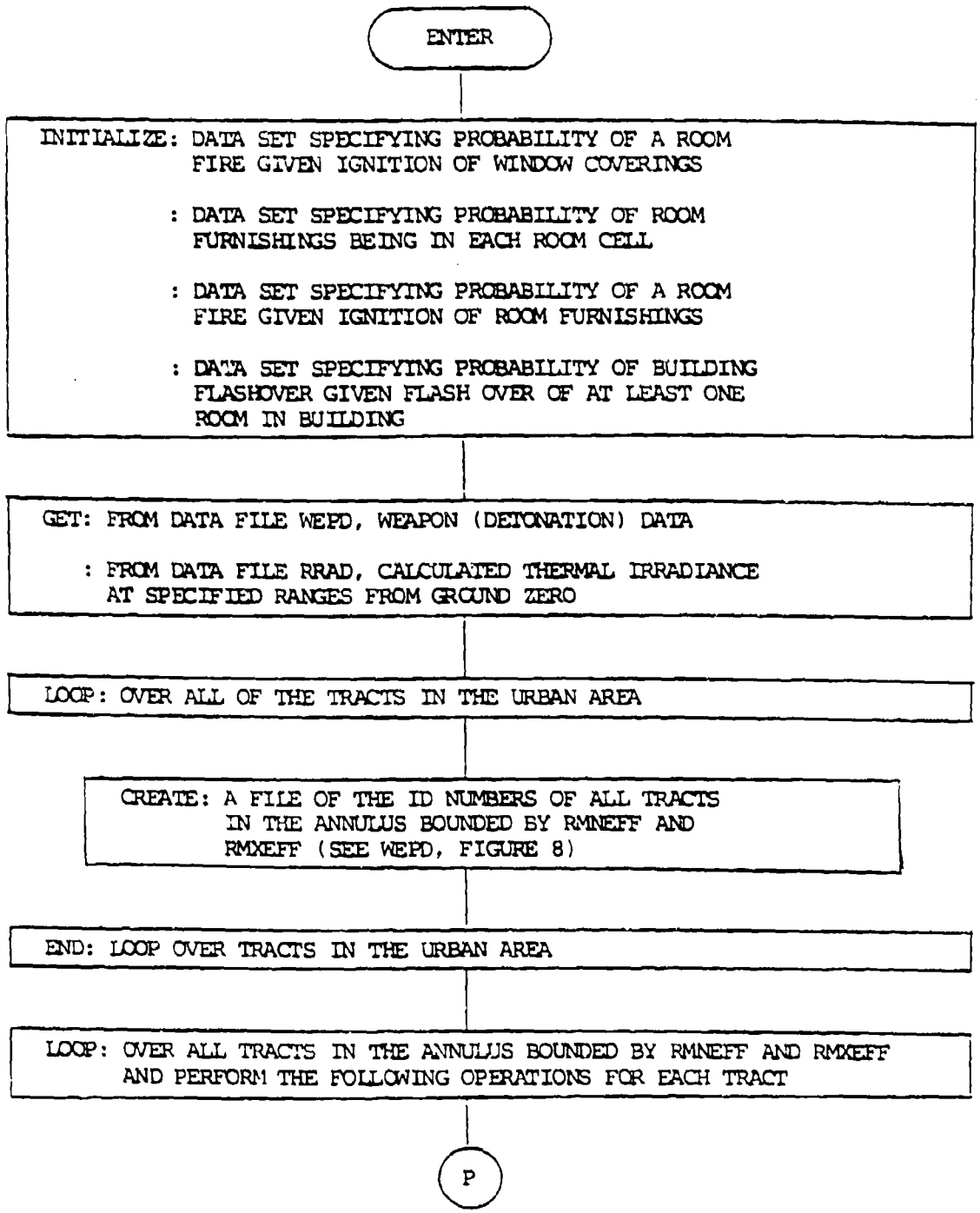

Figure 17. Logic flow diagram for submodule TRTIGN.

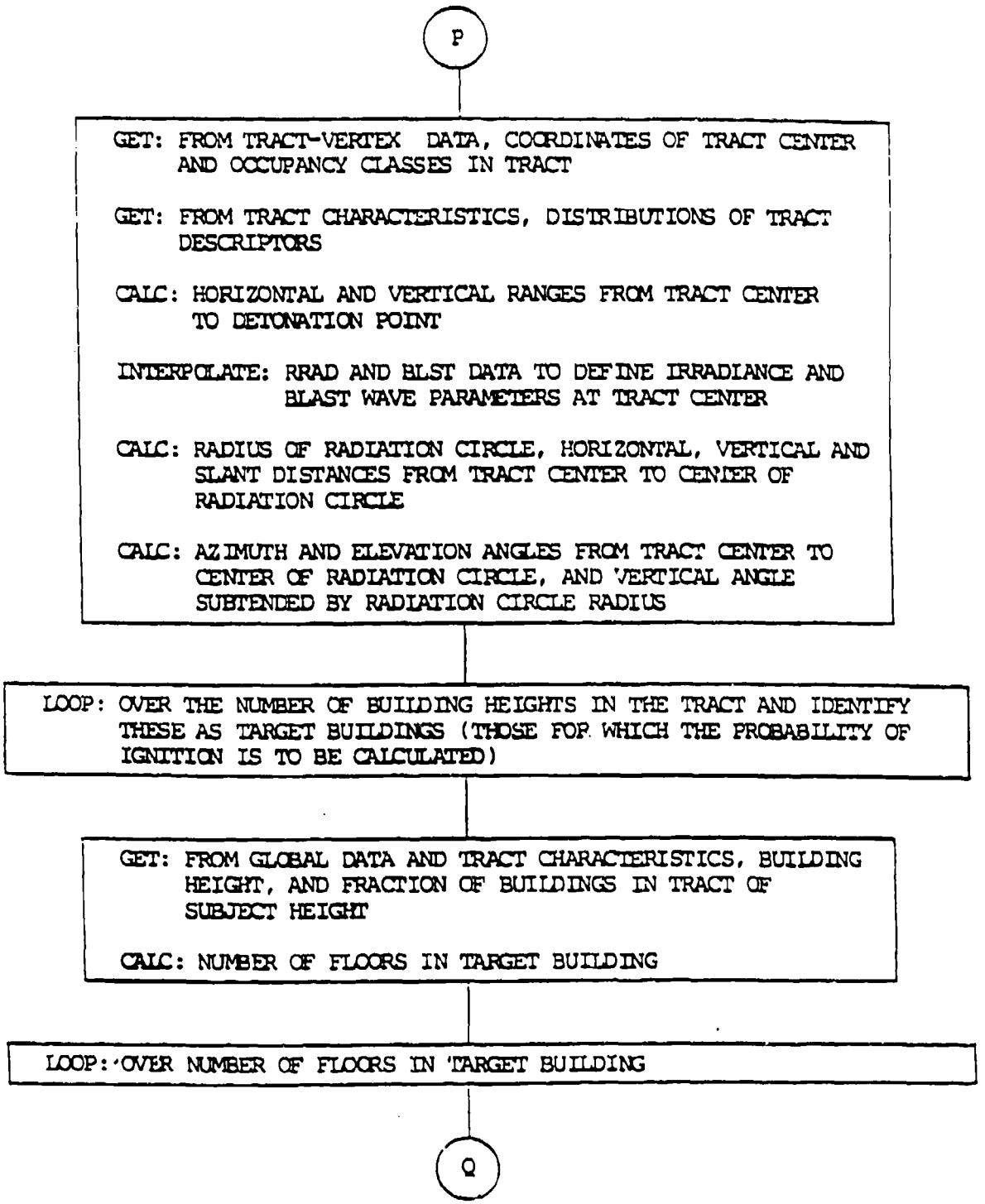

Figure 17. Logic flow diagram for submodule TRTIGN (continued).

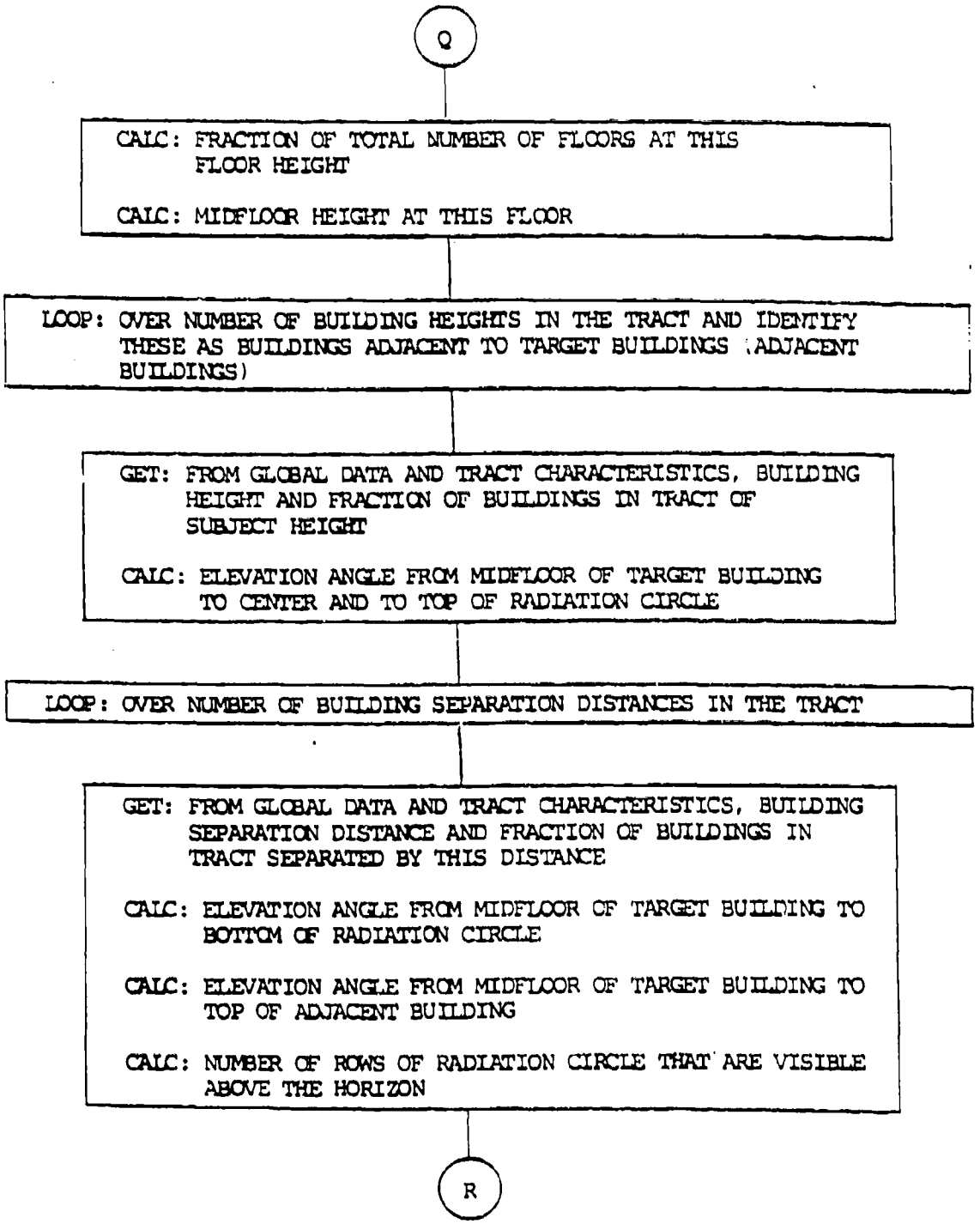

Figure 17. Logic flow diagram for submodule TRTIGN (continued).

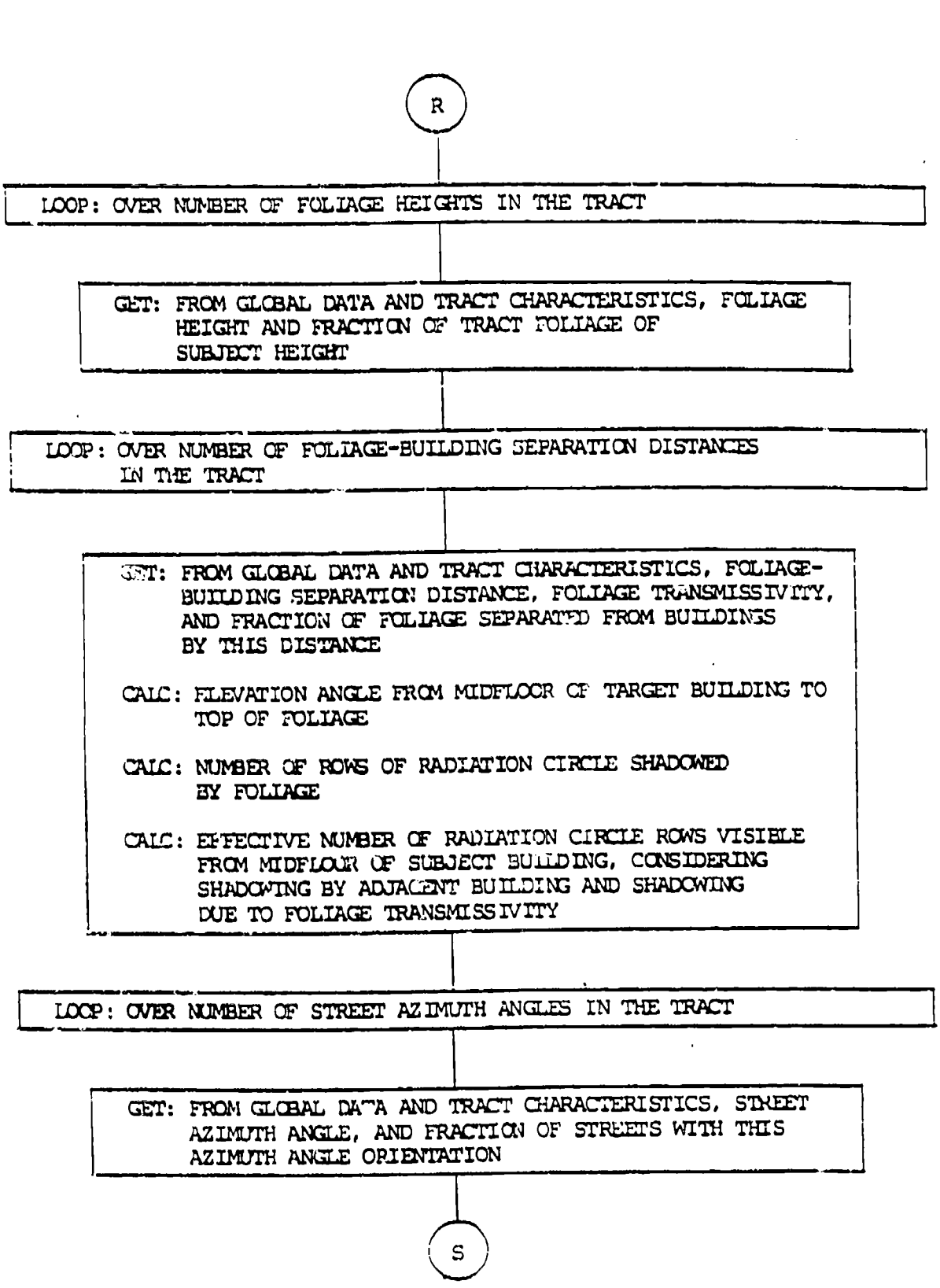

Figure 17. Logic flow diagram for submodule TRTIGN (continued).

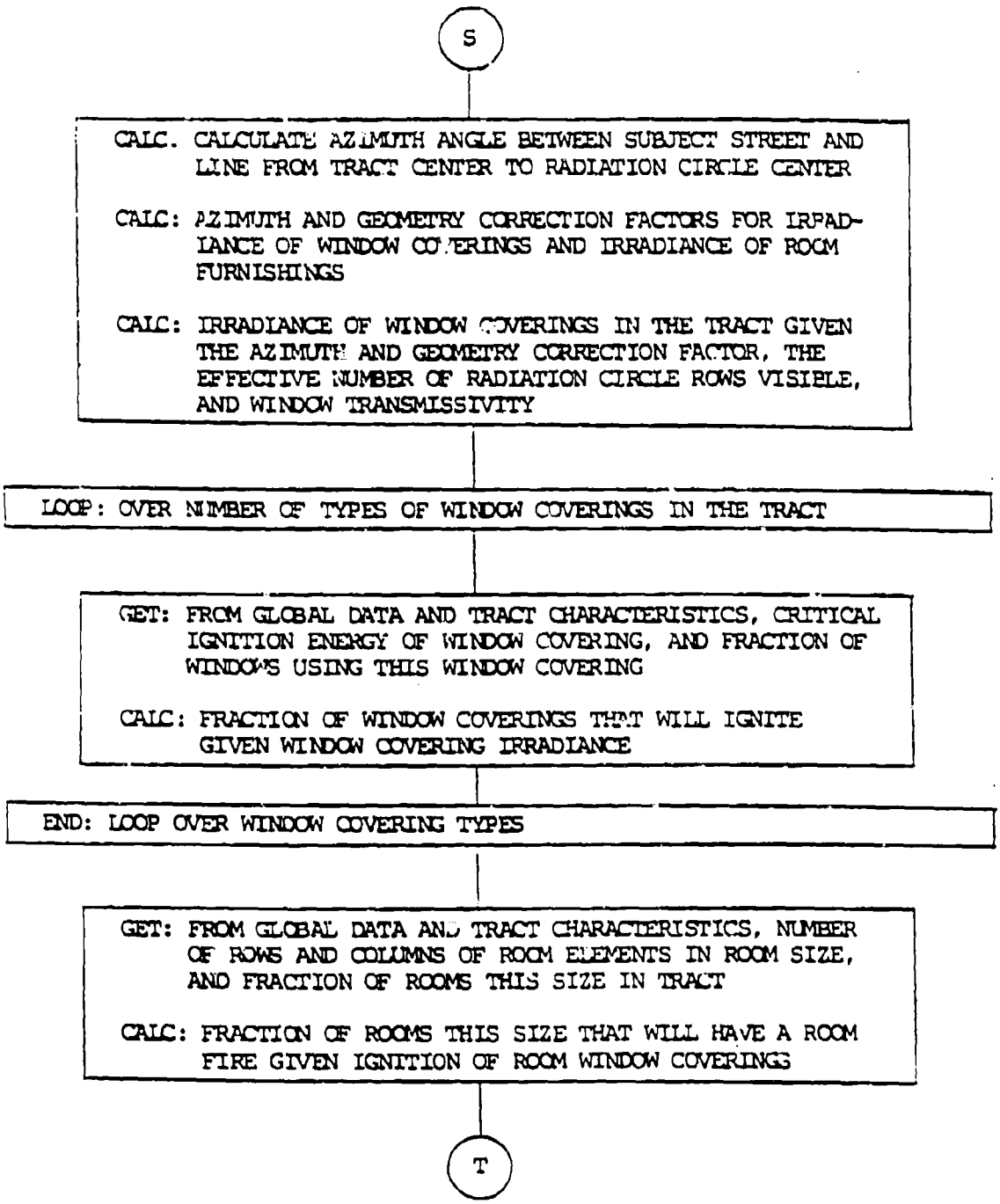

Figure 17. Logic flow diagram for submodule TRTIGN (continued).

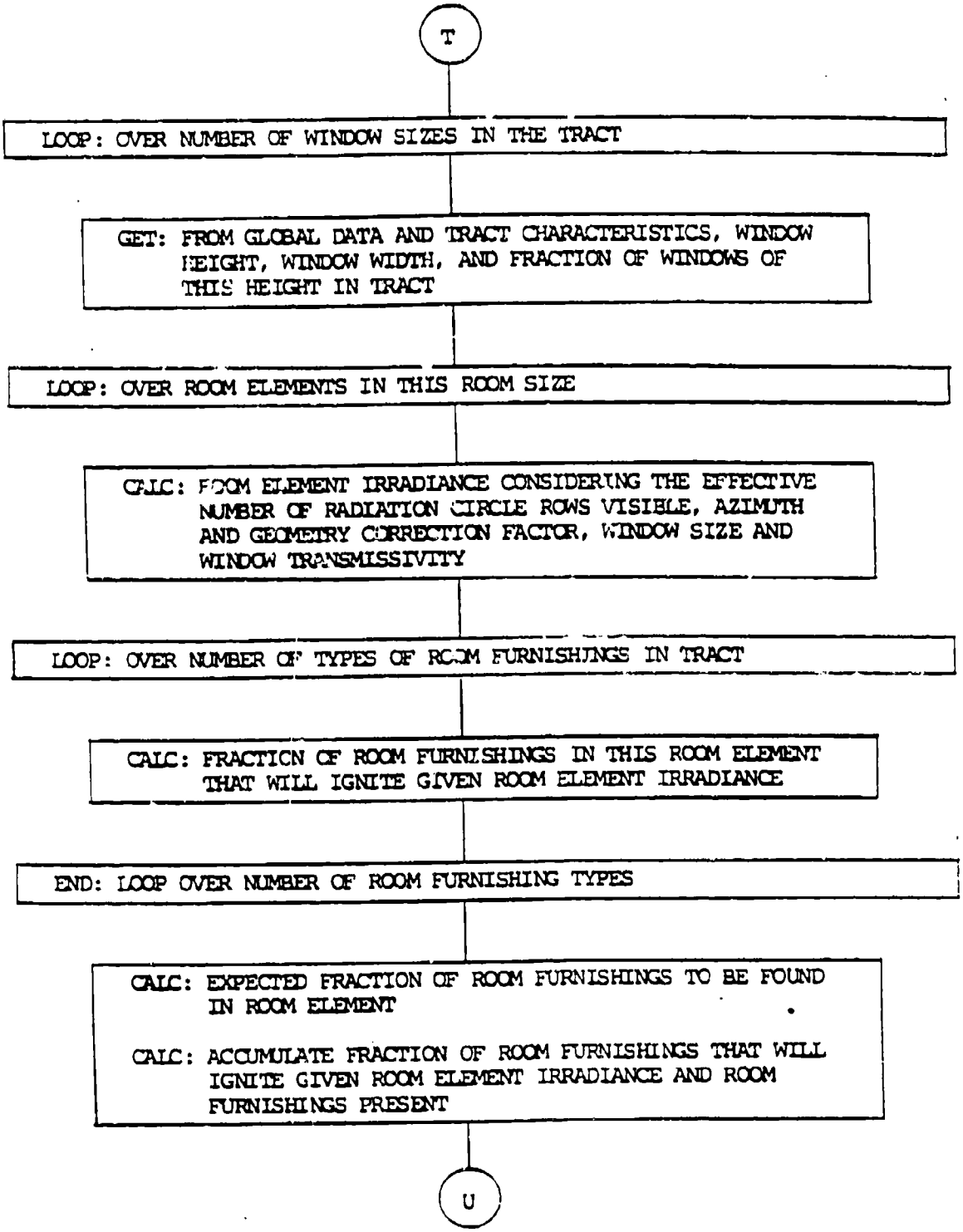

Figure 17. Logic flow diagram for submodule TRTIGN (continued).

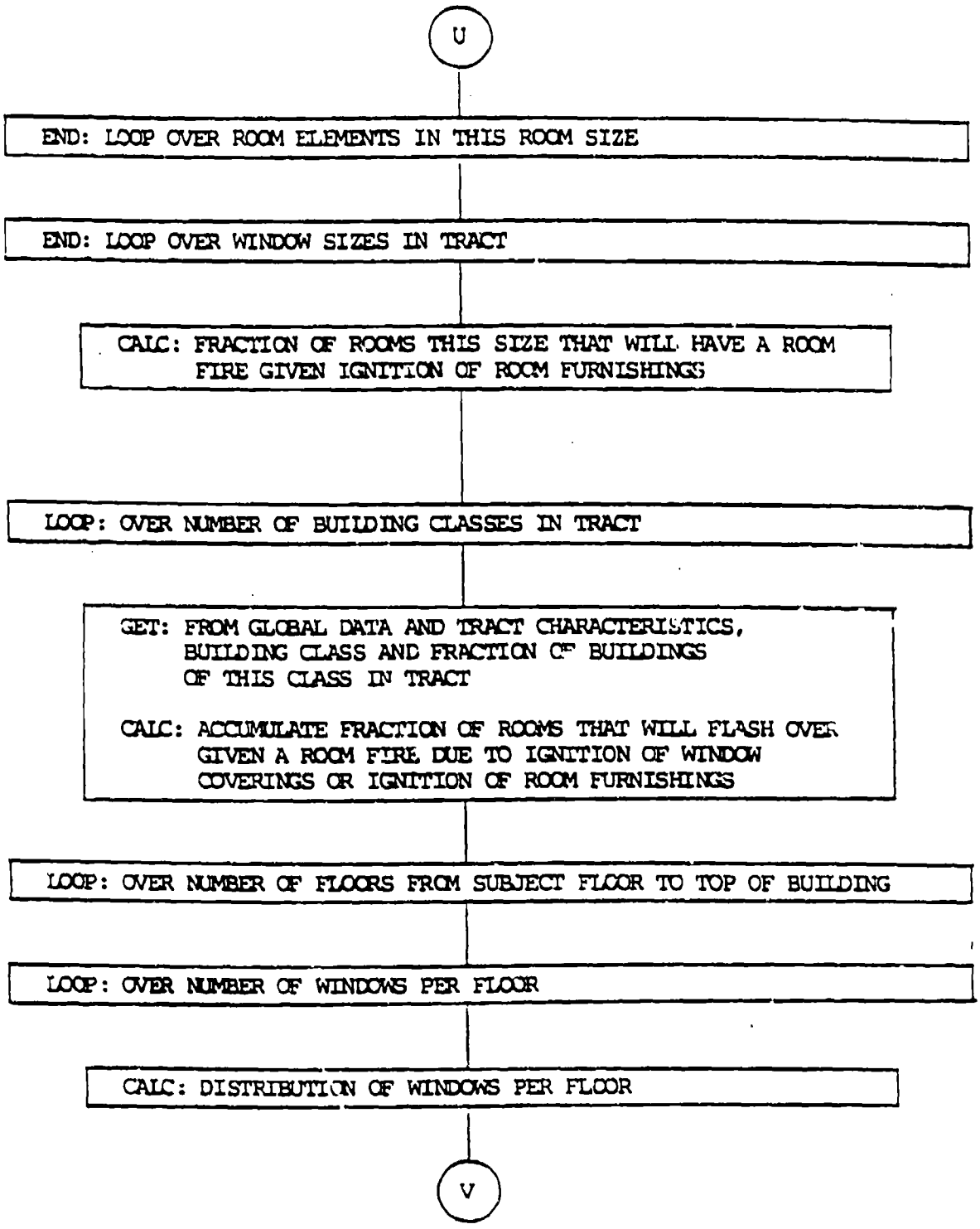

Figure 17. Logic flow diagram for submodule TRTIGN (continued).

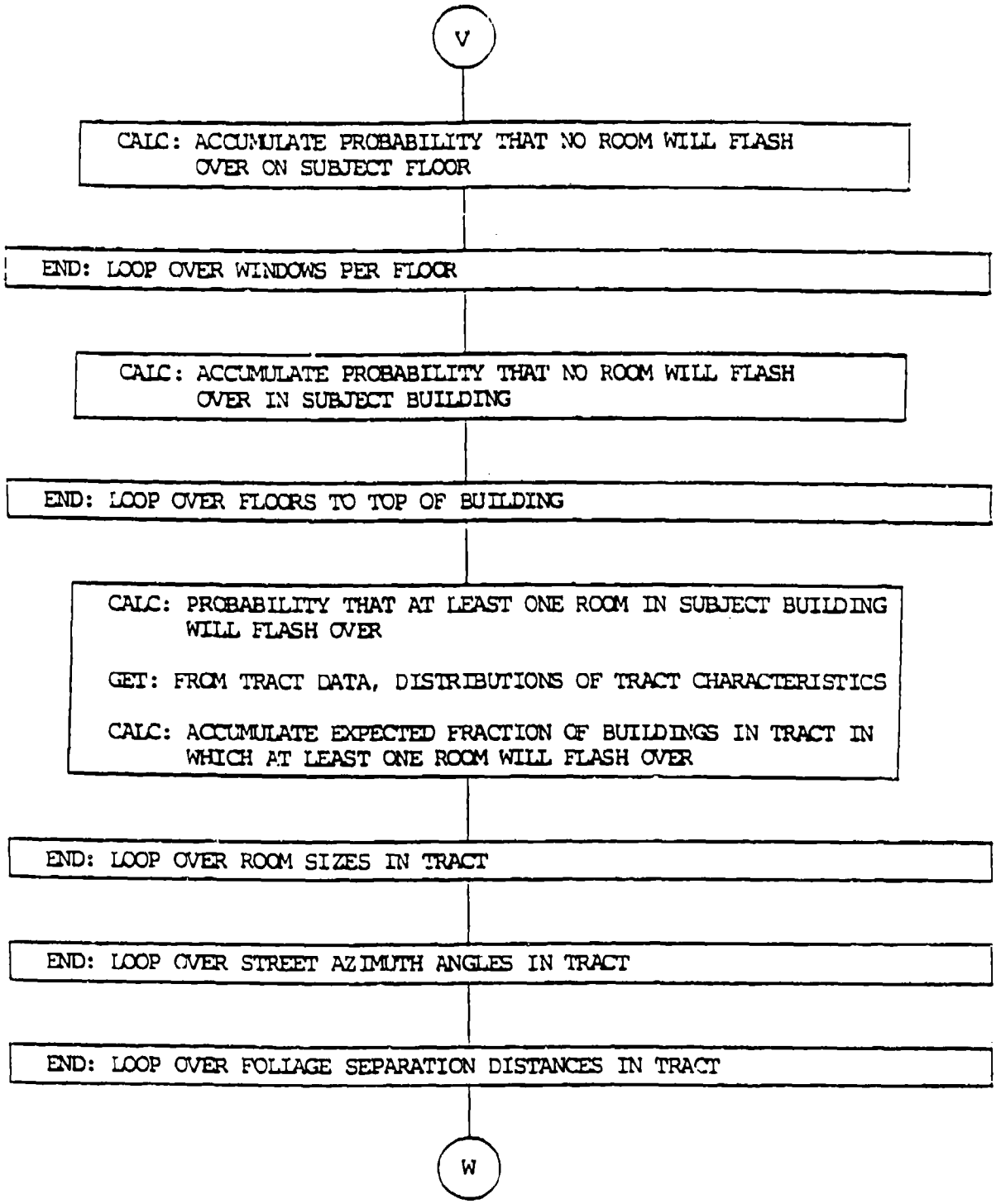

Figure 17. Logic flow diagram for submodule TRTIGN (continued).

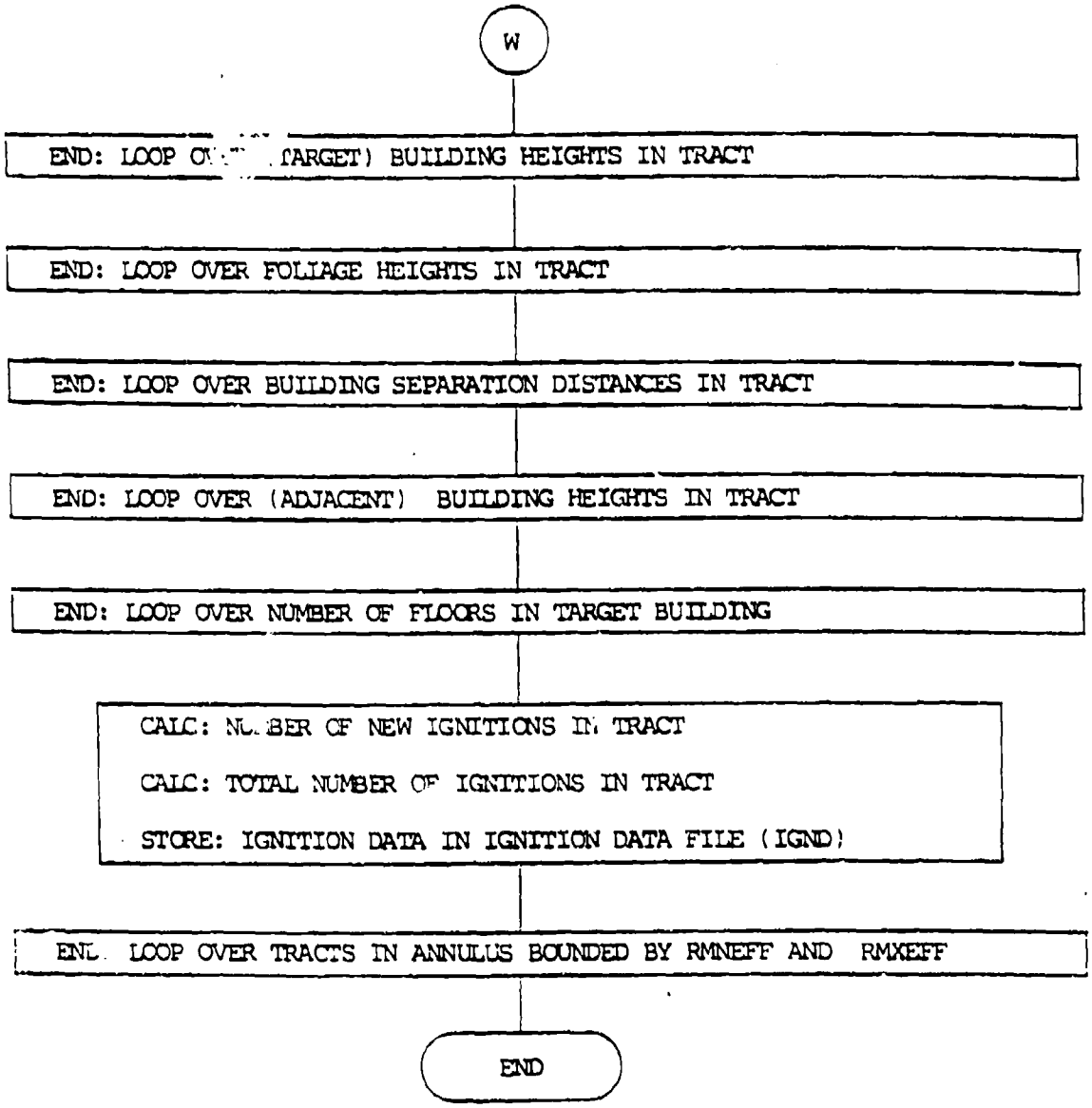

Figure 17. Logic flow diagram for submodule TRTIGN (continued).

The radius of the radiation circle, as viewed from the tract center, together with the vertical and horizontal distances between the tract and radiation circle centers are calculated from (9) through (11).

The azimuth and elevation angles from the tract center to the center of the radiation circle, and the vertical angle from the center to the top of the radiation circle are calculated as shown in Figure 18. The radiation circle is assumed to be normal to the line connecting its center with the tract center. However, windows, window coverings, room furnishings, etc. are not assumed to be oriented normal to the radiation circle-tract centerline.

A loop is formed over the heights of the buildings in the tract. These buildings are identified as the buildings for which the probability of ignition is to be calculated (i.e. target buildings). The global building height data (Figure 5) are accessed using the tract building height data (Figure 9) to quantify the tract building heights. The tract building height data includes the ID numbers of the global tract building heights that are found in the subject tract. Given the building height ID number, the building height is obtained from the global building height data. The presence of all tract descriptors is identified in the tract characteristics data (Figure 9) by the appropriate global ID number. Tract descriptor quantitative data are obtained by entering the global data with the ID number. This procedure is repeated in accessing each of the tract characteristics (Figure 9) data sets.

The number of floors in the target building is calculated from the building height and the specified floor height. One floor height has been specified. In practice, a floor height could be specified for each occupancy class.

A loop is formed over the floors of the subject target building (height). At label (Q) the midfloor height and the fraction of buildings in the tract having this number of floors is calculated. In practice, the fraction of buildings in the tract with this number of floors would be obtained from an empirically based data table. The irradiance of room furnishings is calculated in a plane at the midfloor height. The midfloor height is used here, although the reference plane can be placed at any desired fraction of the floor height.

A loop is formed over the number of building heights in the tract, and the subject buildings are identified as the buildings adjacent to target buildings (adjacent buildings). The adjacent building heights and fractions of adjacent buildings in the tract of each height are obtained from the tract characteristics and the global data.

The elevation angles are calculated from midfloor of the target building to the center and to the top of the radiation circle as shown in Figure 19. In Figure 19 it is assumed that the target building is located at the tract center. All of the building-related calculations assume that the part of the structure for which calculations are being made is also located at the tract center. The tract calculations, in general, assume that the effects of distance from the detonation point on blast and thermal radiation parameters can be adequately accounted for by a calculation at each tract center. That is, the variation over the dimensions of each tract is assumed to be small. Under this assumption, distance variations over structures within tracts can certainly be considered insignificant.

It may be of interest at some time to describe the distributions of the blast and thermal irradiance parameters over each tract. This can be easily done, given the values of the parameters at the tract centers and the extent of each tract in terms of its vertex locations.

R_{rc} = radiation circle radius

D_v = vertical distance from tract center to radiation circle center

D_h = horizontal distance from tract center to radiation circle center

D_s = slant distance from tract center to radiation circle center

E_1 = elevation angle from surface at tract center to radiation circle center

E_2 = elevation angle from surface at tract center to top of radiation circle

E_3 = elevation angle from surface at tract center to bottom of radiation circle

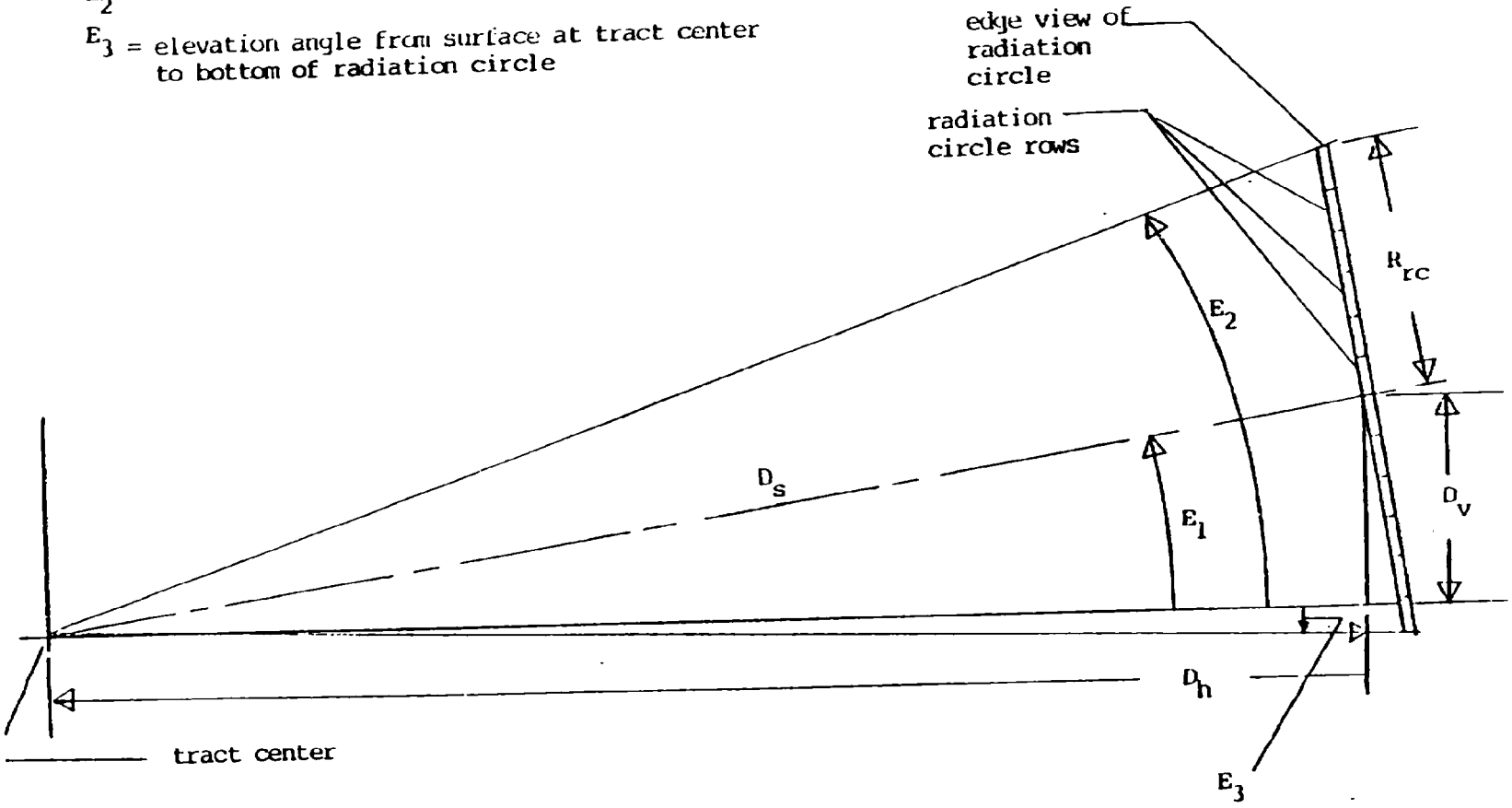

Figure 18. Geometry of radiation circle from tract center.

H_{mf} = midfloor height in building at tract center

E_1' = elevation angle from midfloor height at tract center to radiation circle center

E_2' = elevation angle from midfloor height at tract center to top of radiation circle

E_3' = elevation angle from midfloor height at tract center to bottom of radiation circle

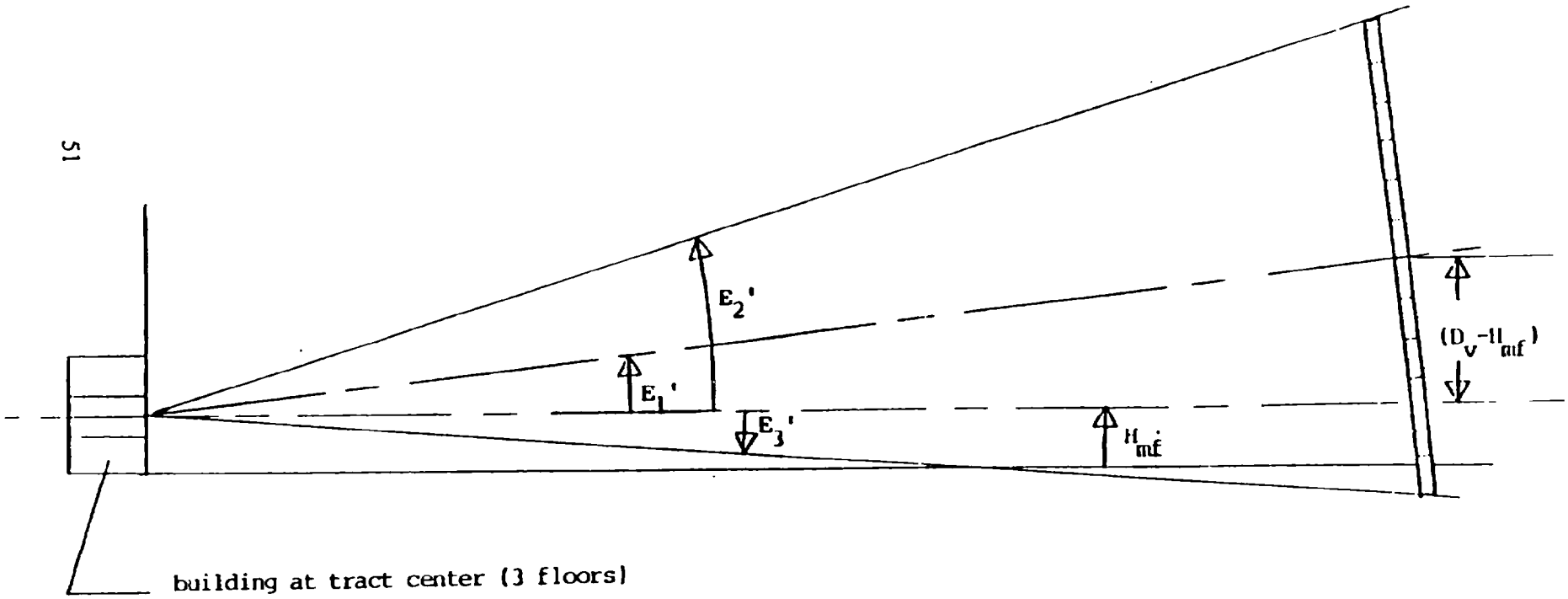

Figure 19. Geometry of radiation circle from midfloor of building at tract center.

A loop is formed over the number of building separation distances in the tract. The building separation distances and the fractions of buildings in the tract separated by those distances are obtained from the tract characteristics and global data sets. The elevation angles are calculated from midfloor of the target building to the top of the adjacent building as shown in Figure 20, and to the bottom of the radiation circle using the geometry of Figure 19. The number of radiation circle rows that are visible above the horizon is calculated using the geometry of Figure 19, the vertical extent of the radiation circle that is visible, and the number of rows defined for the radiation circle

At label (R) a loop is formed over the number of foliage heights in the tract. The foliage heights, transmissivities, and the fractions of foliage in the tract of those heights are obtained from the tract characteristics (Figure 9) and global (Figure 5) data sets.

A loop is formed over the number of foliage-building separation distances in the tract. The foliage-building separation distances and the fractions of foliage separated from buildings by those distances are obtained from the tract characteristics (Figure 9) and global (Figure 5) data sets.

The number of rows of the radiation circle that are shadowed by foliage is calculated using the geometry of Figure 20 where the foliage is treated as a non-opaque adjacent building. The effective number of radiation circle rows visible (Nre) considering shadowing by adjacent buildings and foliage is given by

$$Nre = Nrv - (Nsb + Tf\ Nsf) \qquad (14)$$

where Nrv is the number of radiation circle rows visible,
Nsb is the number of radiation circle rows shadowed by the adjacent building,
Tf is the foliage transmissivity,
Nsf is the number of radiation circle rows shadowed by foliage.

A loop is formed over the number of street azimuths in the tract. The street azimuth angles and the fraction of streets in the tract at those azimuth angles is obtained from the tract characteristics and global data sets. The angle is calculated between the subject street azimuth and a line from tract center to the radiation circle center.

Correction factors are calculated for the irradiance of window coverings (CFwc) and room furnishings (CFrf) to account for the effects of building orientation and geometry. Three representative building shapes are shown in Figure 21; (1) narrow and deep, (2) wide and shallow, and (3) square. Building orientation is defined in terms of the azimuth angle (A) between the incident radiation (Io) and the front face of each building. The building front face is assumed normal to the subject street. Each exterior room of each building is assumed to have a window in each exterior wall. Thus, the correction factors will be symmetrical about normal incidence of radiation on the front face of the building.

S = separation distance between adjacent building or foliage and target building
H_{ab} = height of adjacent building (or foliage)
E_4 = elevation angle from midfloor of building at tract center to top of adjacent building (or foliage)

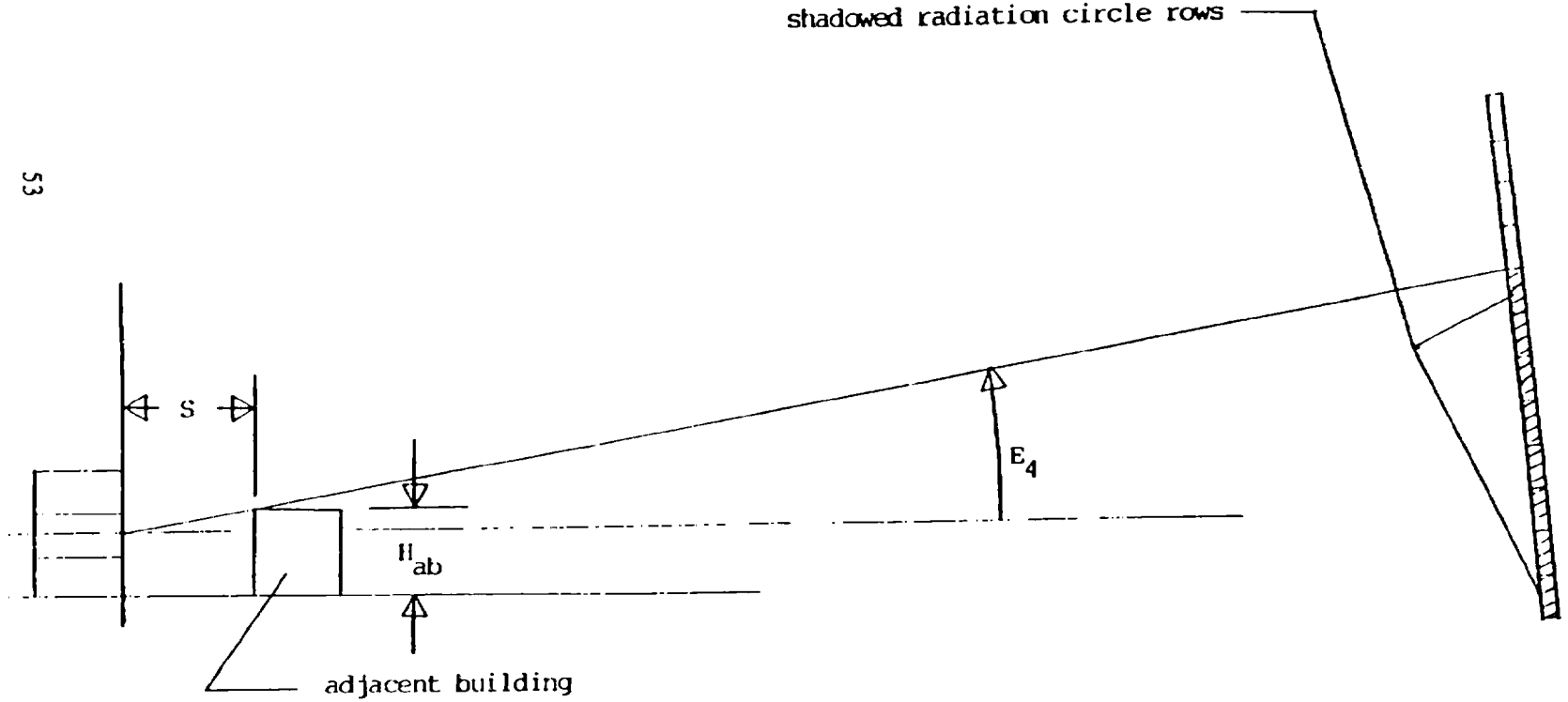

Figure 20. Geometry of radiation circle shadowing by adjacent buildings or foliage.

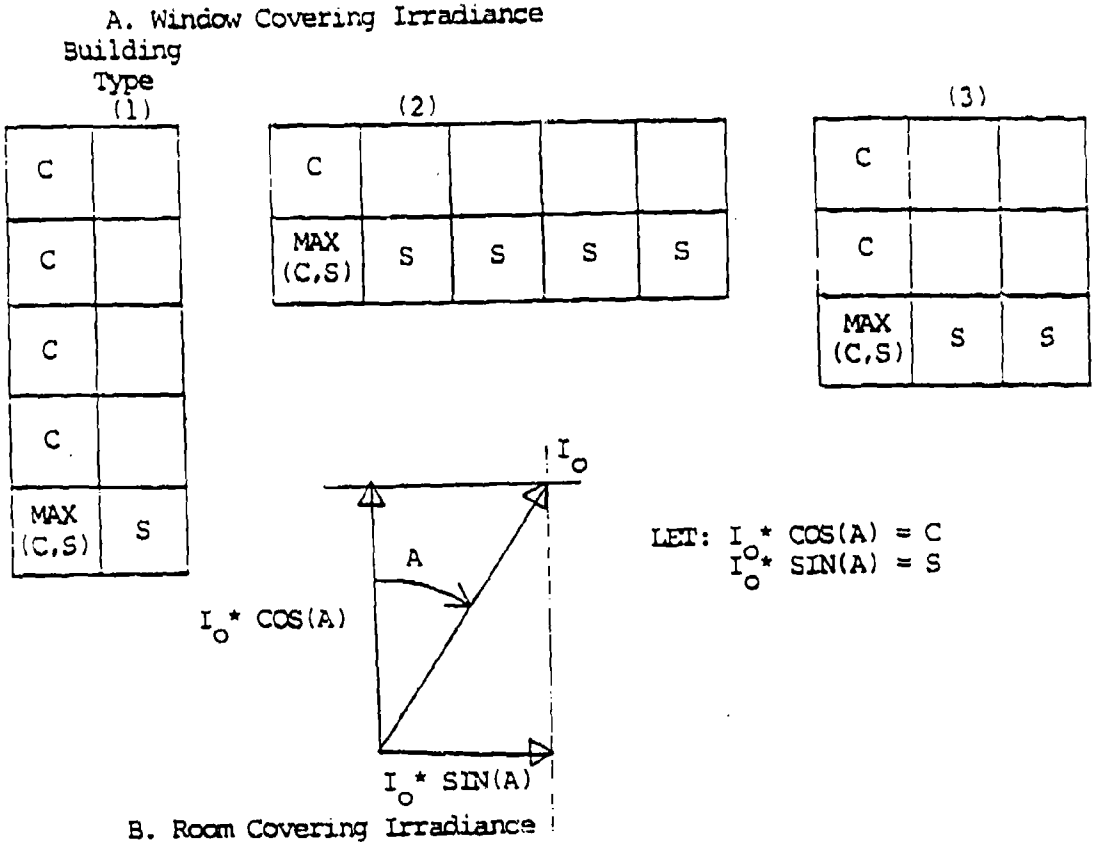

Figure 21. Geometry of room and building irradiance.

Figure 21-A shows the effective irradiance of window coverings in each room of each building type. Only one set of window coverings per room are considered. Thus, in those cases where two windows are irradiated the maximum irradiation is taken. Figure 21-B shows the effective irradiance of room furnishings in each room of each building type. Room furnishing irradiance is taken as the linear combination of the irradiances from each window in those cases where two windows are irradiated.

Table 2-A shows the general form of the total window covering and room furnishing irradiances given in Figure 21. Also, these irradiances are tabulated for three different angles of radiation incidence. The total irradiances in Table 2-A are reorganized in Table 2-B, together with the average window covering and average room furnishing irradiances per room. These are averaged over building types for each angle of incidence, and averaged over angles of incidence.

From Table 2-B the correction factors for window covering and room furnishing irradiances are given by

$$CFWC \begin{cases} = 0.37\ COS(A), \text{ for } COS(A) .GE. 10\ SIN(A), \\ = 0.37\ SIN(A), \text{ for } SIN(A) .GE. 10\ COS(A), \\ = 0.29\ (COS(A) + SIN(A)), \text{ otherwise,} \end{cases} \quad (15)$$

and

$$CFrf = 0.34(COS(A) + SIN(A)). \quad (16)$$

At label (S) of Figure 17 the irradiance of window coverings at the tract center for the effective number of radiation circle rows visible (QWCI, is calculated by interpolating on the global window covering irradiance

QWC(RGZ, NROWS),

and correcting the interpolated value for window transmissivity, together with geometry and building type to obtain

$$QWCI = Tw\ CFwc\ QWC \quad (17)$$

where Tw is the window transmissivity.

A loop is formed over the number of window covering types in the tract, which are defined in terms of their critical ignition energy levels. The fraction of window covering types that will ignite (FWCI), given irradiance QWCI is calculated. The fraction of rooms of the subject size in the tract that will have a room fire, given ignition of window coverings is calculated from

Table 2. Building and room irradiance for example building types.

Let: $A \gg B \rightarrow B \approx A/10$

A. Total Irradiance as a Function of Building Type and Geometry

Bldg. Type	Geom. Case	Total for Building Type	
		Window Coverings	Room Furnishings
1		4*C + S + MAX(C,S)	5*C + 2*S
	C ≫ S	5.2*C	5.2*C
	S ≫ C	2.4*S	3*S
	C ≈ S	6*(C+S)/2	7*(C+S)/2
2		C + 4*S = MAX(C,S)	2*C + 5*S
	C ≫ S	2.4*C	3*C
	S ≫ C	5.2*S	5.2*S
	C ≈ S	6*(C+S)/2	7*(C+S)/2
3		2*C + 2*S + MAX(C,S)	3*C + 3*S
	C ≫ S	3.2*C	3.3*C
	S ≫ C	3.2*S	3.3*S
	C ≈ S	5*(C+S)/2	6*(C+S)/2

B. Average Room Irradiance

Geom. Case	Bldg. Type	Window Coverings		Room Furnishings	
		Total Irrad.	Ave. Irrad. per Room	Total Irrad.	Ave. Irrad. per Room
C ≫ S	1	5.2*C		5.2*C	
	2	2.4*C		2.5*C	
	3	3.2*C		3.3*C	
			0.37*COSA		0.38*COSA
S ≫ C	1	2.4*S		2.5*S	
	2	5.2*S		5.2*S	
	3	3.2*S		3.3*S	
			0.37*SINA		0.38*SINA
S ≈ C	1	3*(C+S)		7*(C+S)	
	2	3*(C+S)		7*(C+S)	
	3	2.5*(C+S)		6*(C+S)	
			0.29*(COSA+SINA)		0.34*(COSA+SINA)

FRFWCI = FWCI RFWCI(RNSIZ, WNDCOV). (18)

The data set RFWCI defines the probability of a room fire given ignition of specified window coverings and room size. This data set was initiated at the beginning of TRTIGN. In practice RFWCI would be an empirically based data table or model of the probability of room ignition given ignition of window coverings.

A loop is formed over the number of room sizes in the tract. The room size, the number of rows and columns of room cells in the room size, and the fraction of rooms of this size in the tract are obtained from the tract characteristics (Figure 9) and global (Figure 5) data sets.

At label (T) a loop is formed over the number of window sizes in the tract. The window dimensions and the fraction of windows having those dimensions is obtained from the tract characteristics (Figure 9) and global (Figure 5) data sets. A single value of transmissivity is defined for all window sizes.

A loop is formed over the room cells in the room size by looping over the number of rows and the number of columns in the room size. The irradiance on vertical room furnishings (QRFI) is calculated for each room by interpolating on the global room furnishing irradiance

QRF(RGZ, NROWS, ROWRM, COLRM, WNDSIZ),

using the defined values of range to ground zero, effective number of radiation circle rows visible, room row and column, and window size. The interpolated value is corrected for window transmissivity, together with geometry and building type to obtain

QRFI = Tw CFrf QRF. (19)

A loop is formed over the room furnishings in the tract, which are defined in terms of their critical ignition energy levels. The fraction of room furnishings that will ignite (FRFI) given irradiance QRFI is calculated. The fraction of room furnishings expected to be found in the subject room cell is obtained from data set

FRFRC(ROWRM, COLRM),

which was one of the data sets initialized at the beginning of Submodule TRTIGN. In practice FRFRC would also be a function of room size, and would represent an empirical average of the fraction of furniture one would expect to find in a given cell of a room of given size in the urban area being evaluated.

The fraction of room furnishings that will ignite(FRMFI), given irradiance QRFI and room furnishings present is accumulated by

$$FRMFI = \sum_{RMROW} \sum_{RMCOL} FRFI \; FRFRC(RMROW, RMCOL) \qquad (20)$$

for all of the room cells in the subject room size.

At label (U) the loops on room columns and rows (i.e. room cells), and window sizes are terminated.

The fraction of rooms in the tract of the subject size that will have a room fire given ignition of room furnishings (FRFRFI) is calculated in terms of the fraction of room furnishings ignited (FRMFI) and the probability of a room fire in a room of this size given ignition of room furnishings. Thus,

$$\text{FRFRFI} = \text{FRMFI RFRFI(RMSIZ, FRFI)}. \tag{21}$$

The data set RFRFI was initiated at the beginning of TRTIGN. In practice this would be an empirical data set or model based on experimental or experiential data defining the relationship between room furnishing ignition and occurrence of a room fire.

A loop is formed over the number of building classes in the tract. The building class and the fraction of buildings in the tract or this class are obtained from the tract characteristics (Figure 9) and global (Figure 5) data sets.

The fraction of rooms that will flash over, given a room fire due either to ignition of window coverings or to ignition of room furnishings is calculated from

$$\text{FFORF} = \text{FBCL FBFo (1 - 0.5 ((1 - FRFWCI) + (1 - FRFRFI)))} \tag{22}$$

where FBCL is the fraction of buildings in the tract of this class,
FBFD is the fraction of buildings in the tract of this class
that will flash over given at least one room flashed over.

A loop is formed over the number of floors from the subject floor to the top of the building. In this case the distribution of windows in the tract per floor (DWPF(FLOORHT)) is calculated under the assumption that the number of buildings of given height decays exponentially with increasing building height. In practice this would be an empirically derived distribution for the given urban area.

The probability that no room on the subject floor will flash over is calculated at label (V) from

$$\text{PNRFOF} = \sum_{\text{FLOORHT}} \text{DWPF(FLOORHT)} \, (1 - \text{FFORF})^{\text{NWPF(FLOORHT)}} \tag{23}$$

where NWPF is the number of windows on the subject floor. The loop over floors to the top of the building is terminated and the probability that no room in the subject building will flash over is calculated from

$$\text{PNRFOB} = \prod_{\text{NTBF}} \text{PNRFOF}. \tag{24}$$

The probability that at least one room in the building will flash over is given by

$$P1RFOB = 1 - PNRFOB. \tag{25}$$

The fraction of buildings in the tract that will flash over is accumulated and normalized by including the distributions of the tract characteristics and summing (24) over all of the defined tract characteristics. The complete expression is given by

$$FBFOT = \sum_{NRMS}\sum_{NSAZ}\sum_{NFSP}\sum_{NFHT}\sum_{NBSP}\sum_{NABH}\sum_{NTBF}\sum_{NTBH} \tag{26}$$

$$(FRMS\ FSAZ\ FFSEP\ FFOLHT\ FBSP\ FB2HT\ FB1HT\ FB1FHT)$$

$$(1 - \prod_{NTBF} TBHT)\left(\sum_{NWPF} WPF(FWPF\ (1 - P1RFOB))\right).$$

The loops are terminated over tract room sizes, street azimuth angles, foliage-building separation distances, foliage heights, building separation distances, adjacent building heights, number of floors in target buildings, and target building heights.

The number of new buildings flashed over in the subject tract is calculated from

$$NNEW = FBFOT\ NBT \tag{27}$$

where NBT = the number of buildings in the subject tract. The total number of buildings flashed over in the tract (NTOT) is updated by accumulating NNEW to NTOT. The number of buildings that have flashed over during the most recent 171 seconds (NLAST) is updated to the current time (T2MX) by accumulating NNEW and deleting those that no longer satisfy the criterion.

The new values of NTOT, NNEW, NLAST, and TLAST are stored in the ignition data (IGND, Figure 22), and submodule TRTIGN and module IGNITE are exited.

3.5 THE BLAST PROPAGATION MODULE (BLSPRP).

The blast propagation module specifies the blast effects event parameters for each tract within the annulus defined by RMXEFF and RMNEFF. The demonstration module simply interpolates on the global BLST data, assuming free field conditions. In practice the module could take into consideration the effects of terrain, structures, and forests on blast wave parameters.

Upon entry to the BLSPRP module, as shown in Figure 23, weapon data are accessed to obtain coordinates of the detonation point. These are used to identify the tract that contains ground zero.

The global irradiance and blast data are accessed, and a loop is formed over the tracts in the annulus bounded by the user specified minimum and maximum effects ranges. The file containing these tracts was created in TRTIGN, and can be accessed by BLSPRP. In general, any data file created by a module in an event can be accessed by all subsequent modules in the event.

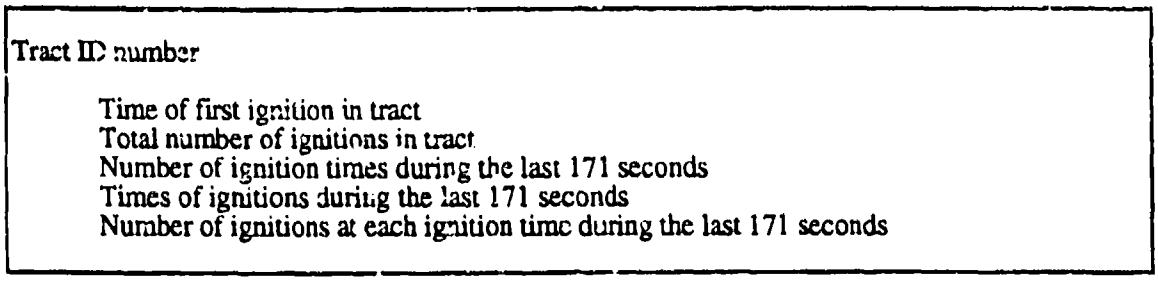

Figure 22. Tract ignition data (IGND).

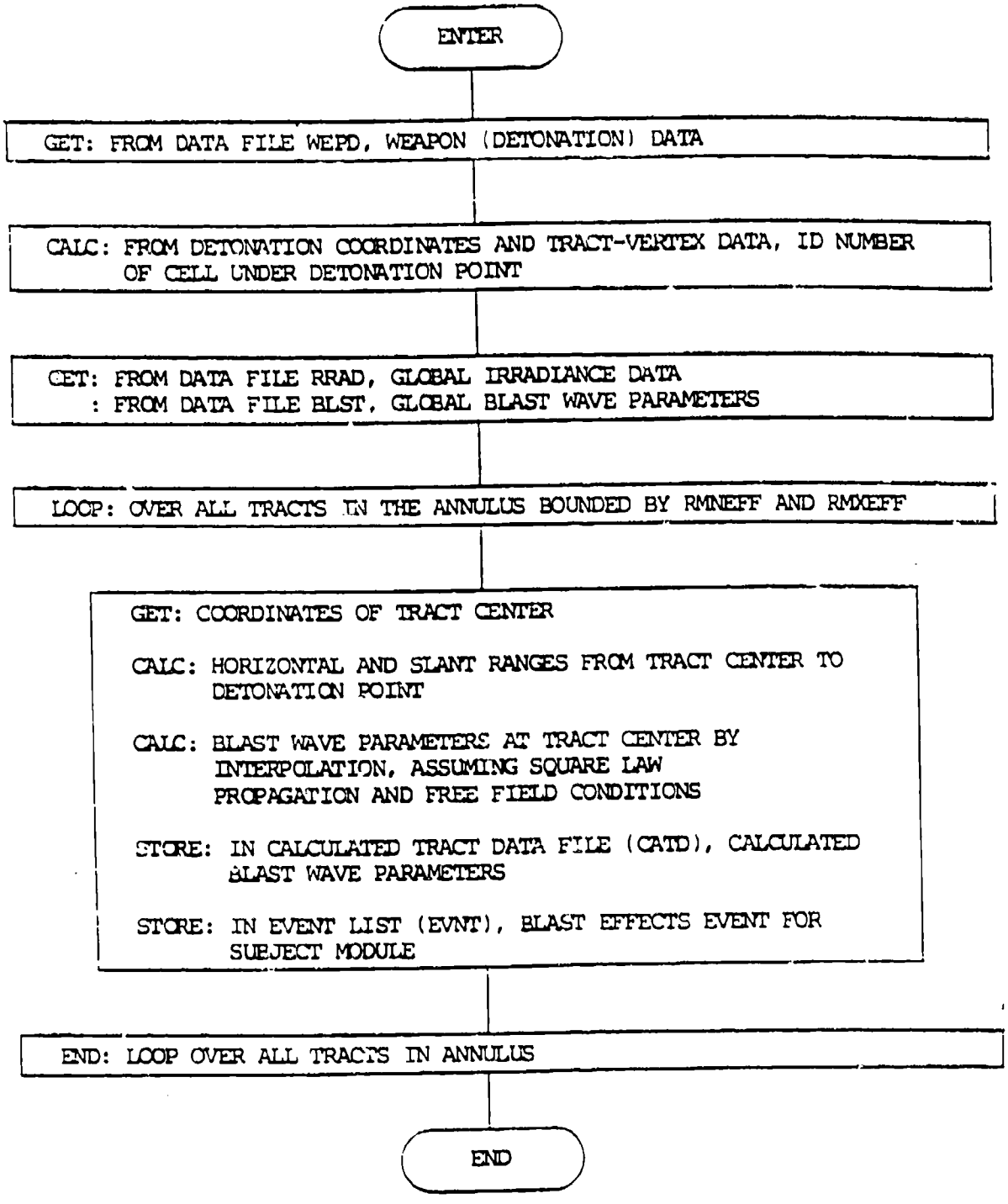

Figure 23. Logic flow diagram for module BLSPRP.

The global thermal irradiance and blast parameters are interpolated to the range of the subject tract center from ground zero. Logarithmic interpolation is used, assuming square law propagation of thermal irradiance and blast wave effects, together with free field conditions. The interpolated values;

TASF = time of shock front arrival,
POP = peak overpressure,
PPDOP = positive phase duration of peak overpressure,
PHDP = peak horizontal dynamic pressure,
PPDHP = positive phase duration of horizontal pressure,
QI = thermal irradiance,

are stored in the calculated tract data file (CATD), shown in Figure 24.

A blast effects event for the subject tract is placed on the event list, shown in Figure 24, to be processed at the interpolated time of shock front arrival at the tract center. The loop over tracts in the annulus is terminated, and module BLSPRP is exited.

This terminates the discussion of the NUCDET event. The blast effects event BLSEFF is discussed in the next section.

Calculated Tract Data File (CATD)

ID number of tract
- Time of shock front arrival at tract center (s)
- Peak overpressure at tract center (g/m^2)
- Peak horizontal dynamic pressure at tract center (g/m^2)
- Positive phase duration, overpressure (s)
- Positive phase duration, dynamic pressure (s)
- Thermal irradiance at tract center (j/m^2)

Event Data File (EVNT) Format for BLSPRP Event

- Simulation time at which event is to be processed (s)
- Event ID number
- Weapon (detonation) ID number
- Tract ID number

Figure 24. Calculated tract data (CATD) and event data (EVNT).

SECTION 4

THE BLAST EFFECTS (BLSEFF) EVENT

The blast effects event addresses the quenching of existing ignitions, structural damage, and secondary ignitions resulting from passage of the blast wave.

The effect of blast wave passage on existing ignitions is estimated in module QUENCH, and the effect on structural integrity is estimated by module FULMOD. Secondary ignitions resulting from the interaction of blast parameters with structures and existing fires is estimated by module SECIGN.

The objective of the blast effects module is to specify the total number of primary and secondary ignitions resulting from detonation of a nuclear weapon in an urban area. The structure of the blast effects event is designed to accommodate sequential detonations as defined in Section 3.0.

4.1 CALCULATION OF BLAST-FIRE INTERACTIONS (QUENCH).

Blast-fire interactions have been the subject of considerable theoretical and empirical investigation (References 7 and 8). These investigations are just beginning to yield results upon which a model can be based. The procedure used in module QUENCH is based on the work of Martin reported in Reference 8.

Module Quench is shown in Figure 25. Upon entry, the ignition data set IGND (Figure 22) is accessed to obtain tract ignition data, and the calculated tract data set CATD (Figure 24) is accessed to obtain tract blast wave parameters.

Only ignitions that have occurred in the past 171 seconds are considered subject to being quenched by blast wave passage. Thus, if there are no ignition times in the past 171 seconds, the module is exited.

If ignition times are found in IGND during the past 171 seconds, the probability is calculated that they will be quenched by the blast wave. The calculation of the probability of quenching an ignition is based on Figure 26.

The boundaries (B1 and B2) between the "quench" and "no quench" regions of Figure 26 are calculated from the time since ignition by

$$B1 = 0.0486\ (TASF - TLAST(I)) \qquad (28)$$

$$B2 = 14.02 - 0.0777\ (TASF - TLAST(I))$$

where TASF is the shock front arrival time, and
TLAST(I) is the I-th ignition time in the past 171 seconds.

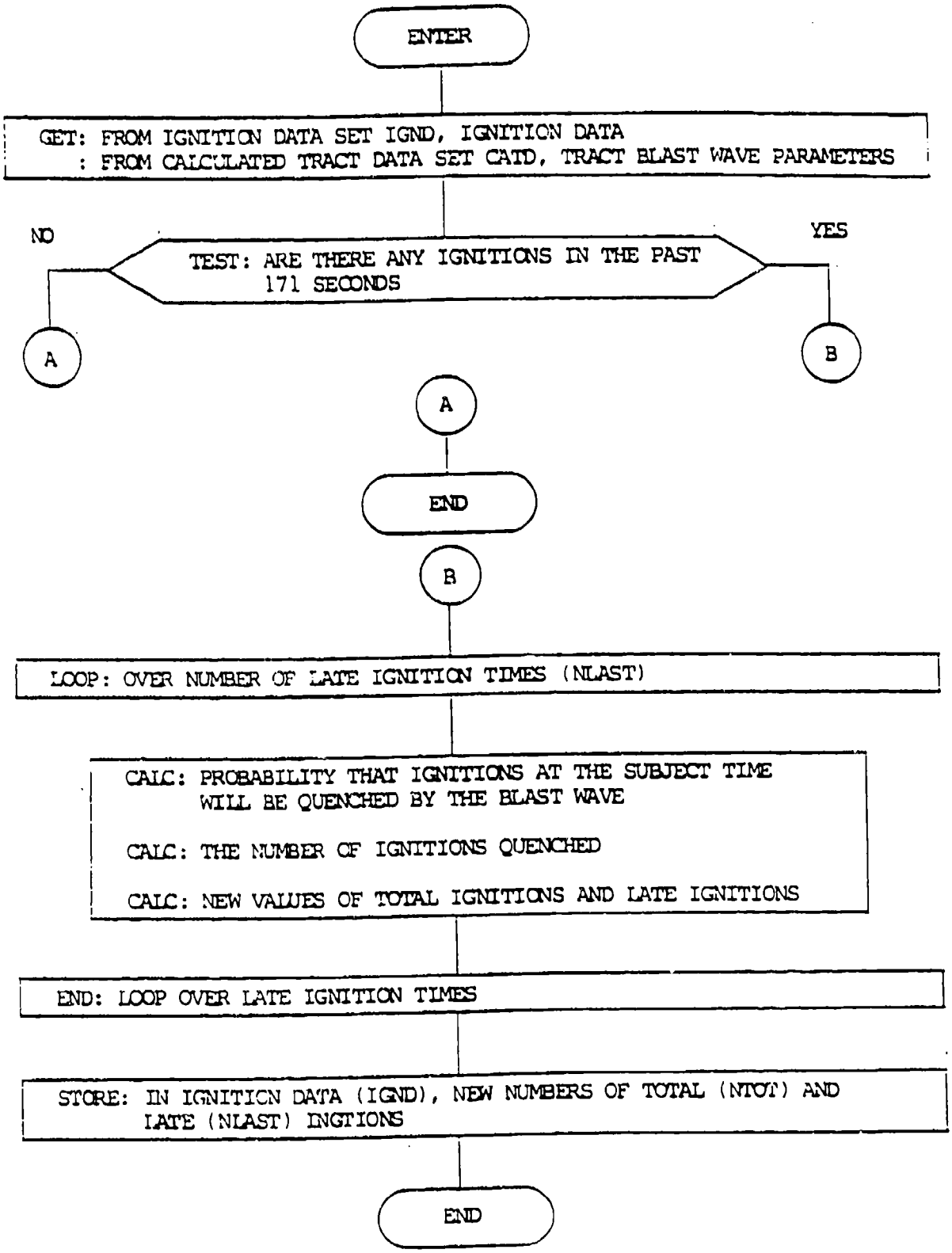

Figure 25. Logic flow diagram for module QUENCH.

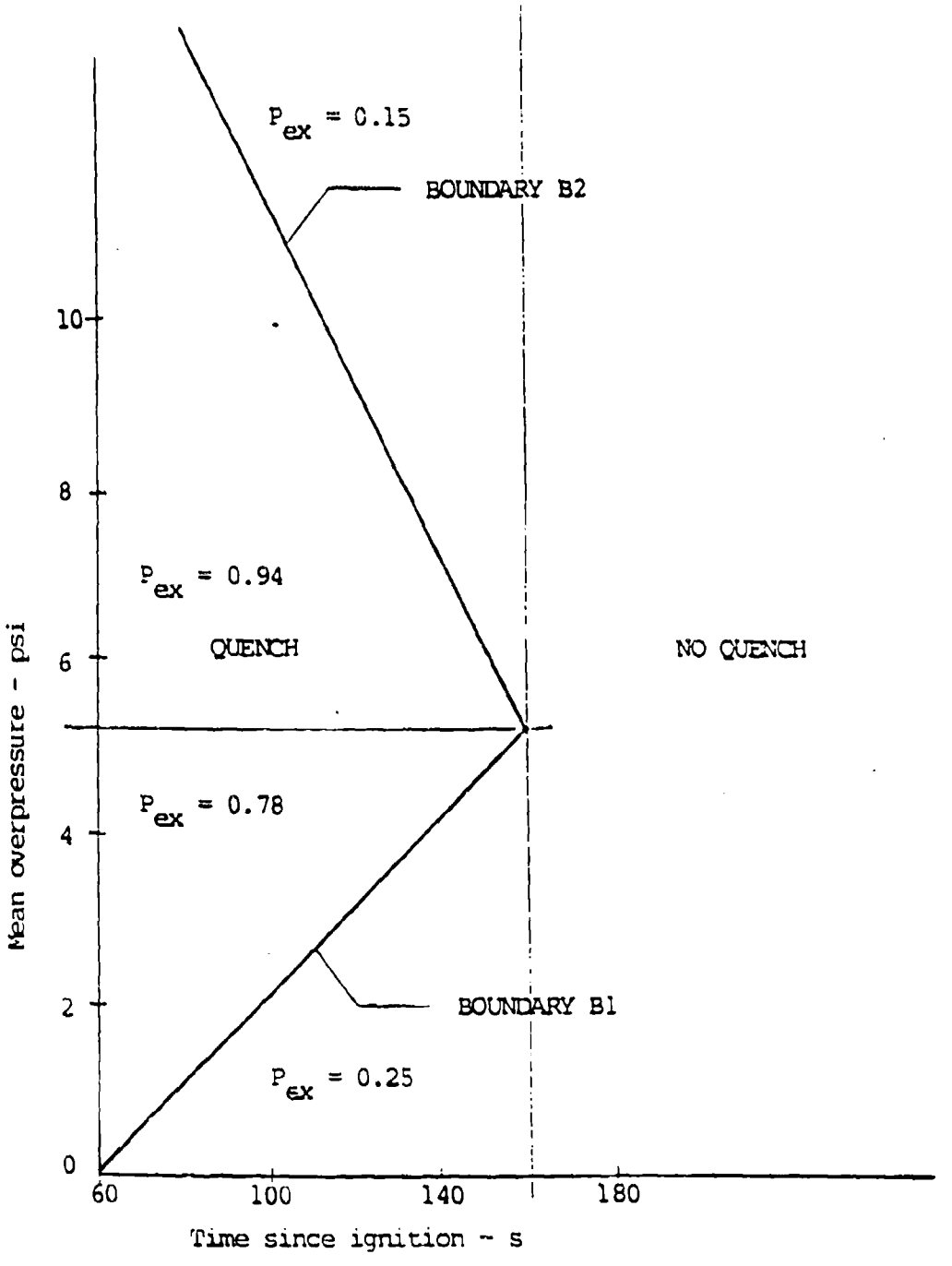

Figure 26. Blast fire interaction.

Based on the peak overpressure experienced, the probability of the ignition being extinguished is calculated from

$$Pex = \begin{cases} 0.25 \text{ if POP .LT. 5.4 (psi) .AND. POP .LT. B1,} \\ 0.78 \text{ if POP .LT. 5.4 (psi) .AND. POP .GT. B1,} \end{cases} \quad (29)$$

$$Pex = \begin{cases} 0.94 \text{ if POP .GT. 5.4 (psi) .AND. POP .LT. B2,} \\ 0.15 \text{ if POP .GT. 5.4 (psi) .AND. POP .GT. B2.} \end{cases} \quad (30)$$

The number of ignitions at TLAST(I) that will be quenched by the blast wave is calculated from

$$Nex = Pex \ NLAST(I). \quad (31)$$

The loop over late ignition times is terminated, the values of total (NTOT) and late (NLAST) ignitions are modified by Nex, the new values are stored in the ignition data set IGND, and module QUENCH is exited.

4.2 BLAST EFFECTS ON FUEL PROPERTIES OF STRUCTURES (FULMOD).

The modification of structures by the passage of the blast wave is of interest because it contributes to secondary ignitions and it affects the way a structure will burn. Blast wave damage results in loss of structural integrity, which in turn results in increased fire ventilation which can reduce the fraction of rooms that may flash over. This causes a slower building burning rate and lower burning temperatures, with reduced impact on the ambient air movement.

Structural fire damage is defined as a function of peak overpressure at the tract center following the procedure described in Reference 9, pp. 38-47. The results of structural damage studies and tests that are available and on-going (References 6, 10, 11) can be used to improve this model.

Upon entry to module FULMOD, shown in Figure 27, the tract building classes are obtained from the tract characteristics (Figure 9), and the blast wave parameters at the tract center are obtained from the calculated tract data (Figure 24)

A loop is formed over the number of structural building classes in the tract. Ten building classes are included, these are defined in Reference 9, pp. 25-32. Within the loop over building classes, a loop is formed over the number of structure damage classes used. Currently three damage classes are used, these are defined in Reference 9, pp. 38-46. Given the peak overpressure, the damage level for each building class is calculated following the procedure shown in Reference 9, p. 47.

The structural damage level for each building class in the tract is stored in the calculated tract data (CATD, Figure 24), and module FULMOD is exited.

4.3 CALCULATION OF SECONDARY IGNITIONS (SECIGN).

The calculation of secondary ignitions is based on the procedure described in Reference 9, pp. 49-64. Reference 9 employs an alignment chart that provides an estimate of the number of secondary ignitions that will occur in a given building structural class as a function of building contents and blast induced damage level. The alignment chart has been represented in the simulation by a set or exponential functions.

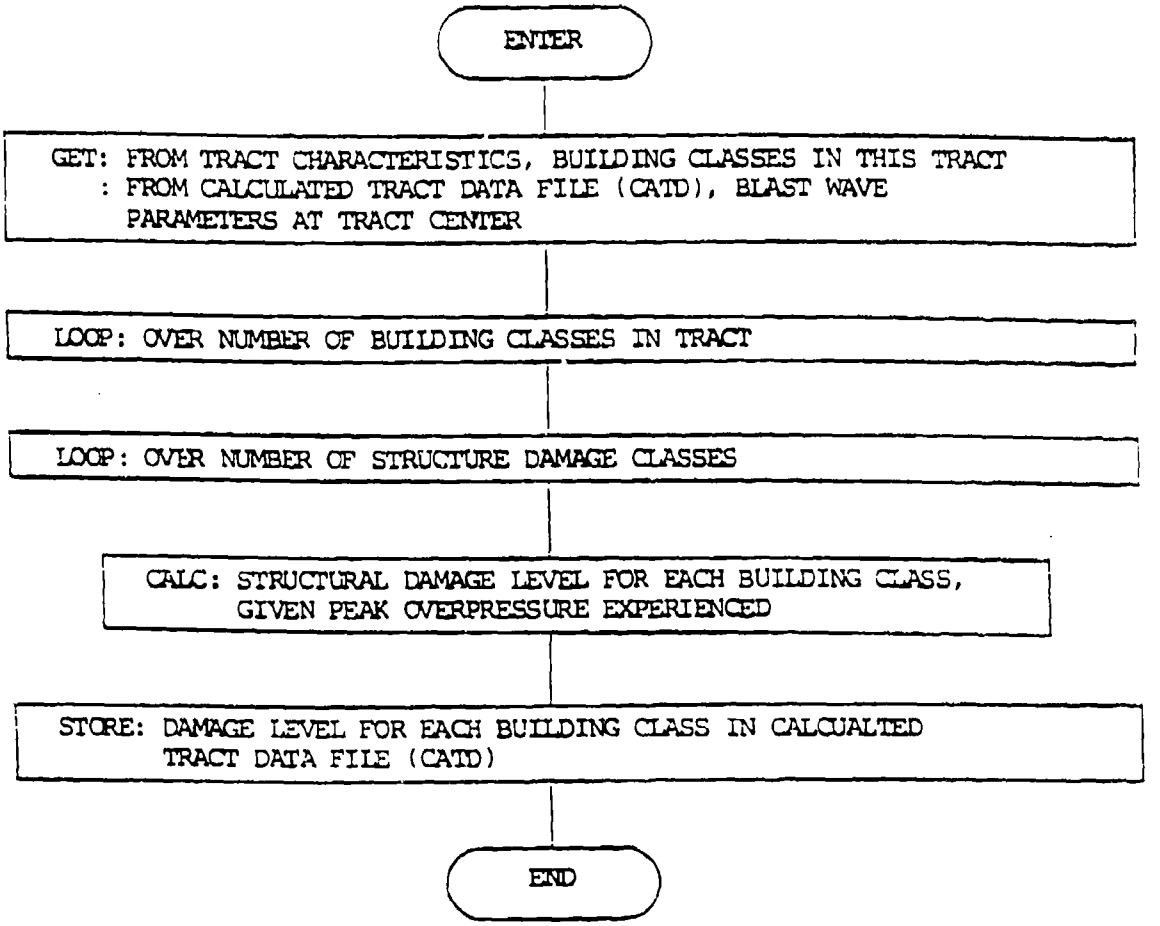

Figure 27. Logic flow diagram for module FULMOD.

Upon entry to module SECIGN, shown in Figure 28, the tract characteristics data is accessed to obtain the number of building classes and building contents in the tract, together with their distributions. The calculated tract data (CATD) is accessed to obtain the damage level experienced by each structural building class. The ignition data (IGND) is accessed to obtain the number of total and late ignitions in the tract.

A loop is formed over the number of structural building classes in the tract. The total number of secondary ignitions (NSEC) is calculated from

$$NSEC = \sum_{ITBCL} A0\ EXP(A1\ ITBCL)\ EXP(A2\ ITBCN)\ NBT\ FTBCL \qquad (32)$$

where A0, A1 and A2 is the coefficients defined by the damage level.
ITBCL is the structural building class ID number,
ITBCN is the building contents ID number,
NBT is the total number of buildings in tract,
FTBCL is the fraction of buildings in tract of subject structural building class.

The loop over building classes is terminated, the numbers of total and late ignitions in the tract are modified in accordance with NSEC, the new values are stored in the ignition data, and module SECIGN is exited.

Module SECIGN is the final module in the execution of the BLSEFF event. At this point the number of ignitions stored in IGND represents the total number of ignitions in each tract in the annulus bounded by RMNEFF and RMXEFF that were caused by detonation of the subject nuclear device.

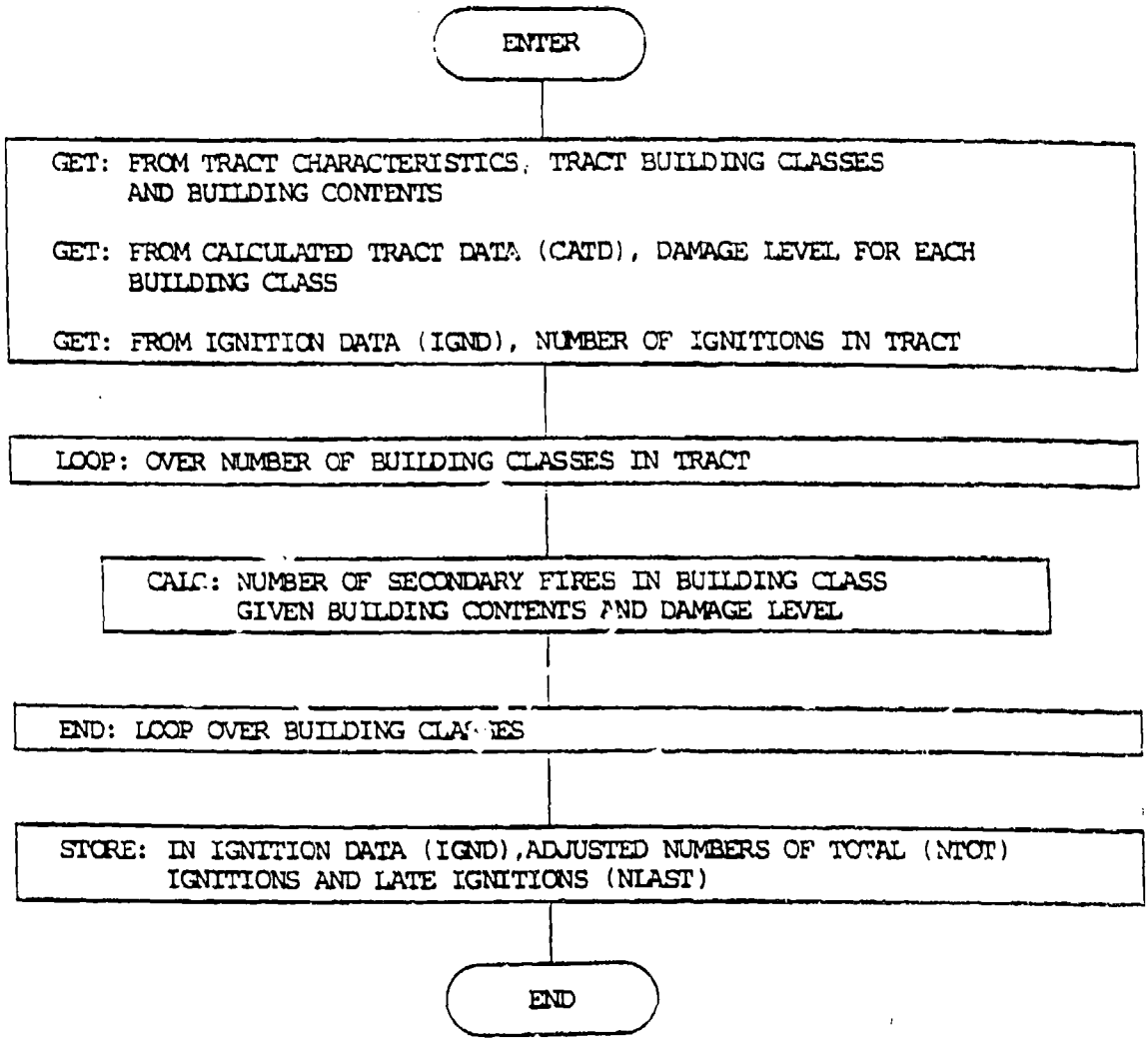

Figure 28. Logic flow diagram for module SECIGN.

SECTION 5

RESULTS FROM NUCLEAR DETONATION AND BLAST EFFECTS EVENTS

The nuclear detonation and blast effects events have been executed many times during the debugging process. The results of some of these executions are presented here to show the types of results that these events will provide.

Figures 29, 30, and 31 present results for tract 76 from three executions of the NUCDET and BLSEFF events for three values of weapon yield and detonation altitude. Tract 76 is 100 percent residential occupancy, 7.5 million square meters in area, and contains 5002 structures. Figure 29 shows thermal irradiance versus distance from ground zero as a function of weapon yield and detonation altitude. It can be seen that weapons of yield greater than 1 MT are dictated to provide extensive areas of sufficient irradiation to reliably ignite window coverings and room furnishings. Figure 30 shows peak overpressure versus distance from ground zero as a function of weapon yield and detonation altitude.

Figure 31 shows primary, secondary, extinguished, and total ignitions in tract 76 for the weapons shown in Figures 29 and 30. The center of tract 76 was about 5 KM from ground zero. Thus, for the 1 MT case, an irradiance of about 4 cal/cm^2, and greater than 1 psi overpressure were experienced. This accounts for the moderate number of primary ignitions and blast extinctions shown in Figure 30. In the 0.01 MT case, an irradiance of about 0.04 cal/cm**2, and about 0.4 psi overpressure were experienced. This is consistent with the small numbers of primary ignitions and blast extinctions shown in Figure 30.

It is somewhat surprising that so many more secondary ignitions than primary ignitions occur at these relatively low levels of overpressure. However, it is important to keep in mind that these results are provided for demonstration of the model structure, and can probably be in error by as much as an order of magnitude. A primary interest in the debugging process was to assure that the results exhibited the correct trends as functions of the important variables.

A 1.0 MT weapon was detonated at coordinates XB = 19 km, YB = 19 km with a burst height of HB = 3.7 km. Thus, the data shown in Figures 29 and 30 apply. The boundaries of the annulus were specified as RMNEFF = 20 km and RMXEFF = 54 km. The burst location, and the collection of all tracts whose centers are located in the annulus are shown in Figure 32. It can be seen that none of the industrial/commercial tracts are located in the annulus. This was done for two reasons. First, it is considered a realistic scenario for use of fire as a collateral damage mechanism. The weapon would most likely be targeted so that the desired level of damage to the commercial/industrial area would be caused by blast effects. It is unlikely that fire would be depended upon to provide sure damage to those targets. Second, the commercial/industrial tracts, as configured, required too long to execute. Tract 75, when evaluated individually, required about 50 minutes to execute with three occupancy classes. This long execution time can be avoided by reconfiguring tract 75 into three smaller tracts, each with one occupancy class. Three such tracts should execute in about 1.5 minutes (i.e. about 0.5 minute each).

Table 3 shows the list of tracts included in the annulus of Figure 32 (see also Figure 2). It can be seen that 19 of the 44 tracts in the annulus have some degree of residential occupancy. Of the 19 tracts containing residential occupancy, 6 are medium density (10 to 30 percent) to high density (30 to 100 percent) occupancy, while 13 are low density (less than 10 percent) occupancy.

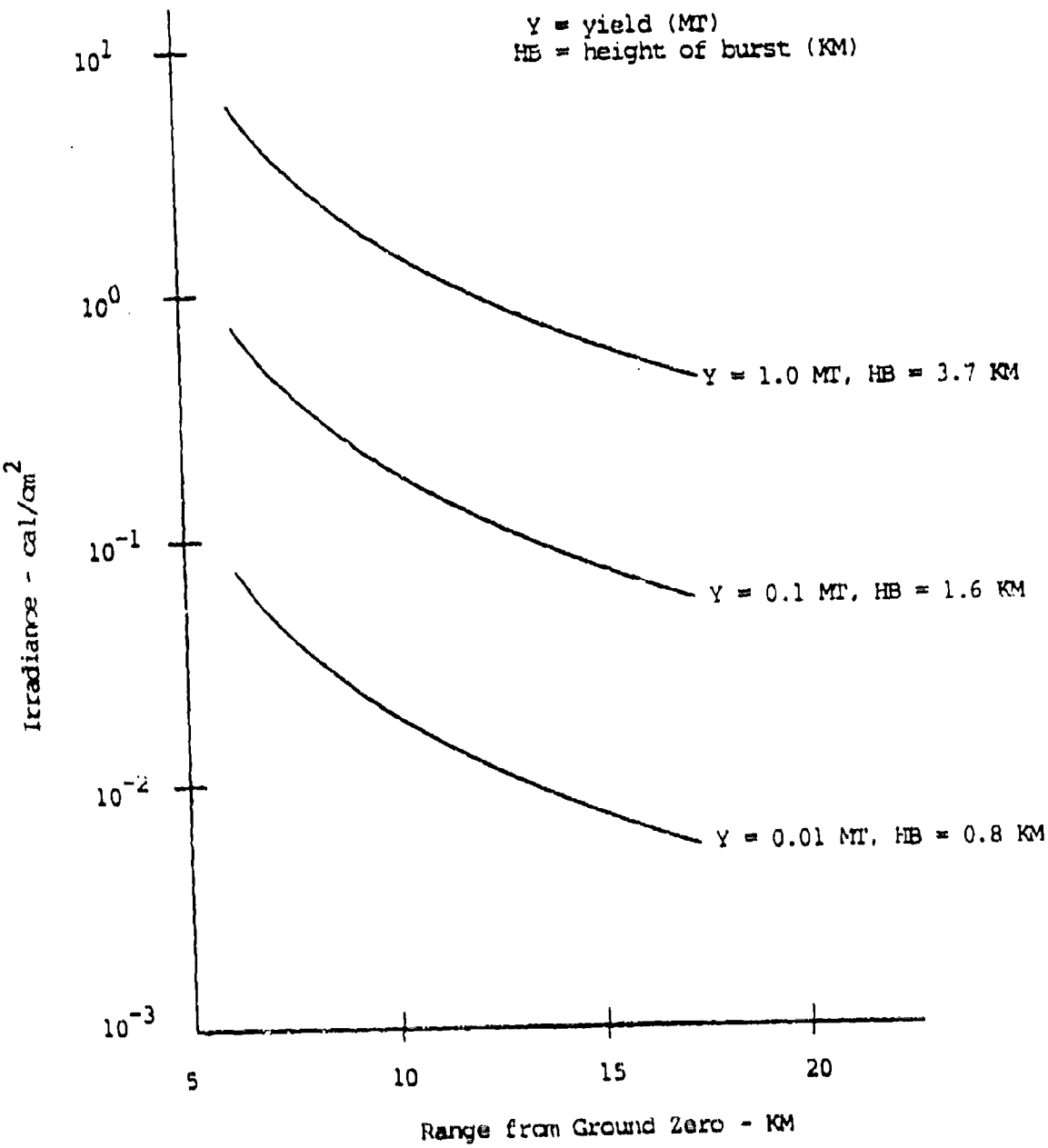

Figure 29. Thermal irradiance at distances from ground zero.

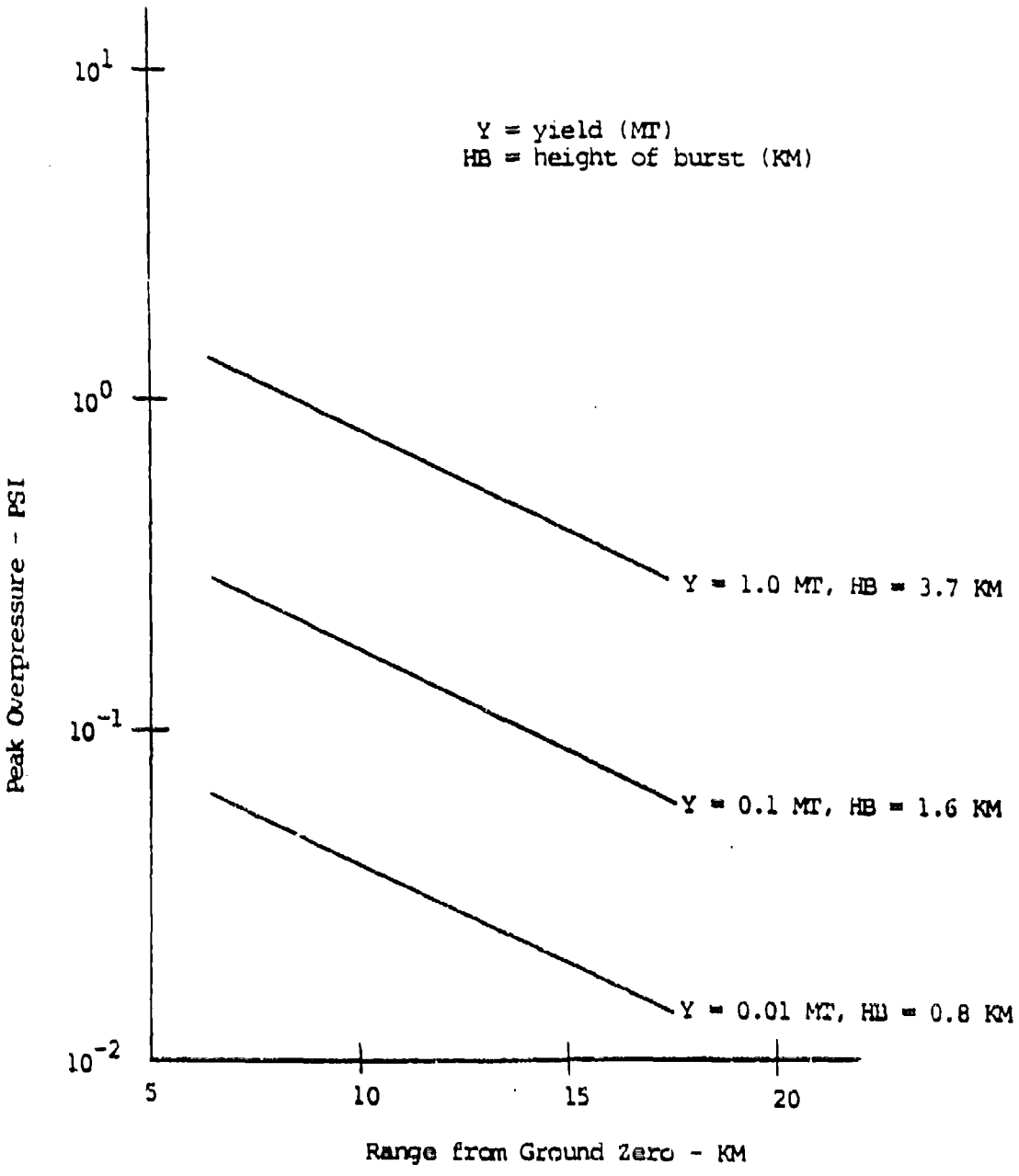

Figure 30. Peak overpressure at ranges from ground zero.

NTOT = total number of ignitions
NSEC = number of secondary ignitions
NPRIM = number of primary ignitions
NEX = number of extinguished ignitions

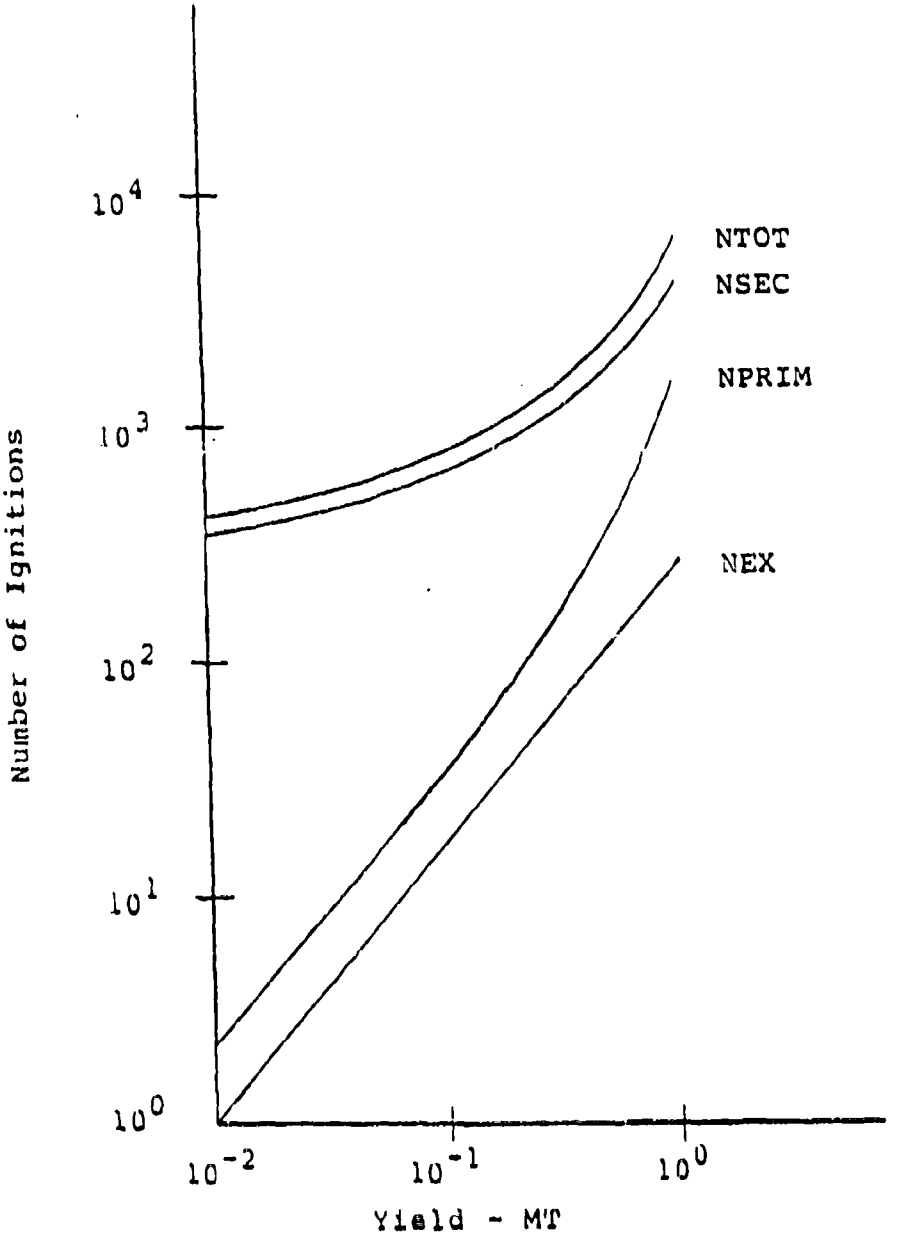

Figure 31. Primary, secondary, and total ignition for three fields.

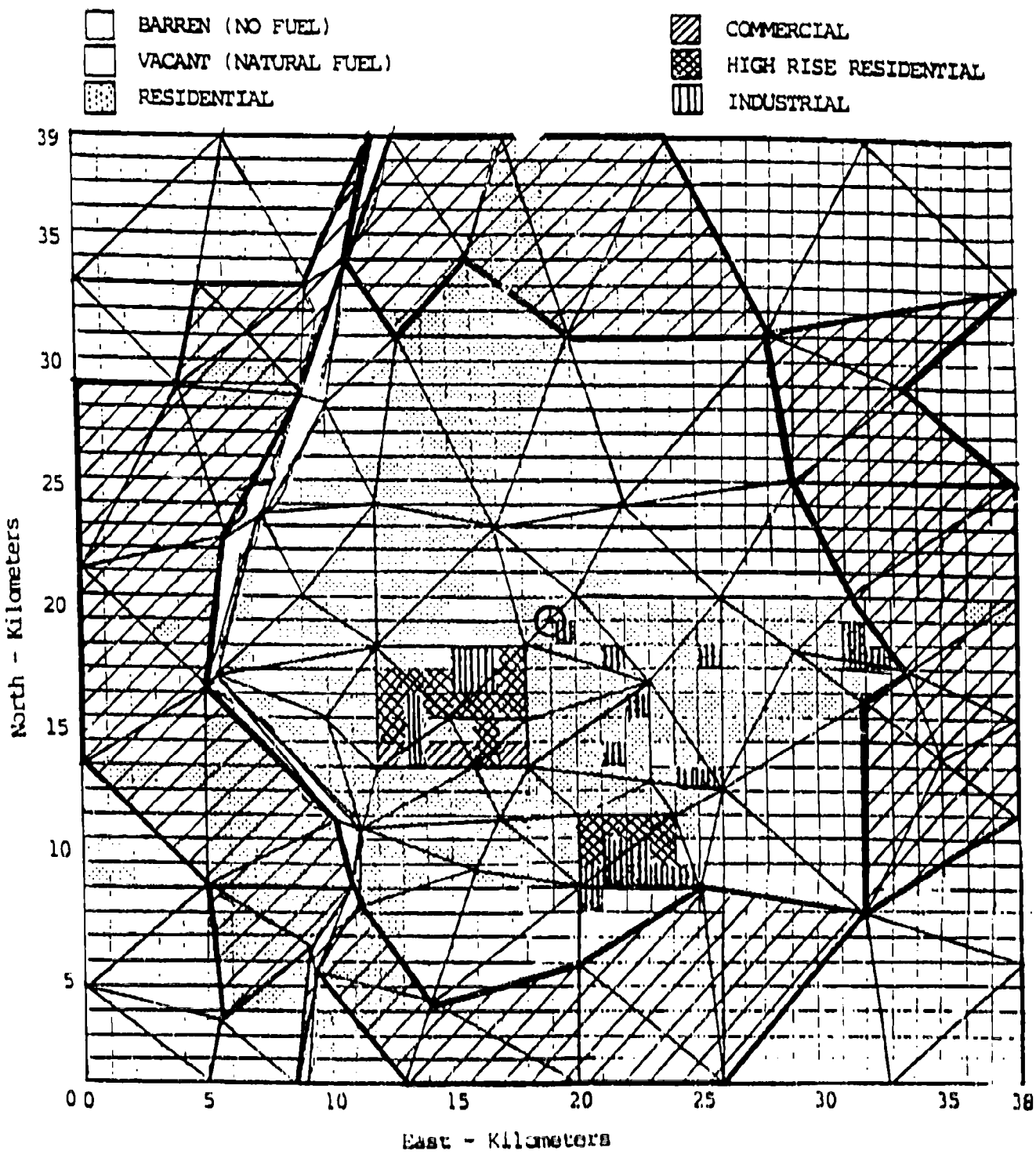

Figure 32. Geometry of annulus and included tracts.

Table 3. Example of tracts in annulus.

TRACT ID	OCCUPANCY CLASS	TRACT ID	OCCUPANCY CLASS
5	B	60	R
7	B	87	R
8	R	88	R
9	R	89	B
10	R	90	B
11	B	91	R
18	B	105	B
19	R	107	B
20	R	109	B
21	B	110	R
24	R	113	B
26	B	114	B
27	B	115	R
28	R	120	B
38	B	121	B
39	B	128	R
40	B	131	R
42	B	132	B
43	R	133	B
57	B	134	B
58	B		
59	R		

B = NO OCCUPANCY (BARREN)
R = RESIDENTIAL OCCUPANCY

Y = 1 MT, XB = 19 KM,
YB = 19 KM, HB = 3.7 KM

RNMEFF = 20 KM
RMXEFF = 54 KM

SUMMARY: 44 TRACTS IN ANNULUS

25 TRACTS IN ANNULUS, NO OCCUPANCY
19 TRACTS IN ANNULUS, RESIDENTIAL OCCUPANCY

6 RESIDENTIAL TRACTS IN ANNULUS, MEDIUM TO HIGH DENSITY
13 RESIDENTIAL TRACTS IN ANNULUS, LOW DENSITY

SECTION 6

TRACT BURNING AND PROPAGATION MODELS

As discussed in Sections 2 through 5, the model of an urban area is described by fuel characteristics and geographical location relative to the burst. A nuclear burst ignites this fuel with its thermal pulse, which is followed by a blast wave. This extinguishes some of the ignitions and may rubblize part of the fuel bed to some radius from Ground Zero. The blast wave is also responsible for initiating secondary ignitions. This is a statement of the initial conditions that lead to the dynamic aspect of tract burning and the propagation of fire through the modeled urban area.

6.1 CHEMICAL REACTION MODEL.

The model of tract burning we call a chemical reaction model, because its form is identical to a simple, coupled reaction involving three species, or substances. It is as though substance A changes into substance B with some rate, and substance B then changes into substance C with some other rate. The rates at which these reactions go can be dependent on many things, but one thing they are certainly dependent on is the amount of the source substances. For example, if the amount of A goes to zero, then B can no longer increase, or if B goes to zero then the channel between A and C is broken. If the rate at which B changes to C is much faster than the rate from A to B, then we could simplify by ignoring the B state and using the A to B rate as the effective rate from A to C. The numerical differential equations that describe this system are integrated forward in time, accounting for changing conditions that affect the rates.

In the tract burning model the three quantities are, for tract index I,

N_1^I the number of unignited buildings

N_2^I the number of burning buildings

N_3^I the number of burnt out buildings.

Their uniform areal densities are

$$\begin{aligned} n_1^I &= N_1^I / A_I \\ n_2^I &= N_2^I / A_I \\ n_3^I &= N_3^I / A_I \end{aligned} \qquad (33)$$

where A_I is area of tract I in square meters. Note that the conservation of buildings gives

$$N^I = N_1^I + N_2^I + N_3^I \qquad (34)$$

where N^i is the total number of buildings in the tract. Now the initial conditions, with primary and secondary ignitions, are that $N_3^i = 0$ and that $N_1^i = N^i - N_{2c}^i$, where N_{2c}^i represents the initial number of ignited buildings.

To write down the governing equation for N_1, which involves the propagation of fire to unburned structures, we equate the rate at which unburned structures are ignited to the product of their effective, average cross section; the number of unburned buildings; and the rate at which brands that would cause ignitions will land per unit area. Symbolically, this becomes

$$\frac{dN_1^i}{dt} = -\sigma_i N_1^i \left[\frac{A_{ii}}{A_i} \frac{1}{\tau^i A_i} + \sum_{k=1}^{3} \frac{A_{ki}}{A_i} \frac{1}{\tau^k A_k} \right] \tag{35}$$

or

$$\frac{dN_1^i}{dt} = -\sigma_i n_1^i \left[\frac{A_{ii}}{A_i} \frac{1}{\tau^i} + \sum_{k=1}^{3} \frac{A_{ki}}{A_k} \frac{1}{\tau^k} \right] \tag{36}$$

where

σ_i is the effective, average cross section of each building in tract i

A_{ii} is the area of tract i that is the source of brands that land in track i starting fires

A_{ki} is the area of tract k that is the source of brands that land in track i starting fires

τ^i is the total brand production period for tract i.

Thus A_{ii} / A_i represents the fraction of tract i area that contributes to new fires in tract i, A_{ki} / A_k represents the fraction of tract k area that contributes to new fires in tract i, $1 / (\tau^i A_i)$ is the total brand production rate per unit area in tract i over all occupancy classes, and $\sigma_i n_1^i$ is the probability that a brand landing in A_i will start a new fire. Only tracts that have a common boundary are considered for contagion, which is represented in the sum to three. Obviously tracts on the boundary of the urban area modeled may have two or only one neighboring tract, so the sum to three is symbolic of the typical case, and is not to be interpreted as a sum over the first three tracts.

The other two governing equations are

$$\frac{dN_2^i}{dt} = -\frac{dN_1^i}{dt} + \left(\frac{dN_1^i}{dt} \right)_{\text{evaluated at } t - T_0^i} \tag{37}$$

and

$$\frac{dN_3^i}{dt} = \left(\frac{dN_1^i}{dt} \right)_{\text{evaluated at } t - T_0^i} \tag{38}$$

where $\overline{T}_o^i$ is the average burnout time for buildings in tract i, which is the weighted average over occupancy classes. In this version of the Urban Fire Simulation (UFS-2) the burnout time for a building in occupancy class j is a constant T_o^j. Thus the rate at which new class j fires started in tract i T_o^j seconds ago is also the rate at which burning buildings are now reaching the burnt out state. Obviously the model could be enhanced at this point for added realism, but as it stands the UFS-2 is adequate for demonstrating the process from ignition to final burnout. One such extension would be to account for multiple ignitions per structure, which would lead to a quicker burnout and a more rapid increase in $\dot{Q}_o^j$, the heat production rate.

The branding rate per building, or its reciprocal the branding period in seconds, is taken as a function of the average heat production rate in the burning building given in watts

$$\frac{1}{T_{Bo}} = 10^{-9}\,\overline{\dot{Q}}_o \tag{39}$$

This branding rate is 100 times the rate used in the previous Urban Fire Simulation (Ref. 1). This is consistent, because the average branding range assumed in the previous work was about 1 km, because of the grid cell size. In the model described here a distance of 100 m is much more consistent with the concepts modeled. To extend this branding rate to the total branding rate for a tract, set

$$\tau^i = T_{Bo} / N_2^i = 10^9 \Big/ \left(\sum_{j}^{\text{all classes}} N_2^{ij}\,\overline{\dot{Q}}_o^j \right) = 10^9 / \dot{Q}_T^i \tag{40}$$

where $\dot{Q}_T^i$ is the total heat production rate for tract i.

The effective, average building cross section is computed as follows:

$$\sigma_i = \frac{A_i}{\sum_{j}^{\text{all classes}} N^{ij} / f_{ij}} \tag{41}$$

where f_{ij} is the fractional area of tract i covered by buildings of class j. However, in the computations in UFS-2 the term $\sigma_i N_1^i / A_i$ is developed by evaluating

$$\frac{\sigma_i N_1^i}{A_i} = \frac{1}{A_i} \sum_{j}^{\text{all classes}} \sigma_{ij} N_1^{ij} = \sum_{j}^{\text{all classes}} \frac{f_{ij} N_1^{ij}}{N^{ij}} \tag{42}$$

As a simple test of the branding rate constant an urban residential tract (14000 structures in 20 km^2) with σ = 1000 m^2, was initially 50 percent randomly ignited. In 24 minutes 90 percent of the structures in the tract were on fire.

For each of the initial fire starts, primary and secondary ignitions, a burnout event is scheduled at T_o^{ij}. Similarly, ignitions that are the result of branding at time t will have burnout events scheduled at $t + T_o^{ij}$ for each building. Another obvious extension to UFM would be to draw T_o^{ij} from a distribution rather than treat it as a constant, or to update the burnout fraction of each burning building, and switch it to category 3 when this fraction exceeded .99. This last method would allow, for example, wind to affect $\dot{Q}_o^{ij}$ as well as T_o^{ij}.

Wind in UFM is the vector sum of ambient wind, which the user defines, and winds induced by the fire. Conceptually a tract would have an image associated with it (for a short while) in the moving air mass above it. Refer to Figure 33, where the displacement is greatly exaggerated. The overlapped areas are proportional to the rate of self-branding, A_{ii} tract i into tract i, and contagion, A_{ki} tract k into tract i and A_{ij} tract i into tract j.

When updating tract i, the branding rates must be computed. Because the wind velocity differs from tract center to tract center, using the wind at the center of tract i to estimate the branding that occurs at tract i boundaries would introduce errors. If only the wind at tract i is considered, then the contagion branding rates will not agree with those computed when neighboring tracts are updated. For example, assume that two tracts like i and j in Figure 33 lie west and east respectively, and that the wind in tract i is blowing to the southeast while the wind in tract j is southwest. In such a case an update of tract i would show brands landing in tract j and vise versa. A better solution is to make a linear estimate of the wind at the ij boundary and use this wind to predict the branding along that boundary. This is in fact what is done in UFS-2. The overlapped areas are computed as the product of the length of a boundary and the component of wind perpendicular to the boundary for contagion. Self-branding then becomes

$$A_{ii} = A_i - \sum_{k=1}^{3} A_{ki} + A_{ik} \qquad (43)$$

where either A_{ki} or A_{ik} will be zero for each k.

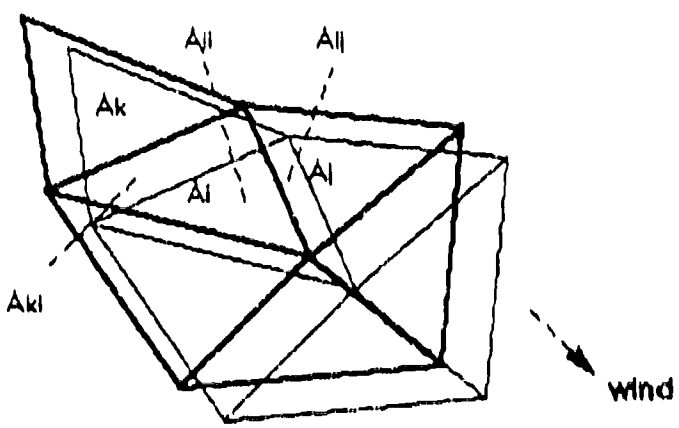

Figure 33. Displacement of air mass because of winds.

Contagion is assumed to occur just along the boundary where branding exists; it is not averaged over the tract area. This would result in a serious numerical diffusion error in simulated fire propagation. The spread of fire across a tract that had been previously unignited would be effectively instantaneous. Because this would seriously violate the intent of UFS-2, an average propagation time is kept and updated for the progress of the fire front across a tract ignited by contagion. This propagation time delay ΔT_p^{ij} for tract j ignited from tract i is

$$\Delta T_p^{ij} = \frac{\tau^i}{L_i} \sqrt{A_j} \tag{44}$$

where

$L_i = v_w t_{Bi}$ is the effective branding range (m)

v_w is the wind velocity perpendicular to the ij boundary (m/s)

$t_{Bi} = 0.1 \left(\dot{Q}_T^i / N_2^i\right)^{1/3}$ is the average brand flight time (s) (45)

and

$A_{ij} = L_i s_{ij}$, branding range times the ij boundary length (m2).

When the fire front has crossed such a tract then it can contribute brands to its neighbors. An Allowed Propagation from tract j event is scheduled at $t_n - \Delta T_p^{ij}$, where t_n is the current update time. Subsequent tract updates will include more branding from tract i, and perhaps other tracts as well, and self-branding of tract j. Because the branding rates and flight times are functions of the rate of energy release, a fire that is increasing rapidly in intensity can cause the fire front to accelerate across a tract. To account for this a tract that is prevented from propagating the fire to its neighbors will have Allowed Propagation events stored at each update. The first of these that is encountered during the simulation will allow the tract to contribute to fire spread; all others will be ignored.

To carry out a tract update the generating differential equations must be transformed into their numerical equivalents. The equation for N_3 simply becomes a tallying of burnout events. The equation for N_2 is the accumulated result of the new fire starts since the last update reduced by the number of burnouts. And the equation for the change in N_1 is the product of the average ignition rate and the update interval. Symbolically

$$\Delta N_1^i = -\frac{1}{2}\left(\left.\frac{dN_1^i}{dt}\right|_{t_n} + \left.\frac{dN_1^i}{dt}\right|_{t_m}\right)\left(t_n - t_m\right) + \rho \tag{46}$$

where the update time has advanced from t_m to t_n, ρ is a uniform random number on (0,1), and ΔN_1^i, which is defined as a positive number, is constrained by $\Delta N_1^i \leq N_1^i$. The random number ρ causes an appropriate rounding to whole numbers of buildings. For example, 3.2 fire starts in

the update interval will round to 4 fire starts 20 percent of the time and to 3 fire starts 80 percent of the time. Thus, at update time t_n, N_1^i is reduced by ΔN_1^i, N_2^i is increased by ΔN_1^i and reduced by the number of burn out events in the update interval, and N_3^i just accumulates burn out events.

The next update time for tract i is estimated by linear extrapolation as the time by which a 10 percent change could occur in N_1^i, N_2^i, or N_3^i with a minimum and maximum allowed time step. The actual formulation that appears in UFS-2 is as follows:

$$\frac{dN_s^i}{dt} = 0 \quad \text{implies } \Delta T_s^{i\,'} = 600 \quad \text{else } \Delta T_s^{i\,'} = 0.1 \frac{N_s^i}{dN_s^i / dt}$$

$$N_s^i = 0 \quad \text{implies } \Delta T_s^{i\,''} = 600 \quad \text{else } \Delta T_s^{i\,''} = \min\left\{600,\ 6\ N^i / N_s^i\right\}$$

$$\Delta T^i = \min\left\{1800,\ \max\left\{30,\ \Delta T_s^{i\,'},\ \Delta T_s^{i\,''}\right\}\right\} \qquad (47)$$

Note that tracts are not updated in lockstep at some specified interval, but are updated individually, asynchronously. The next update event for each burning tract is placed on the event list at the time of the current update. This asynchronous updating is a feature of the UFS-2 design. It provides a combination of good accuracy and computational efficiency. The only exception to this is that all tracts are updated prior to an output event requested by the user.

The energy, power, and burn out time per building in each occupancy class is given in Table 4. The "Vacant" class, which represents natural fuel, has been left blank in the current model. It could be filled in, for example, with an appropriate energy per tree, power per tree, and burn out time for a tree and the number of trees in a vacant tract would replace the number of buildings on input.

Blast from the nuclear weapon can rubblize part of the fuel in the urban area. If a tract is rubblized, the effective number of buildings in each class is halved, T_o^j is halved, and $\dot{Q}_o^j$ is reduced to one third of its normal value. Thus, Q_o^j is one sixth of the energy per building, which allows only one twelfth of the total energy to be released when the tract is burnt out.

Table 4. Approximate constants for rectangular burn curves by occupancy class.

Occupancy Class	Q_o (joules)	$\dot{Q}_o$ (watts)	T_o (s)
Barren	0	0	0
Vacant	0	0	0
Residential	$2(10)^{10}$	$4(10)^6$	$5(10)^3$
Commercial	$8(10)^{10}$	$8(10)^6$	$1(10)^4$
High Rise Residential	$1(10)^{11}$	$1(10)^7$	$1(10)^4$
Industrial	$6(10)^{11}$	$6(10)^7$	$1(10)^4$

6.2 FIRE INDUCED WIND MODEL.

Surface winds resulting from a fire column are an inflow response to the entrainment and lofting of surface air. In the UFS-2 wind model each burning tract is considered to be a subfire with its own fire column. Nieghboring subfire columns coalesce at some altitude above the ground, and this larger, combined column spreads in a conical fashion as it rises. The center of each triangular tract is regarded as the subfire center, with an effective radius r_f^i given by

$$r_f^i = (A_i / \pi)^{1/2} \tag{48}$$

Each subfire is made up of the fire columns from each of the burning buildings in the tract, N_2^i fire columns. The coalescence height of fire columns is

$$z_c^i = 4.6263 \left(\frac{A_i}{\pi N_2^i} \right)^{1/2} \tag{49}$$

where there is more than one column, and the origin displacement below the surface is

$$z_o^i = 4.6263\ r_f^i - z_c^i \tag{50}$$

in meters. These distances are constrained by

$$0 < z_o^i < 4.6263\ r_f^i \tag{51}$$

and

$$0 < z_c^i < 4.6263\ r_f^i \tag{52}$$

Geometrically, the coalesced fire columns in a subfire are depicted in Figure 34. In the construction of Figure 34 about ten fire columns were assumed, which makes z_o about twice z_c. In addition, to make the figure more legible the horizontal scale has been exaggerated by about two times.

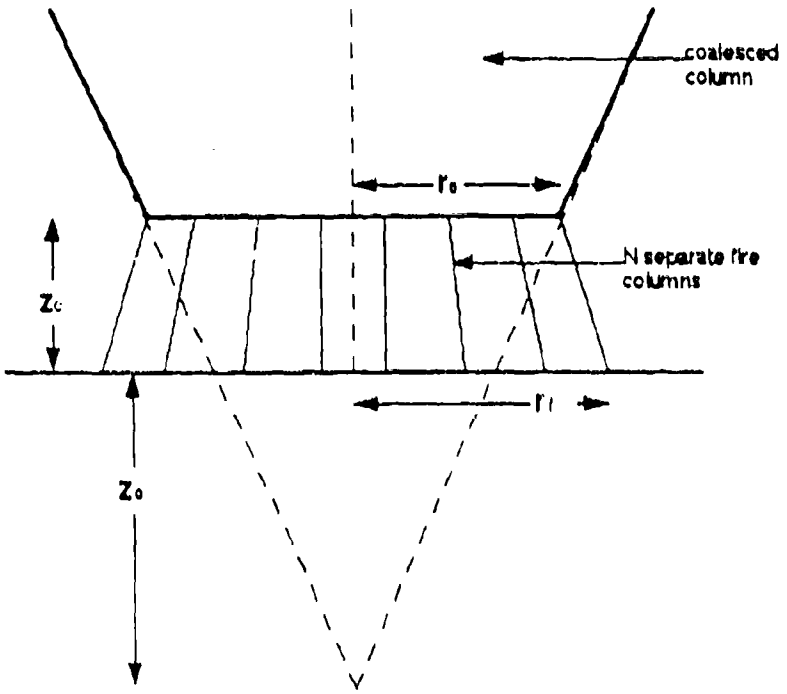

Figure 34. Geometry of coalescing fire columns.

The radial indraft component of surface wind is defined as a vector pointing to the subfire (tract) center. Let these location vectors be given by $\vec{R^i}$ and the test point where indraft is to be evaluated given by $\vec{R_p}$. The radial component is directed along the vector $\vec{R^i} - \vec{R_p}$. After a wind velocity is assigned to each of these vectors (one for each subfire) they are summed to obtain the combined indraft wind. Let

$$r = \left| \vec{R^i} - \vec{R_p} \right| \tag{53}$$

be the distance from the center of tract i to the test point.

If $r > r_f^i$, the test point lies outside the tract i subfire, then the normalized velocity of the indraft wind is given by

$$v_r^i(r) = \frac{\dot{V}_a^i}{2\pi r^2} + \frac{3}{5}\frac{\alpha k}{\eta}\left(\frac{\dot{Q}_T^i}{N_2^i}\right)^{1/3} N_2^i \frac{r_f^i}{r^2} z_c^{i\,2/3} +$$

$$\frac{\alpha k}{\eta}\left(\frac{\dot{Q}_T^i}{r}\right)^{1/3}\left[f(\omega_T^i,\omega_o^i) - f(\omega_c^i,\omega_o^i)\right] \qquad (54)$$

where the first term is the air required by the burning rate, the second term is the air entrained by the lower column, and the third term is the air entrained by the upper column. The new symbols in Equation 54 are as follows:

$$\dot{V}_a^i = \frac{A\,\dot{Q}_T^i}{Q\,d}$$ is the volume rate of air required (m3/s) (55)

where

A is the mass of air needed to burn a mass of fuel (kg air / kg fuel)

Q is the heat produced by a mass of fuel (J/kg)

d is the air density (kg/m3)

$\alpha - 0.1$, $k = 3.897(10)^{-2}$, and $\eta = 5.51$ are constants

and

$$f(\omega_T^i,\omega_o^i) = \int_0^{\omega_T^i} \frac{\left(\omega + \omega_o^i\right)^{2/3}}{\left(1 + \omega^2\right)^{3/2}}\,d\omega \qquad (56)$$

is the truncated column entrainment factor, a tabulated function, where the scaled reciprocal distances are

$$\omega_T^i = z_T^i / r$$

$$\omega_c^i = z_c^i / r \qquad (57)$$

$$\omega_o^i = z_o^i / r$$

and

$$z_T^i = 0.234\ \dot{Q}_T^{i\,1/4}\ \Delta T_B^{i\,3/4} \quad \text{is the column top from tract i (m)} \tag{58}$$

ΔT_B^i is the length of time tract i has been burning.

The UFM-2 model enforces the following constraints on the truncated column entrainment parameters:

$$0 \le \omega_o \le 4.6263 \tag{59}$$

$$0 \le \omega_c \le \omega_T \le 50$$

A plot of $f(\omega_T, \omega_o)$ is shown in Figure 35.

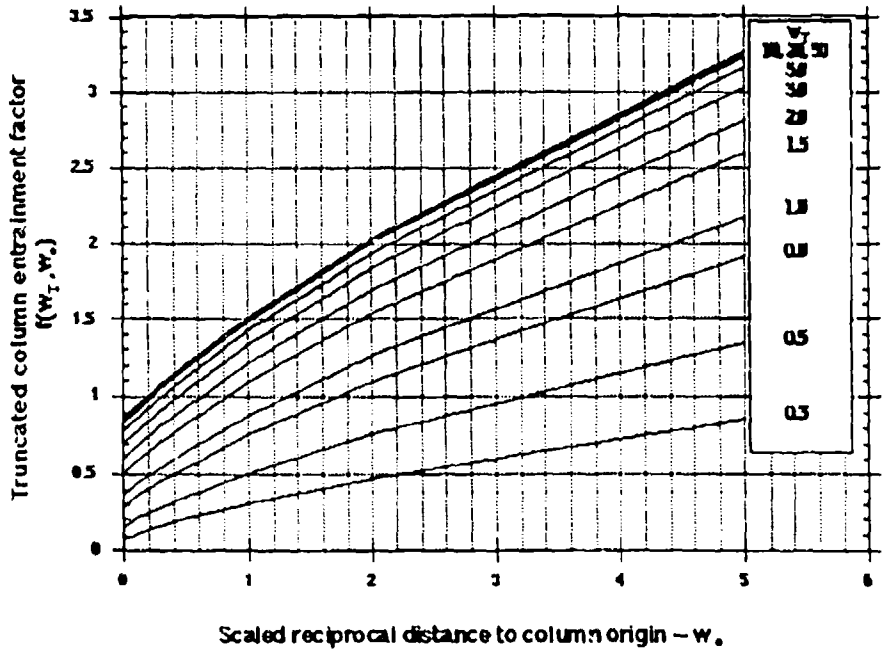

Figure 35. Truncated column entrainment function.

If $r < r_f^i$, then the test point is inside the tract i subfire and the wind velocity from this subfire is scaled linearly from the tract center. The wind velocity is given by Equation 54 evaluated at r_f^i times the distance to the tract center;

$$v_r^i(r) = v_r^i(r_f^i)\,\frac{r}{r_f^i} \tag{60}$$

The radial indraft and the ambient wind is then summed over all velocity components to obtain the wind at test point p

$$\vec{V_p} = \vec{V_a} + \sum_{i}^{\text{all burning tracts}} v_r^i(r^i)\,\frac{\left(\vec{R^i} - \vec{R_p}\right)}{r^i} \tag{61}$$

which can never have a zero distance for r^i when the test point is on a tract boundary. The contagion area A_{ij} can then be expressed as

$$A_{ij} = t_{Bi}\left|\vec{V_p} \times \vec{S_{ij}}\right| \tag{62}$$

where $\vec{S_{ij}}$ is a tract edge vector.

6.3 UFM-2 OUTPUT EXAMPLES.

As a final test of the UFM-2 software, three test problems were executed. These tests used the urban map and tract layout shown as an example in Sections 2 through 5. The three tests involved three different ambient wind conditions: no wind, 1 m/s wind, and 10 m/s wind from the southeast. A 1.0 mT burst is assumed to occur over the boundary of tracts 52 and 77 (19km,19km) at an altitude of 3700 meters. All three tests completed successfully with expected results.

Although almost all of the occupied tracts are on fire by 2000 seconds, the major contributors to energy release rate are the residential tracts 33, 34, and 50, and the high rise residential and industrial tracts 67, 68, 69, 100, and 101. There is little difference between the zero ambient wind case and the 1 m/s wind case. Tract burn out occurs in the same order an with insignificant differences in burnout times, which results from the Monte Carlo simulation design. The last five tracts listed above are also the first to burn out; tract 68 at about 5400 seconds is the first. The only apparent difference in these two cases is that tract 108 caught fire from tract 109 brands at 6540 seconds presumably because of the 1 m/s southeast wind. This wind component is in the right direction to influence that contagion, while radial inflow alone would not. Tracts 108 and 109 are in the southwest corner of the urban map. Bear in mind, however, that the Monte Carlo simulation design would allow this contagion event to occur earlier, later, or not at all in other trial runs using different pseudo random number seeds. The major reason for the similarity of results is that the largest indraft component at a tract center at 2000 seconds is 13 m/s and is 10.5 m.s at 4000 seconds. This indraft clearly dominates in the principal fire areas.

In the 10 m/s ambient wind case the order of tract burnout is affected to some degree, and the ambient wind sped up the burning. The first tract to burn out is 138 at 5140 seconds followed by tract 68 at 5250 seconds. Tracts that quit burning early in the simulation typically leave ten or fewer structures unburned out of several thousand. Tracts that quit burning toward the end of the

simulation (18000 seconds, 5 hours, in this case) typically leave a few percent to about twenty percent of structures unburned.

Output from the 1 m/s ambient wind case, that is plots of quantities recorded at requested simulation times and tract maps plotted by UFM-2 of relative wind, tract burning, and $\dot{Q}$, are shown in Figures 36 through 53. Figure 36 is a plot of the number of tracts unignited, burning, and burned out. Figure 37 is a plot of the maximum wind speed at tract centers. Figures 38 through 42 are tract maps of relative wind vectors. Figures 43 through 47 are tract maps of tract burning and burned out status. Figures 48 through 53 are tract maps of $\dot{Q}$. The values of $\dot{Q}$ associated with each tract are coded on a logarithmic scale, base 10 with an offset of 10^4. Thus, 1 means 1.e5, 2 means 1.e6, etc.

Other parametric studies with UFS-2 involved multiple detonations and patterns of yield and altitude, wind, and fuel loading that might disclose modeling errors. One such pattern placed the bursts over the northeast corner of the urban map and used single detonations of 0.001 mT at 325m, 0.01 mT at 750m, 0.1 mT at 1500m and 1.0 mT at 3500m. Another pattern was a 2x2 matrix of low and high ambient wind and low and high fuel loading. All of these tests were performed satisfactorily.

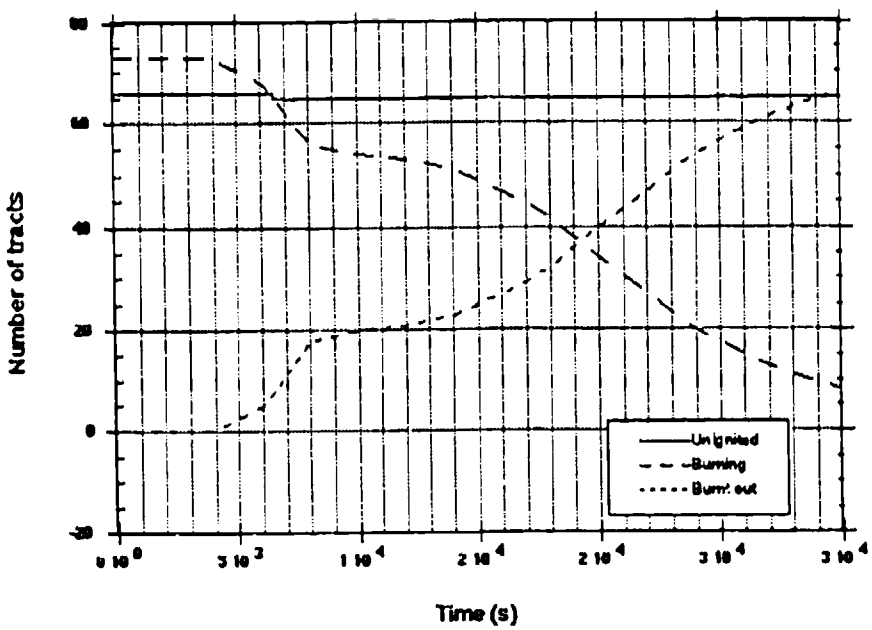

Figure 36. History of tract status for 1 m/s ambient southeast wind.

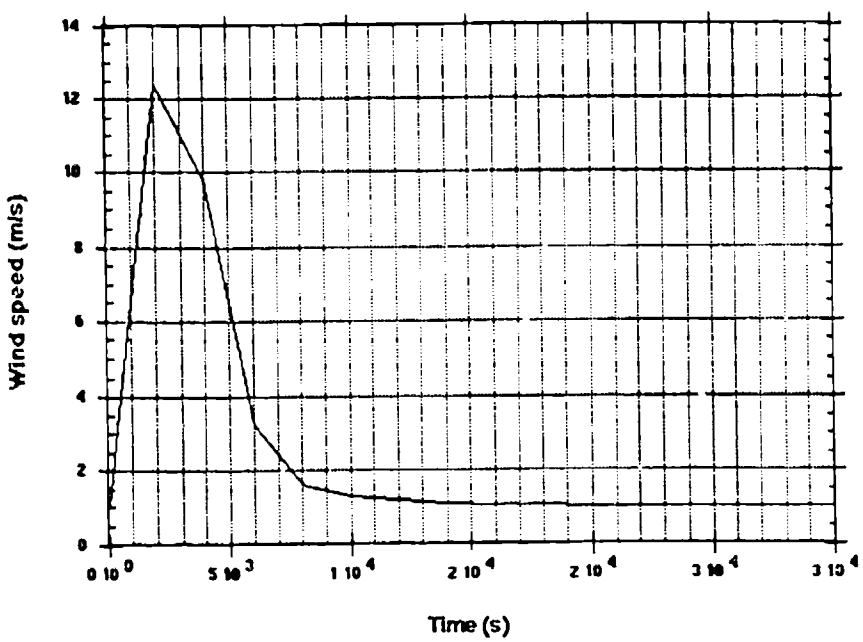

Figure 37. Maximum wind speed at tract centers.

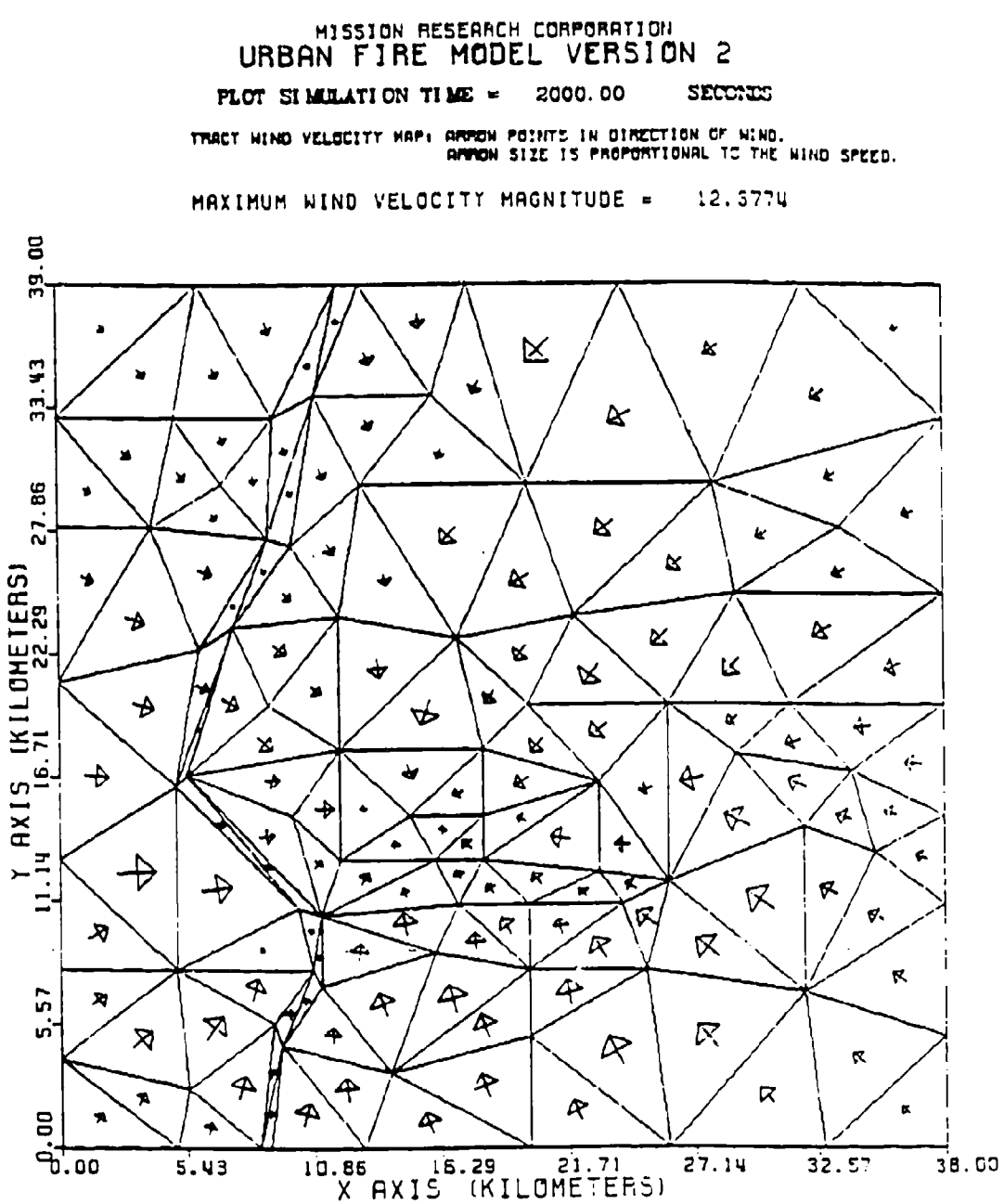

Figure 38. Tract map of relative wind vectors at 2000 s.

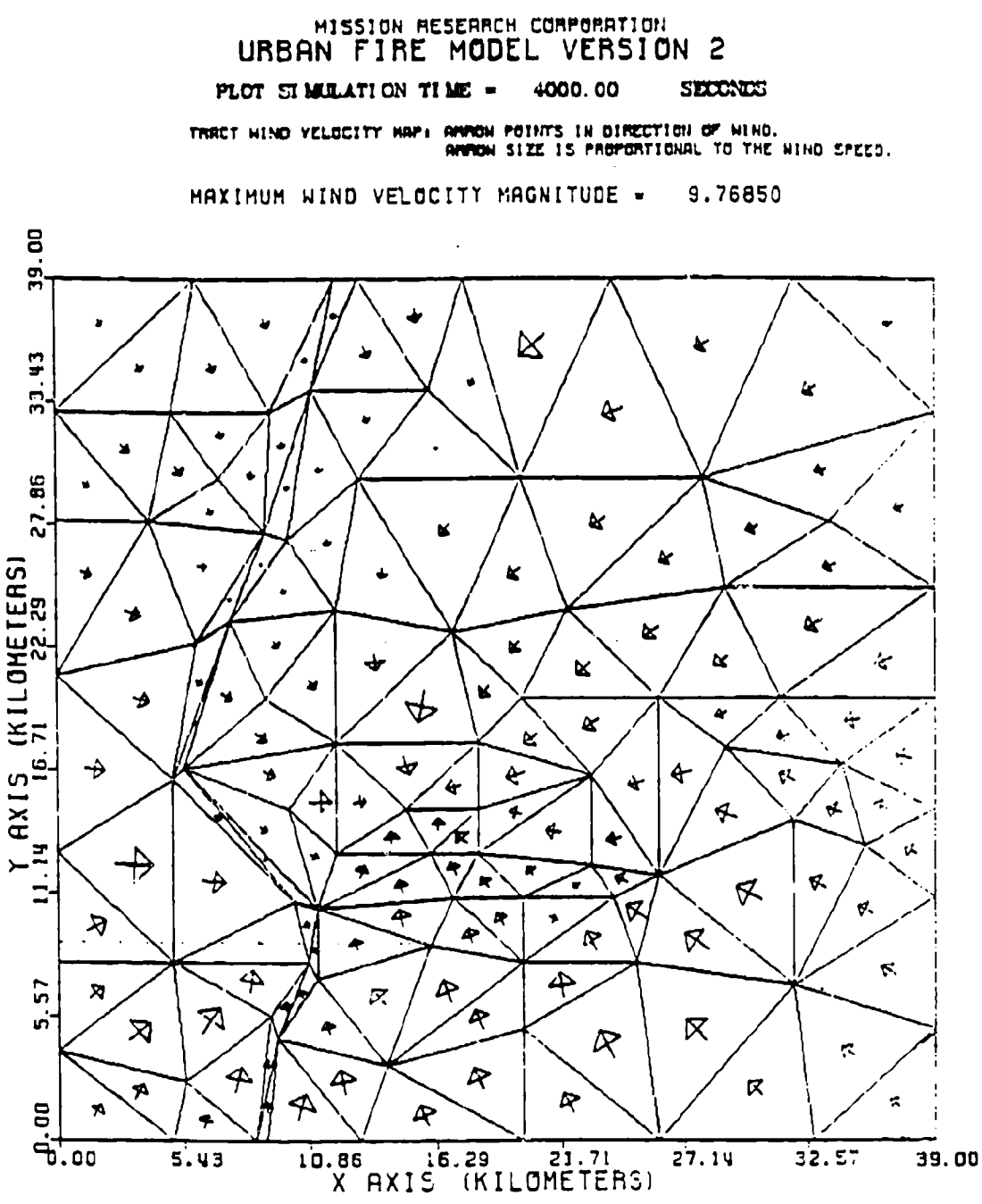

Figure 39. Tract map of relative wind vectors at 4000 s.

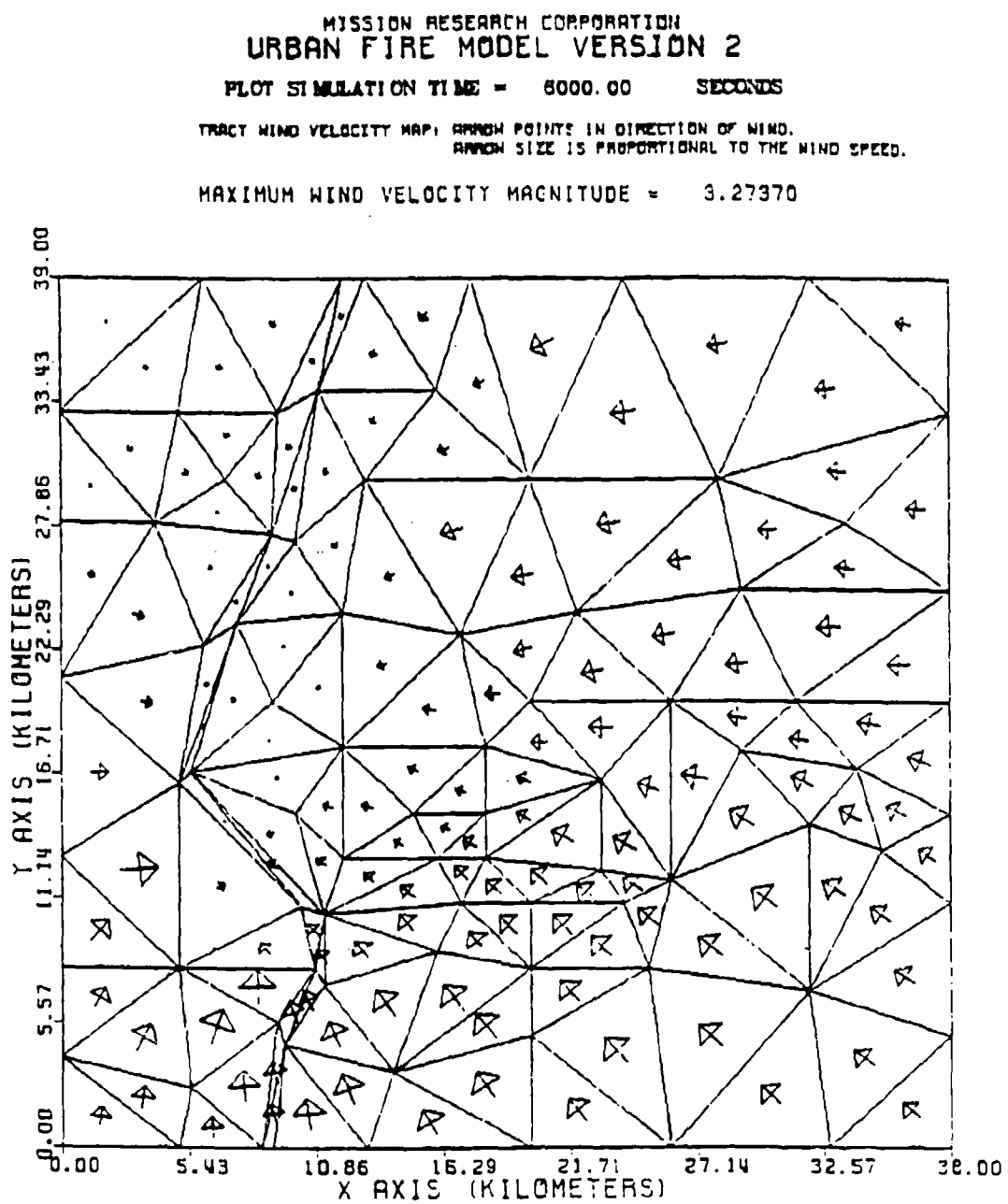

Figure 40. Tract map of relative wind vectors at 6000 s.

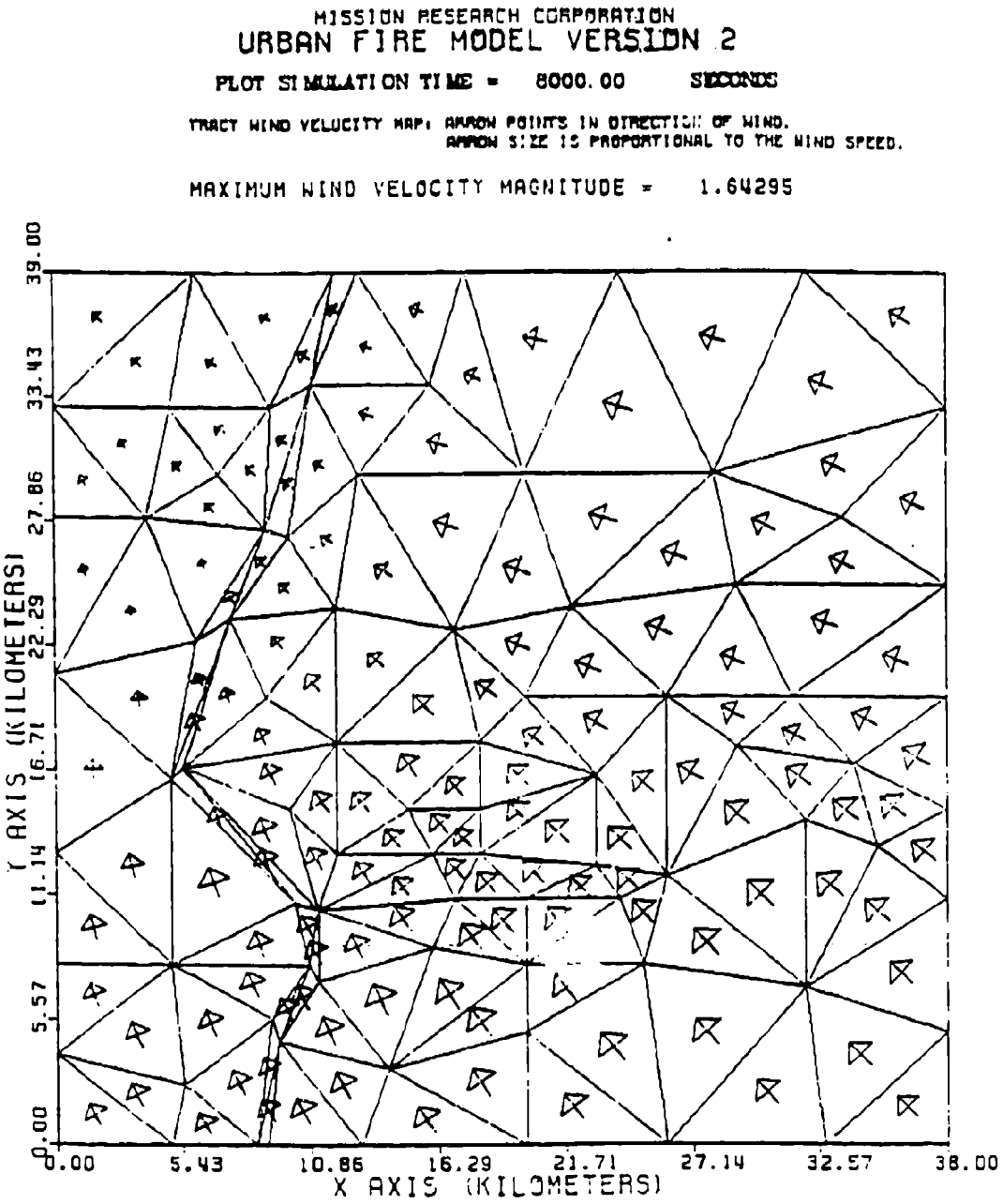

Figure 41. Tract map of relative wind vectors at 8000 s.

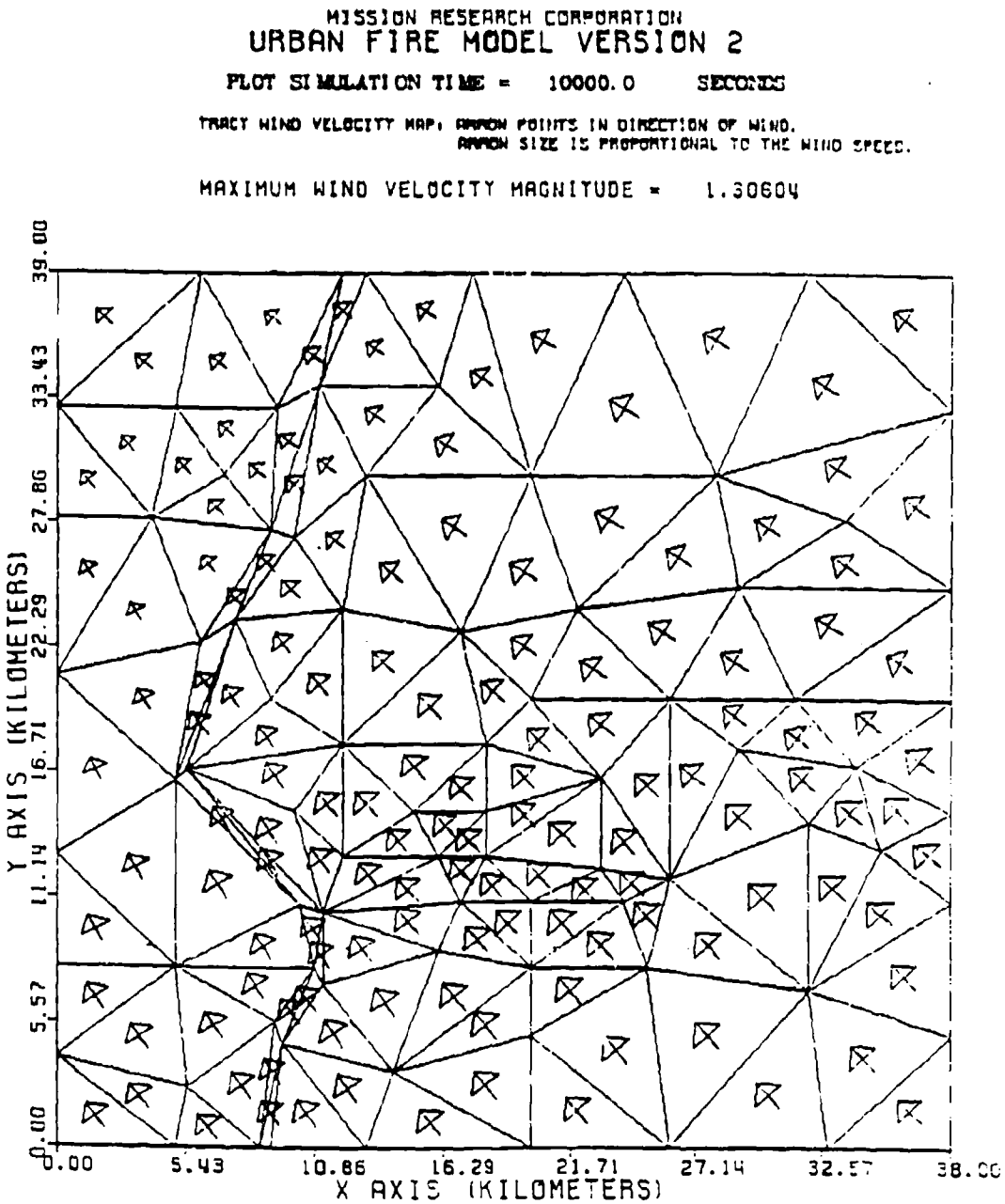

Figure 42. Tract map of relative wind vectors at 10000 s.

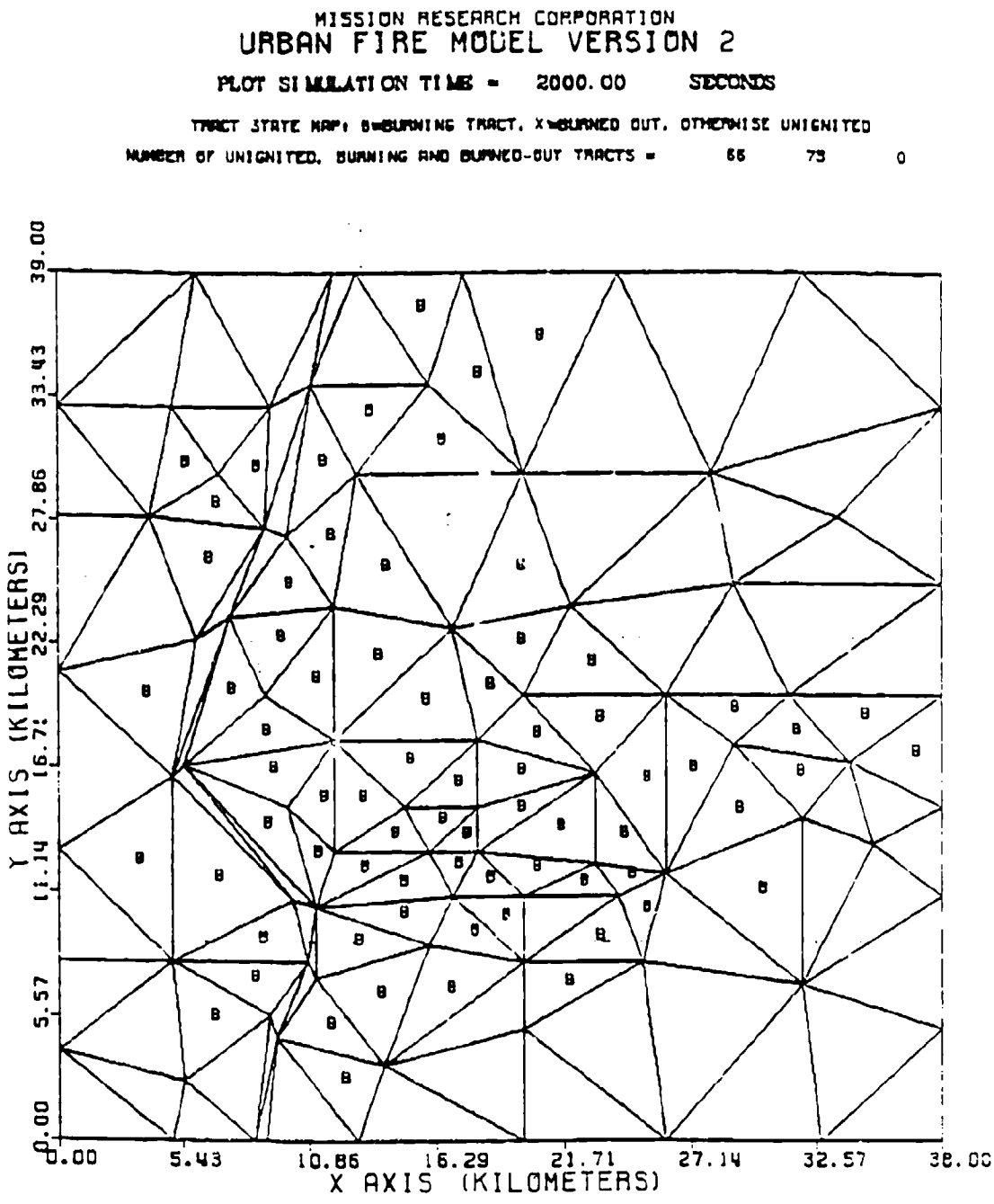

Figure 43. Tract map of unignited, burning, and burned out tracts at 2000 s.

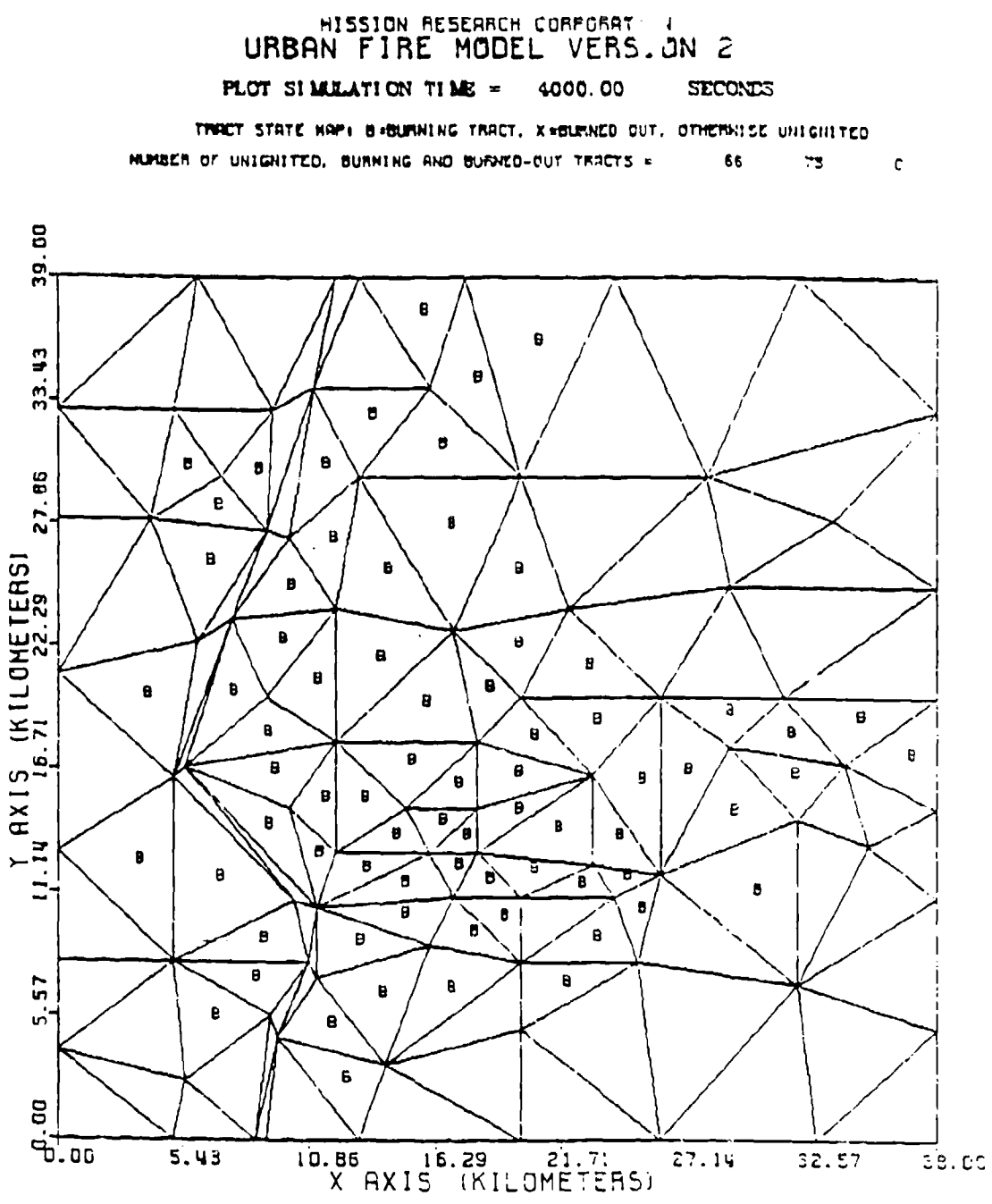

Figure 44. Tract map of unignited, burning, and burned out tracts at 4000 s.

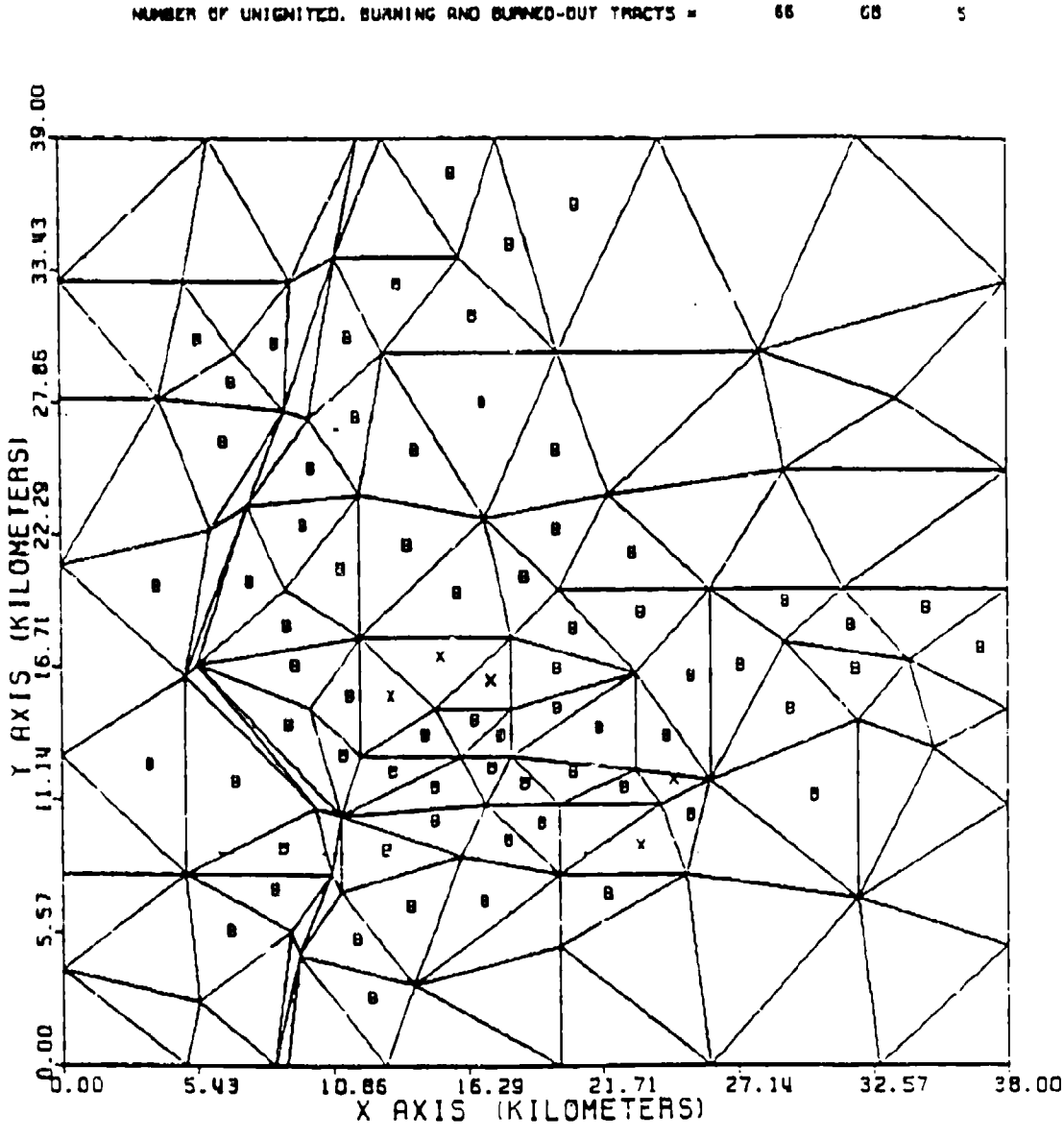

Figure 45. Tract map of unignited, burning, and burned out tracts at 6000 s.

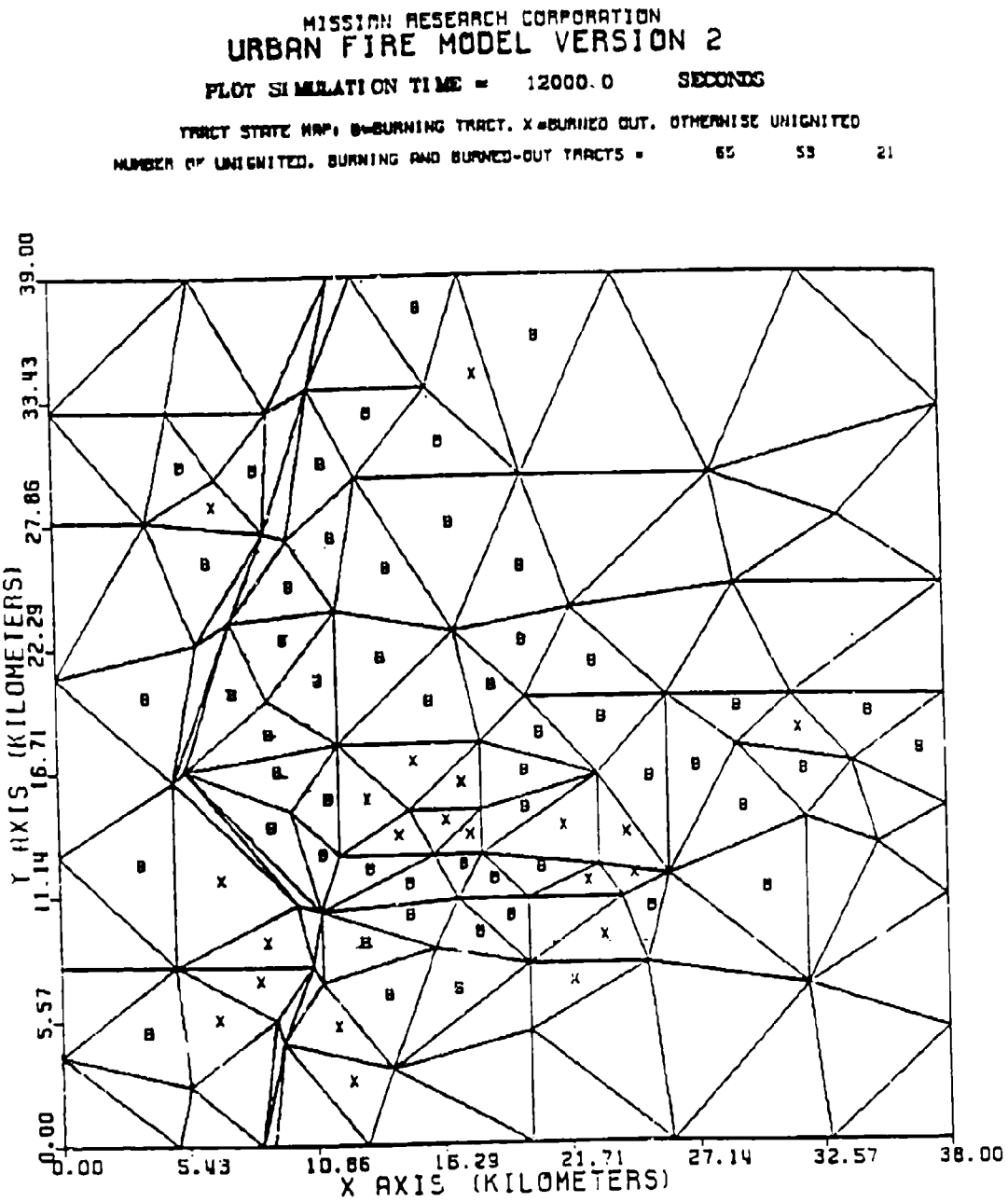

Figure 46. Tract map of unignited, burning, and burned out tracts at 12000 s.

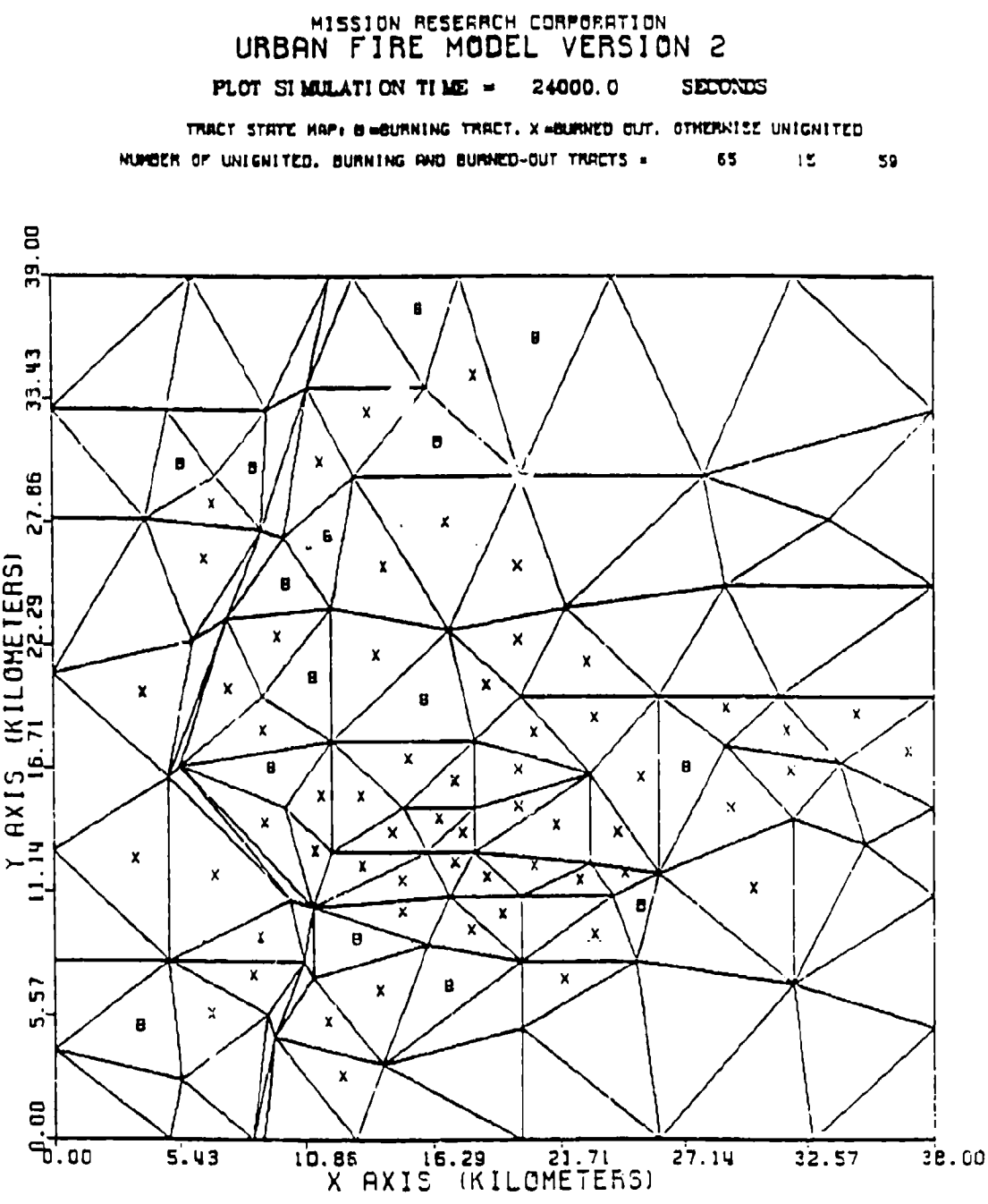

Figure 47. Tract map of unignited, burning, and burned out tracts at 24000 s.

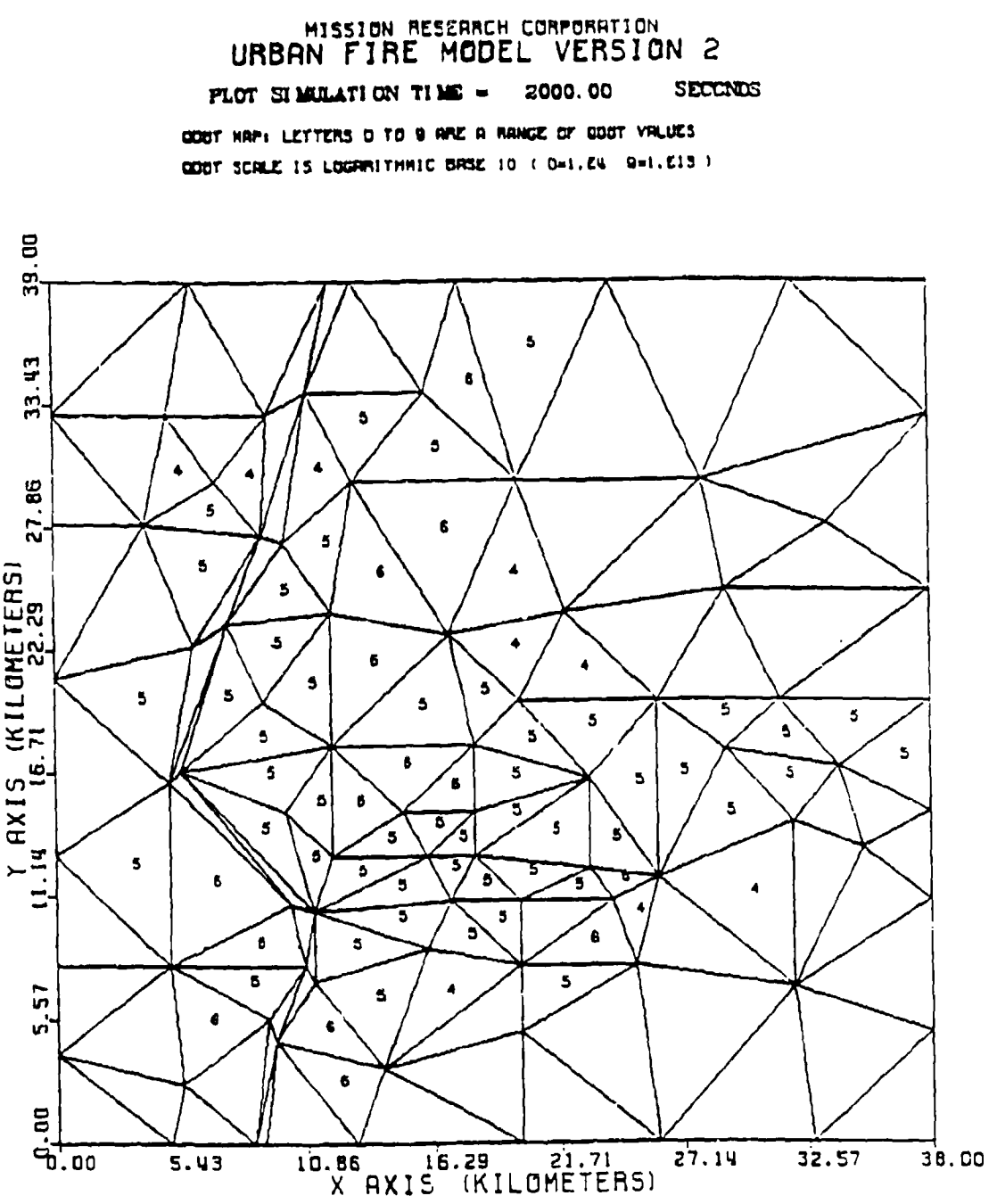

Figure 48. Tract map of $\dot{Q}$ at 2000 s.

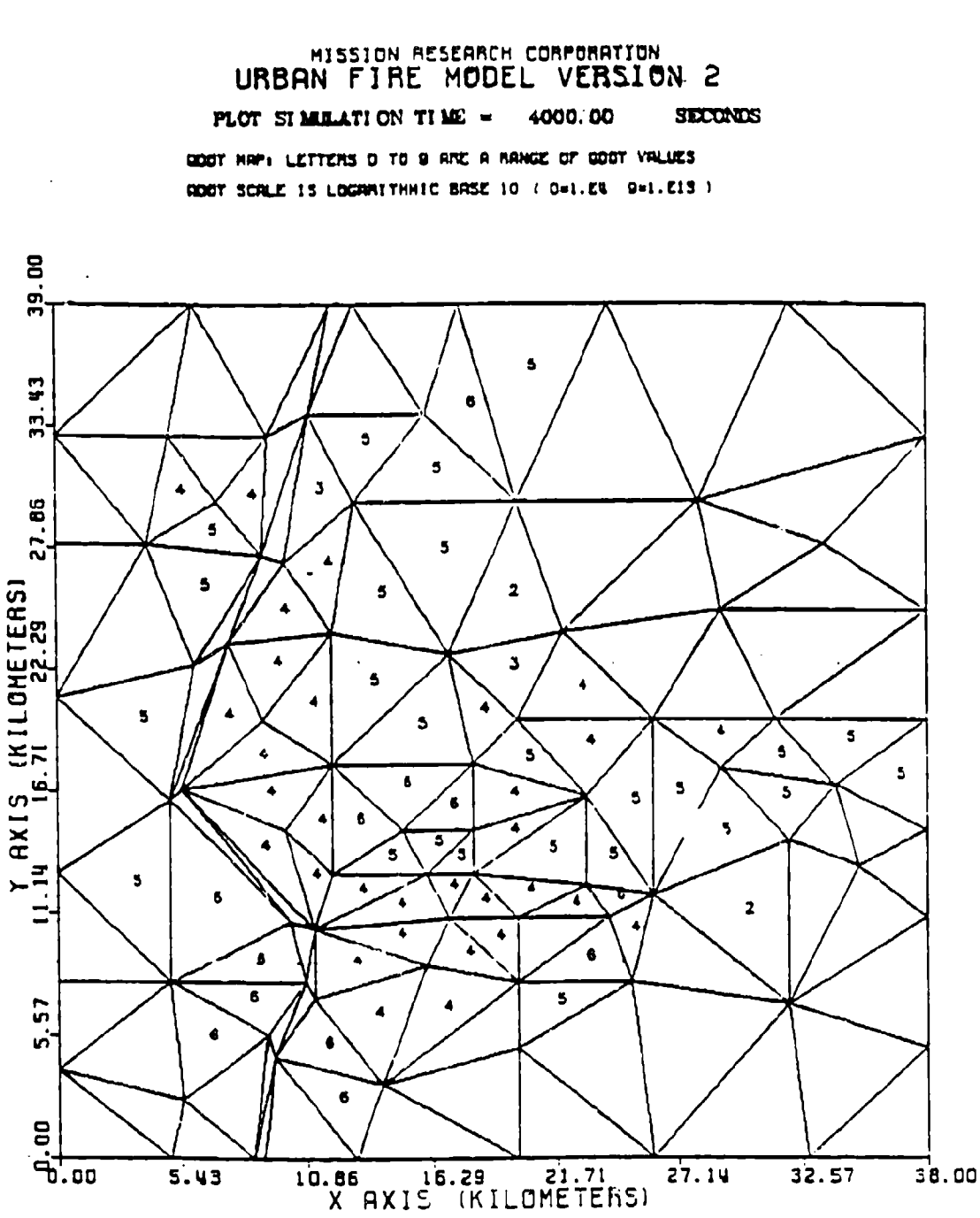

Figure 49. Tract map of $\dot{Q}$ at 4000 s.

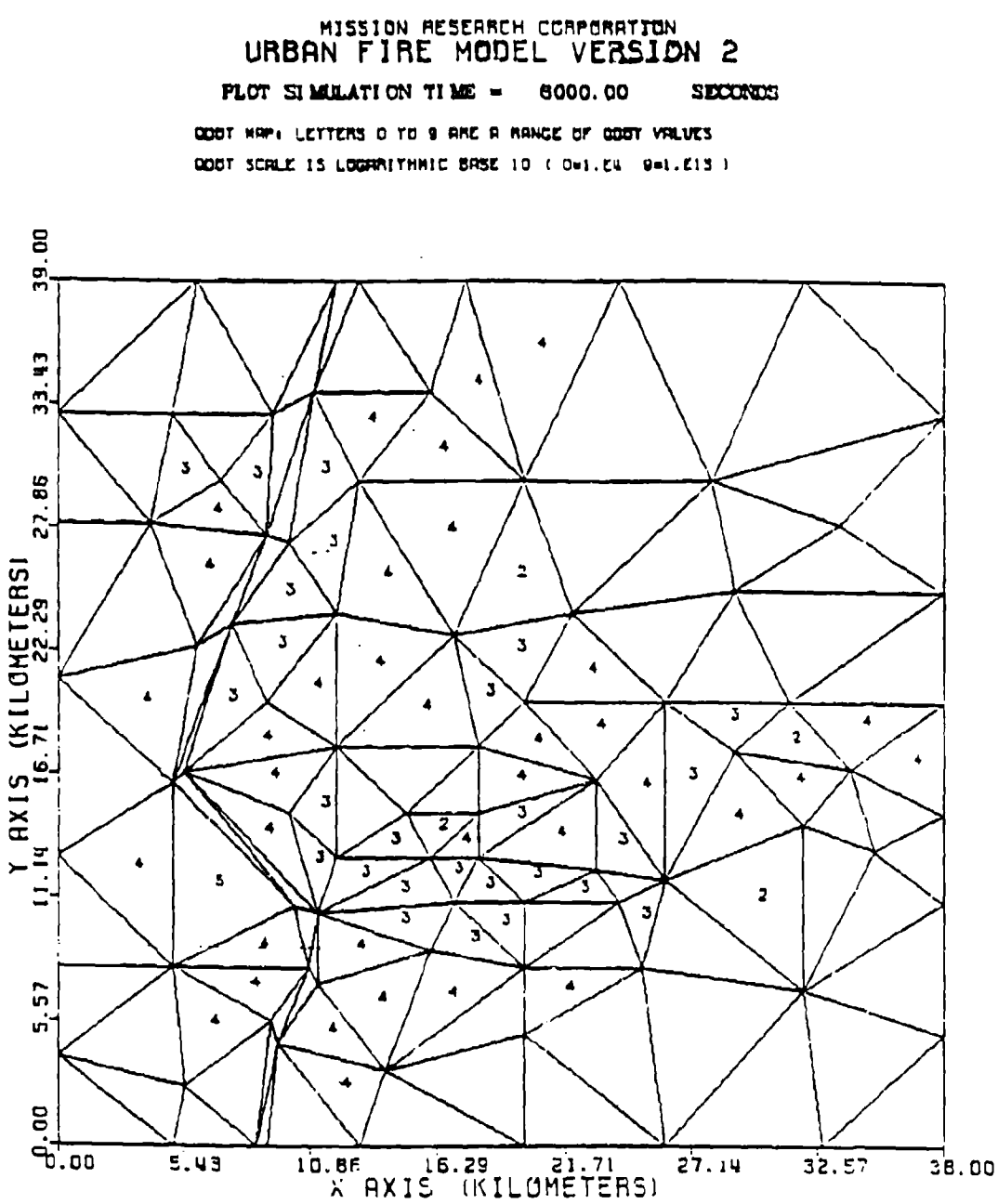

Figure 50. Tract map of $\dot{Q}$ at 6000 s.

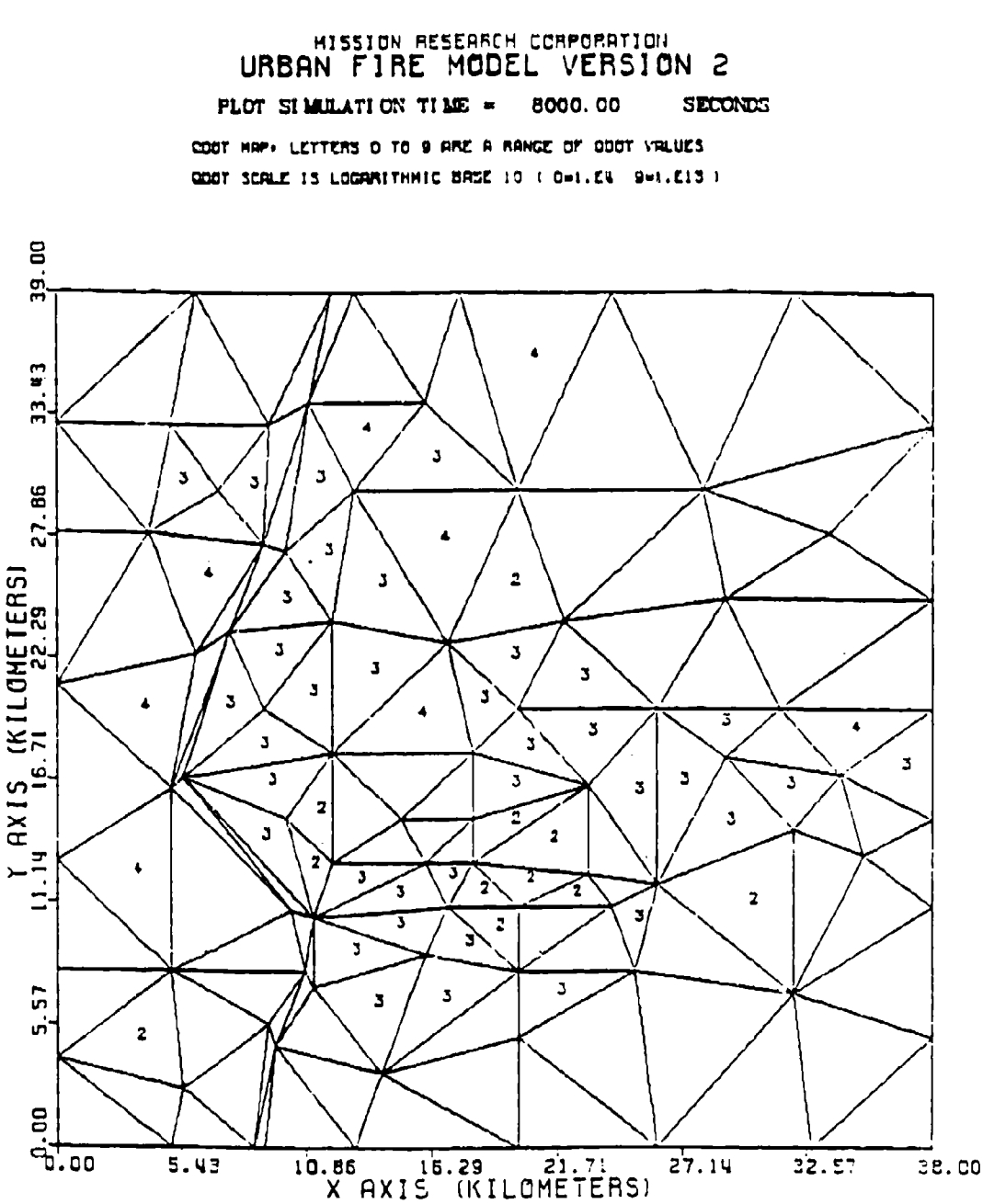

Figure 51. Tract map of $\dot{Q}$ at 8000 s.

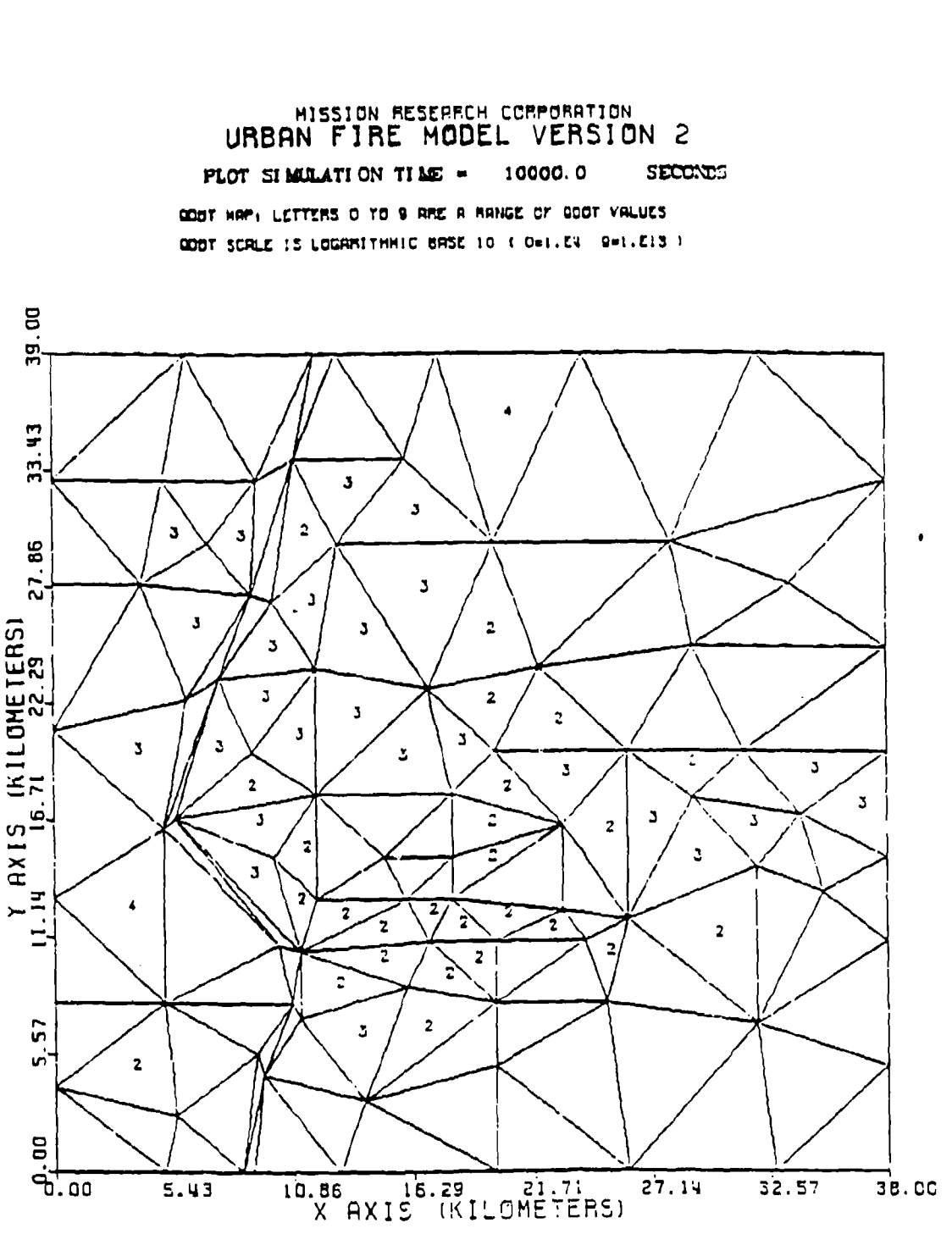

Figure 52. Tract map of $\dot{Q}$ at 10000 s.

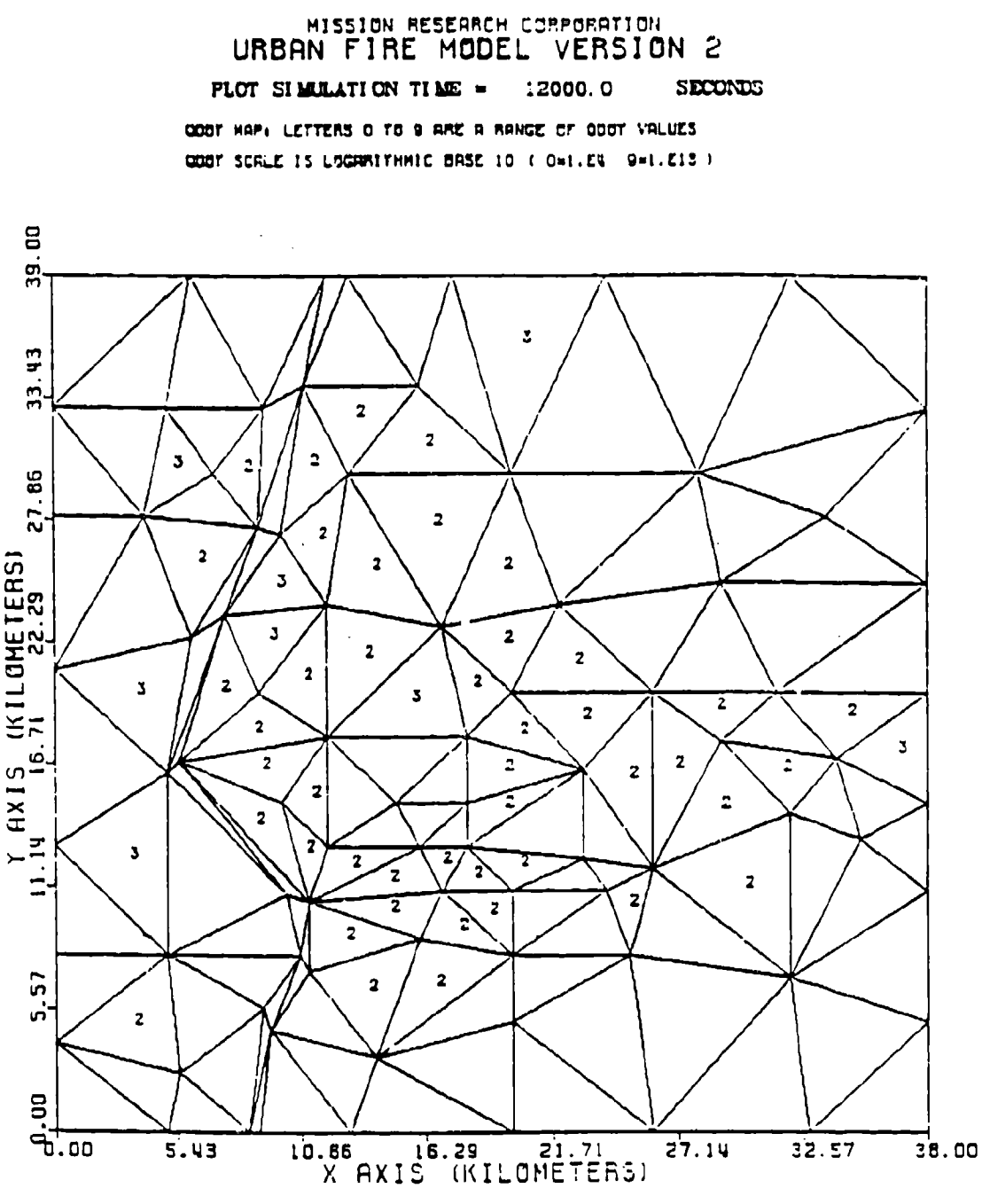

Figure 53. Fract map of $\dot{Q}$ at 12000 s.

SECTION 7

LIST OF REFERENCES

1. Sanderlin, J. C., J. A. Ball, and G. A. Johanson, "Mass Fire Model Concept," (Unclassified) Mission Research Corporation Report MRC-R-636 (DNA 5803F), May, 1981. (Unclassified)

2. Martin, S. B., and S. Holton, "Preliminary Computer Program for Estimating Primary Ignition Ranges for Nuclear Weapons, (Unclassified) USNRDL-TR-866, 3 June, 1965. (Unclassified)

3. Wolf, William L., "Handbook of Military Infrared Technology," (Unclassified) Office of Naval Research, Department of the Navy, Washington, D.C., 1965. (Unclassified)

4. Glasstone, Samuel and Phillip J. Dolan, "The Effects of Nuclear Weapons," (Unclassified) U.S. Government Printing Office, Washington, D.C, 1977. (Unclassified).

5. Takata, Arthur N. and Frederick Salzberg, "Development and Application of a Complete Fire Spread Model: Volume I (Development Phase)," (Unclassified) Illinois Institute of Technology, June, 1968. (Unclassified)

6. martin, Stanley B., and Raymond s. Alger, "Blast/Fire Interactions: Proceedings of the 1981 Conference," (Unclassified) Stanford Research Institute Project PYU 3110, August, 1981. (Unclassified)

7. McAuliffe, Jonn and Kendall Moll, "Secondary Ignitions in Nuclear Attack," (Unclassified) Stanford Research Institute, Menlo Park, CA, July 1965 (Unclassified)

8. Backovsky, Jana, Stanley Martin, and Robert McKee, "Blast Effects on Fires," (Unclassified) Stanford Research Institute Project PYU 8421, December 1981. (Unclassified)

9. Wilton, C., D.J. Myrouk, and J.V. Zaccor, "Secondary Fire Analysis," (Unclassified) Scientific Services Incorporated Report SSi 8048-6, September 1981. (Unclassified)

10. Rotz, J., et al., "Formation of Debris from Buildings and Their Contents By Blast and Fire Effects of Nuclear Weapons," (Unclassified) United Research Services Report URS 651-4, April, 1966. (Unclassified)

11. Rotz, J., "Debris Model Research with Building Damage, Fire Spread, and Debris Predictions for Five-City Study," (Unclassified) United Research Services Report URS 651-8, March 1967. (Unclassified)

DISTRIBUTION LIST

DNA-TR-92-20

DEPARTMENT OF DEFENSE

DEFENSE INTELLIGENCE AGENCY
ATTN: DIW-4
ATTN: OGA-4B2
ATTN: WDB-4CR

DEFENSE NUCLEAR AGENCY
ATTN: RARP
2 CYS ATTN: TITL

DEFENSE TECHNICAL INFORMATION CENTER
2 CYS ATTN: DTIC/FDAB

FIELD COMMAND DEFENSE NUCLEAR AGENCY
ATTN: FCNM

DEPARTMENT OF THE AIR FORCE

UNITED STATES STRATEGIC COMMAND
ATTN: J 535

DEPARTMENT OF ENERGY

LAWRENCE LIVERMORE NATIONAL LAB
ATTN: J PENNER
ATTN: M MACCRACKEN
ATTN: R PERRETT

LOS ALAMOS NATIONAL LABORATORY
ATTN: M GILLESPIE

SANDIA NATIONAL LABORATORIES
ATTN: B ZAK

OTHER GOVERNMENT

FEDERAL EMERGENCY MANAGEMENT AGENCY
ATTN: OFC OF CIVIL DEFENSE R SANDS

NASA
ATTN: O TOON

NATIONAL CENTER ATMOSPHERIC RESEARCH
ATTN: L RADKE
ATTN: S SCHNEIDER

NATIONAL INSTITUTE OF STANDARDS & TECHNOLOGY
ATTN: H BAUM
ATTN: R LEVINE

NATIONAL INST OF STANDARDS AND TECHNOLOGY
ATTN: G MULHOLLAND

OFFICE OF SCIENCE AND TECH POLICY
ATTN: MAJ S HARRISON

DEPARTMENT OF DEFENSE CONTRACTORS

DESERT RESEARCH INSTITUTE
ATTN: J HUDSON

INSTITUTE FOR DEFENSE ANALYSES
ATTN: E BAUER

KAMAN SCIENCES CORP
ATTN: DASIAC

KAMAN SCIENCES CORPORATION
ATTN: DASIAC

MISSION RESEARCH CORP
2 CYS ATTN: G JOHANSON
2 CYS ATTN: J BALL
2 CYS ATTN: J SANDERLIN
2 CYS ATTN: L EWING

PACIFIC-SIERRA RESEARCH CORP
ATTN: H BRODE
ATTN: R SMALL

SCIENCE APPLICATIONS INTL CORP
ATTN: L HUNT

SCIENCE APPLICATIONS INTL CORP
ATTN: D BACON
ATTN: J COCKAYNE
ATTN: J MCGAHAN

STAN MARTIN AND ASSOCIATES
ATTN: S B MARTIN
ATTN: S MARTIN

UNIVERSITY OF NEW MEXICO
ATTN: H GLOVER

DIRECTORY OF OTHER

HARVARD UNIVERSITY
ATTN: G CARRIER

MARYLAND UNIVERSITY OF
ATTN: A ROBOCK DEPT METEOROLOGY

UCLA
ATTN: R TURCO